

AN IN-SITU INVESTIGATION OF THE ANODIC BEHAVIOR OF
Ni and Ni-30 Cu USING ELECTROCHEMICAL AND OPTICAL TECHNIQUES

By

RANDALL J. SMITH

A DISSERTATION PRESENTED TO THE GRADUATE SCHOOL
OF THE UNIVERSITY OF FLORIDA IN PARTIAL FULFILLMENT OF
THE REQUIREMENTS FOR THE DEGREE OF DOCTOR OF PHILOSOPHY

UNIVERSITY OF FLORIDA

1984

ACKNOWLEDGEMENTS

The author wishes to express his sincere appreciation to his advisor, Dr. Rolf E. Hummel, for his patience and confidence throughout this work. Special thanks are extended to Dr. Ellis D. Verink, Jr., for his unwavering confidence and guidance over the past four years. The refreshing humor of Dr. Paul Holloway and his efforts in securing financial support for the final year of research are also gratefully acknowledged. Dr. John R. Ambrose and Mesuit Akkaya are also to be thanked for their many stimulating conversations regarding the present research. Sincere appreciation is expressed to each member of the supervisory committee (R. E. Hummel, E. D. Verink, Jr., J. R. Ambrose, P. H. Holloway, R. T. DeHoff and D. O. Shah) for their support over the past years.

The author would also like to thank Dr. Mike Kosinski for his elegant and timely operation of the ESCA-AES system which were necessary for the completion of this research.

TABLE OF CONTENTS

	<u>Page</u>
ACKNOWLEDGEMENTS.....	i
ABSTRACT.....	iv
CHAPTER	
1 INTRODUCTION.....	1
2 LITERATURE REVIEW.....	6
The Corrosion Behavior of Pure Nickel.....	6
Behavior of Nickel in Neutral Solutions.....	15
The Behavior of Nickel in Alkali Solutions.....	18
The Transpassive Behavior of Nickel.....	20
The Effect of Chloride Ions on the Passive Behavior of Nickel.....	24
The Corrosion Behavior of Pure Copper.....	28
The Corrosion Behavior of Nickel-Copper Alloys.....	31
Summary.....	35
3 EXPERIMENTAL PROCEDURE.....	38
Sample Preparation.....	38
Solution Preparation.....	41
The Corrosion Cell.....	41
Polarization Techniques.....	43
4 RESULTS AND DISCUSSION.....	44
Identification of Anodic Surface Films.....	44
Anodic Films on a Copper Electrode.....	44
Anodic Films on a Nickel Electrode.....	51
Anodic Behavior of Nickel in 0.15 N Na ₂ SO ₄	66
Anodic Behavior of pH = 4.0.....	66
Anodic Behavior of pH = 8.0.....	76
Anodic Behavior of pH = 12.0.....	81
Anodic Behavior of Nickel in 0.15 N Na ₂ SO ₄ Containing Chlorides.....	89
Anodic Behavior at pH = 4.0.....	89
Anodic Behavior at pH = 8.0.....	91
Anodic Behavior at pH = 12.0.....	97

CHAPTER	Page
4	RESULTS AND DISCUSSION (continued)
	Anodic Behavior of Nickel - 30 Copper in 0.15 N Na_2SO_497
	Anodic Behavior at pH = 4.0.....97
	Anodic Behavior at pH = 12.0.....112
	Summary.....112
5	CONCLUSIONS AND SUGGESTIONS FOR FURTHER RESEARCH.....117
	BIBLIOGRAPHY.....121
	BIOGRAPHICAL SKETCH.....126

Abstract of Dissertation Presented to the Graduate School
of the University of Florida in Partial Fulfillment of the
Requirements for the Degree of Doctor of Philosophy

AN IN-SITU INVESTIGATION OF THE ANODIC BEHAVIOR OF
Ni and Ni-30 Cu USING ELECTROCHEMICAL AND OPTICAL TECHNIQUES

By

Randall J. Smith

December, 1984

Chairman: Professor R. E. Hummel
Major Department: Materials Science and Engineering

Although the passivation of nickel was observed by Faraday over a hundred years ago, the composition of the passivating film still has not been conclusively determined. This investigation was undertaken, therefore, to positively identify the film responsible for the passive behavior of nickel and to illustrate the mechanism of film formation. Also, of particular interest were the possible roles that alloying additions of copper and the presence of chlorides in solution might have on the stability of this film. To accomplish these goals standard electrochemical polarization techniques were used in conjunction with ex situ surface analytical techniques such as electron spectroscopy for chemical analysis and Auger electron spectroscopy, as well as Differential Reflectometry, which is capable of film identification both in situ and ex situ.

On the basis of this research it is concluded that the film which causes nickel to passivate in 0.15 N Na_2SO_4 (pH = 4.0 - 12.0) is $\text{Ni}(\text{OH})_2$. It is suggested that the film forms via a precipitation mechanism in the acid solutions while a solid state mechanism is operative in the alkaline solutions. Both NiO and NiOOH are also observed to form subsequent to $\text{Ni}(\text{OH})_2$ but only at the higher pHs.

The film responsible for the passivation of the Ni-30 Cu alloy is again $\text{Ni}(\text{OH})_2$. In addition to dealloying, small amounts of Cu_2O are detected to form in the acid solutions. However, the film that passivates this alloy at the alkaline pHs is pure $\text{Ni}(\text{OH})_2$. Although the presence of a 0.1 M chloride concentration does not alter the composition of the film that forms on pure nickel, it does delay the growth of this film at pHs of 4.0 and 8.0. In fact, in these solutions film breakdown as well as severe pitting occurs subsequent to passivation. However, at a pH of 12.0 the chlorides affect neither the film formation process nor film stability.

CHAPTER 1 INTRODUCTION

Nickel and nickel base alloys are widely used to prevent or limit corrosion in many environments. Nickel is quite resistant to alkalis and is often used to solve corrosion problems involving caustic solutions. Organic acids and compounds do not generally attack nickel; this leads to its widespread use in the food industry. Nickel also shows good resistance to neutral and slightly acid solutions but is attacked by strongly oxidizing acids [1].

However, nickel is most commonly used in the form of an alloying ingredient. While markedly improving the corrosion resistance, the mechanical properties of the alloy are often improved as well. Nickel is also metallurgically compatible with a wide range of important elements (e.g., Cu, Cr, Fe, Mo, W) and can be used to bring together in one alloy elements that are otherwise mutually immiscible (e.g., Cu and Cr).

Perhaps the most commercially important nickel base alloys are the Monels,* a class of alloys containing approximately 30% Cu along with varying amounts of secondary additions (e.g., 1% Fe). These alloys, while retaining the natural corrosion resistance of pure nickel to alkalis, have improved resistance to chloride ions and reducing media. They are commonly used to handle sulfuric acid, dilute hydrochloric and hydrofluoric acid of all concentrations. They also find considerable use in flowing seawater [2].

*Trademark of the International Nickel Company

Although the standard reduction potential of nickel ($-.25 V_{SHE}$) in the electromotive force series is less noble than that of hydrogen, nickel often passivates in many deareated acids and alkalies. This somewhat unexpected behavior is commonly believed to be the result of a film formed at the metal-solution interface. The passive state of nickel was observed by Faraday in 1844 and the concept of a passive film was put forth at this same time; however, the exact composition and nature of the film has still not been conclusively determined despite literally hundreds of papers published on the topic [3,4]. Indeed, without a basic understanding of the nature and composition of the passivating film, it is difficult, if not impossible, to develop a means of perfecting the performance of this film or to invent ways of improving its stability in hostile environments (e.g., chloride solutions).

The reason that an understanding of this passivating film has so long eluded researchers is that to date no technique has been available which can provide data suitable for making conclusive, unambiguous film identification. Perhaps the most common method of film identification uses thermodynamic parameters in an attempt to explain certain features of experimentally obtained polarization curves. However, not only are the thermodynamically calculated equilibrium potentials for the various nickel oxides and hydroxides questionable [5,6], but also an objection must be raised on the basis that, although a given film may at a certain potential be thermodynamically possible, it may not form in sufficient quantities for detection because of kinetic limitations. In addition, it must be recognized that a considerable overpotential may be required for the formation of those films that are not thermodynamically

prohibited. The combination of the debatable equilibrium potential along with unknown required overpotentials makes film identification using this technique rather tenuous.

A second method that has become increasingly popular with the advent of surface sensitive analytical techniques is identification of the corrosion film ex situ. After potentiostatically inducing passivation in a suitable solution, the metal sample is removed and then inserted into a vacuum chamber. One of several techniques (e.g., Electron Spectroscopy for Chemical Analysis (ESCA), Auger Electron Spectroscopy (AES)) can then be used to unambiguously determine film composition. However, upon removing the sample from solution and the subsequent rinsing, drying and exposure to high vacuum, it cannot reasonably be assumed that the film composition and/or thickness has not changed. This uncertainty must be reflected in the conclusions drawn from these data.

One in situ technique capable of providing corrosion data has been used with increasing frequency over the past 25 years--ellipsometry. The basis for ellipsometric studies is the influence that various corrosion films have on the relative phase retardation and relative amplitude diminution of incident elliptically polarized light. Although automated ellipsometers have simplified data collection, interpretation of these data is by no means straightforward [7]. Often simplifying assumptions are necessary in order to facilitate interpretation of these data (e.g., assuming a smooth substrate), but the nature of these assumptions renders many of the subsequent conclusions suspect.

A second in situ technique developed more recently is the A-C impedance method. This method yields the value of the polarization

resistance which can be useful in determining corrosion mechanisms and in corrosion rate monitoring [8]. However, this method is of no value in determining film composition.

Recently a third in situ technique has been developed that allows not only unambiguous film identification but at the same time is capable of continuously monitoring corrosion film thickness. This technique is based on the Differential Reflectometer (DR), which employs a monochromatic light beam that is alternately reflected (at 60 Hz) from two adjacent samples in solution, one corroding, one not corroding (the standard). The intensity of the reflected light from each sample is measured using a photomultiplier tube and this signal is subsequently electronically processed to yield a plot of $\Delta R/\bar{R}$ as a function of incident light wavelength, where ΔR is the difference in reflectivity between the two samples and \bar{R} is the average of the reflectivity of two samples. The monochromatic light is scanned from 200 nm to 800 nm in about two minutes. Because of the differential nature of this technique, the spectral response of both the cell window and the electrolyte cancel. The operation of the DR has been discussed in detail elsewhere [9,10].

Since each type of corrosion film has a unique band structure, the spectral response of each film is different which is evidenced in the reflectograms by a single peak or more often by a series of peaks. From the magnitude of a given peak the film thickness can often be determined.

Although the DR has an unequalled capacity for in situ film characterization, the limitations of this technique should also be considered. First, in order to be able to correlate a given set of

peaks in a reflectogram with a specific film composition, an independent method of film identification must be used. Second, an independent method must also be used to initially correlate a given peak height with the film thickness. Third, it is necessary to maintain one sample in solution at a standard reflectivity during the course of the experiment; i.e. one sample must remain uncorroded while the second sample is growing the corrosion film(s). These limitations are not nearly as ominous as they might seem at first and the methods of dealing with them are discussed in detail in the Experimental Procedure section.

The object of the present research is to obtain a general understanding of the anodic behavior of nickel in aqueous solution through corrosion film identification. Of particular interest are the processes and mechanisms that induce and destroy passive behavior. It is also of interest to establish an experimental basis for further research concerning the role of copper in the passivation of nickel and the role of chloride ions in the breakdown of this passive state.

CHAPTER 2 LITERATURE REVIEW

The Corrosion Behavior of Pure Nickel

Almost all corrosion studies directed at explaining the behavior of nickel in aqueous solutions employ electrochemical techniques in conjunction with independent analytical techniques such as ellipsometry, impedance measurements, ESCA, etc. Some studies draw only on a comparison of electrochemical behavior with thermodynamically predicted reaction values in an attempt to determine the processes that occur at the electrode-solution interface. However, some authors claim to have identified the complete reaction scheme at the electrode interface, including film compositions, using only electrochemical data.

In one such paper [11], MacDougall and Cohen anodize Ni in .15 N H_2SO_4 (pH = 2.8) for short times--typically 90 seconds, and then monitor the galvanostatic reduction of the surface films. Two arrests appear on the reduction curve. The major arrest is attributed to NiO reduction and the surface activity is recovered during this arrest. The rate of recovery slows down after completion of this arrest leading the authors to conclude that two different oxide species are present. Referencing the behavior of Ni in vacuum, they conclude that oxygen chemisorbs onto the surface as the first step in passivation. This chemisorbed monolayer converts to $\text{NiO}_{\text{adsorbed}}$ and finally to NiO. The second arrest, then, is due to the reduction of some unconverted, chemisorbed oxygen. However, an arrest on a galvanostatic reduction curve merely indicates that a charge consuming reaction is occurring at the surface.

The development of a detailed, mechanistic theory from such data alone seems unjustified.

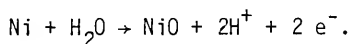
A second study [12] based solely on the electrochemical data was performed by Vilche and Arvia in 1N NiSO_4 + .05N H_2SO_4 , solution (pH = 1.75). Again, based on polarization curves alone, they conclude that three films form on the surface. The first film, Ni(OH)_2 , is a pre-passive film and is formed through the NiOH^+ intermediate. The second film, NiO , is formed by Ni(OH)_2 dehydration while the final and truly passivating film, Ni_2O_3 , forms from Ni(OH)_2 via the NiOOH intermediate. Considering the limitations of polarization curves, these conclusions should be viewed with suspicion.

Perhaps the uncertainty involved in interpreting polarization data alone is best exemplified by examination of a paper by MacDougall and Cohen [13] and a second paper by Vilche and Arvia [14]. In the paper by MacDougall and Cohen, a series of polarization curves are obtained for Ni in sodium sulfate solution (pH = 3.0) after cathodic pretreatments at various N_2 bubbling rates. As the bubbling becomes more vigorous or at longer polarization times, the active-passive peak diminishes and a new peak appears and grows at a more cathodic potential. The authors conclude that this is the result of impurities in the solution adsorbing onto the surface and blocking the normal film formation process. In a subsequent paper Vilche and Arvia observed this same type of behavior but as a function of various sweep rates. They conclude that the "adsorption-of-impurity" theory is an inadequate and hasty interpretation and point to the "complexity of kinetic results. . .and the difficulty of deriving from them prompt mechanistic interpretations which are not fully substantiated."

[page 1063] It is interesting to note that this statement was made

by the same authors who used polarization curves alone to defend the argument that Ni(OH)_2 , NiO , Ni_2O_3 , NiOOH and NiOH^+ are all formed on the Ni surface.

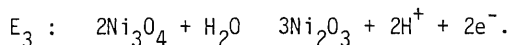
A series of three papers by Okamoto and Sato [15-17] are perhaps the most often referenced studies on the anodic behavior of Ni contained in the corrosion literature. In the first paper of this series the authors observe three distinct arrests on the potential decay curve of Ni in H_2SO_4 ($\text{pH} = 4.5$). The first arrest has a corresponding potential of $E = .103 \text{ V}_{\text{SHE}}$ and compares favorably with the reversible potential for $.081 \text{ V}_{\text{SHE}}$ for the reaction



The second and third arrests occur at $E_2 = .453 \text{ V}_{\text{SHE}}$ and $E_3 = 1.573 \text{ V}_{\text{SHE}}$ and are stated to compare favorably with the thermodynamically expected values for the reactions



and



These values, however, are never actually stated for comparison.

The values found in Pourbaix's Atlas [18] for these reactions are $E_2 = .870 \text{ V}_{\text{SHE}}$ (cf .453) and $E_3 = 1.273 \text{ V}_{\text{SHE}}$ (cf 1.573) which differ significantly from the experimental arrest values. The authors consider the second arrest to correspond to the Flade potential and therefore conclude that the passivation of Ni is the result of a transformation of NiO (prepassive film) to Ni_3O_4 (passive film).

Building on these somewhat questionable conclusions, Sato and Okamoto in the second paper [16] suggest the mechanisms by which the various films are formed. They conclude that both NiO and Ni_3O_4 are formed through NiOH^+ intermediate. This argument would be more persuasive if they had presented evidence for the existence of this species.

In the third and final paper qualitative arguments are given to show that passivation of nickel cannot occur either by a film precipitation mechanism or by a direct oxidation film mechanism. Instead the authors advance a new theory based on their two previous papers, which they call "Higher Valence Oxide Film Theory." This theory states that passivation can only occur via the conversion of a surface intermediate, such as the NiOH^+ complex. Unfortunately, again no analytical evidence for the existence of NiOH^+ was provided. Hence the support for this theory rests solely on the correlation of a potential arrest with an unstated reversible potential.

Cowan and Staehle [19] also attempted to identify surface corrosion films by comparison of thermodynamically calculated reversible potentials with the experimental arrest potentials obtained for Ni in .050 N H_2SO_4 + 0.5 N K_2SO_4 (pH = 1.3) and .001 N H_2SO_4 + .099 N K_2SO_4 (pH = 3.4) solutions. Although the principal concern of their paper was the establishment of high temperature Pourbaix diagrams, they conclude from the single arrest observed in room temperature solutions that the film is Ni_3O_4 since the experimental arrest was consistently within 20 mV of the thermodynamically predicted values.

Using a .15 N Na_2SO_4 solution (pH = 2.8), Mitrovic-Scepanovic and Ives [20] obtained a potential plateau at $-300 \text{ mV}_{\text{SCE}}$ which corresponds well with the thermodynamically predicted reversible potential of -299.4

mV_{SCE} which they quote for the Ni/NiO electrode. Other plateaus were observed in addition to the one at -300 mV_{SCE} but they did not lie close to equilibrium values for any of the Ni/NiO_n or NiO_n/NiO_m electrodes.

Gromoboy and Shreir [21] conclude that up to four Ni oxides are possible for a Ni electrode in a sulfuric acid solution (pH = 1.3) containing various amounts of thiourea. Instead of using potential decay curves, the authors determined the experimental reversible potentials from inflections in the potentiostatic and galvanostatic polarization curves. The four inflections noted all occur within millivolts of the reversible potentials for Ni/NiO, Ni/Ni₃O₄, Ni/Ni₂O₃ and Ni/NiO₂. All four of these inflections were never observed on a single polarization scan but rather on curves obtained in solutions of various thiourea concentrations. Also it could be argued that many more plateaus exist on the galvanostatic curve than were noted and explained by the authors. Although the excellent agreement between inflections on the polarization curve and the various reversible potentials is remarkable, one must wonder what effects the thiourea have on the actual film formation processes and compositions. Unfortunately, no surface analytical data were presented.

The adaptation of ellipsometry to in situ studies represents a major advance in the methods available to the corrosion scientist. Although only one paper was found which reported utilization of the ellipsometer to study the anodic behavior of Ni in acid solutions [22], it is regarded by many as a classic. The basis for the study is the comparison of a polarization curve obtained in .01 N H₂SO₄ + .5 M K₂SO₄ (pH = 3.15) with ellipsometric data obtained concurrently. A correlation is found between the onset of film formation (as evidenced

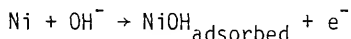
by ellipsometry) and a slight inflection in the polarization curve. It is suggested by the authors that since passivation does not occur immediately that this film must be merely a "precursor film." Then, at the current maximum, the absorption coefficient, κ , begins to increase indicating an increase in film conductivity which becomes roughly equal to that of a semiconductor. From comparison of refractive indices, it is concluded that this passivating film has a composition of $\text{NiO}_{1.5-1.7}$. Based on these data, Bockris and Reddy describe the passivation process as follows: a thick ($> 45 \text{ \AA}$) precursor film (Ni(OH)_2) forms via a precipitation mechanism, this film is subsequently converted to a nonstoichiometric film at the passivation potential. Since the electrical conductivity of this nonstoichiometric film is much higher than that of the precursor, there exists no high field ionic conductivity through this film--hence passivation.

The conversion of an insulating film to an electrically conducting film as the cause of passivation is a unique explanation and capable of explaining passivation behavior. However, several questions must be raised as to the validity of the data upon which this theory is based. First of all, in order to determine film thickness, certain assumptions must be made as to the ranges of values for the refractive index, n , the absorption coefficient, κ , and even the composition of the film. These values are then used in an iterative process that yields various $\Delta\psi$ plots, to which the experimental values must be compared for a "best fit." This process led the authors to conclude that the film thickness was approximately 60 \AA --a value which is much higher than generally reported in the literature [13]. Perhaps one variable that was not considered that could account for such an abnormally high value is the

roughening of the electrode surface during active dissolution. Such roughening has been reported to influence ellipsometric data significantly [7].

Secondly, it is not surprising that a film appears on the electrode prior to passivation. It does not seem necessary that such a film be a precursor that must be converted, but rather the passivation film could form initially on grains more favorably oriented for such a process to occur while less favorably oriented grains are still experiencing active dissolution. In fact, there is evidence that film kinetics are indeed a function of crystal orientation [23,24].

Finally, it is stated that ellipsometry is suitable for detecting even monolayer changes. However, the authors then suggest



as the reaction that leads to the electrode dissolution, but there is no change in ellipsometric response accompanying this proposed reaction. It would therefore seem necessary that more substantial evidence be obtained before giving credence to the ionic-electronic conduction conversion theory.

Although impedance measurements do not result in data that can be directly used for film identification, nevertheless it has become a useful technique for determining important film characteristics. Lovrecek and Lipanovic [25] concluded from a study in 1N H_2SO_4 that the impedance response of the Ni electrode indicates that the surface film cannot be electrically represented as a serial joining of resistive and capacitive components. This indicates that relaxation phenomena must be occurring within the film which suggests that the film is not merely an

insulator or simple semiconductor but, according to the authors, a "quite complex film." However, a complex anodization scheme may be partially responsible for their results. The electrode was initially anodized at +1800 mV_{SCE} (well above the oxygen evolution potential) for 15 minutes and then held at +450 mV_{SCE} for ten days. This unusual experimental procedure makes it difficult to compare their data with that found elsewhere in the literature.

Turner, Thompson and Brook [26] also employed AC impedance techniques to study the Ni electrode but in concentrations of H₂SO₄ varying from .5 - 18.8 M. The impedance data they obtained suggested that the passivation film is thinner in the more highly concentrated solutions. They also determined that Ni dissolves as a divalent ion in the active region while passivation is accomplished by a solid state mechanism. This latter conclusion is in direct contrast with the mechanism proposed by Bockris and Reddy [27].

The use of ex situ film identification procedures has also become increasingly popular in the last ten to fifteen years. MacDougall and Cohen [28] were able to elucidate several mechanisms responsible for the electrochemical behavior of pure Ni. From cathodic decay curves in a solution of pH = 2.8 obtained after various anodic treatments, the authors deduced the following model: oxygen absorbs onto the surface as a monolayer while NiO is concurrently nucleating at "active sites." The NiO eventually spreads to complete coverage but with pores of "non-stoichiometric or noncrystalline" NiO. This pore material subsequently converts to stoichiometric NiO at more anodic potentials which accounts for the small current passed in the passive region. The breakdown of the film on the cathodic cycle occurs by dissolution of the pores and

then "undermining" of the remaining NiO. The authors also conclude, from x-ray spectroscopy, that the anodic film thickness and composition are independent of the anodic polarization potential.

It is somewhat surprising that the cathodic arrests are not interpreted as being the interconversion of higher oxides, as previous authors have suggested, but rather the dissolution of pore material. Although film composition and thickness have been determined using ex situ methods, the mechanistic model itself is based solely on the electrochemical response of the electrode. There is no independent analytical evidence offered to confirm the existence of the chemisorbed oxygen, pores, non-stoichiometric pore material or undermining.

In the third paper concerning the anodic behavior of Ni, MacDougall [29] concludes from galvanostatic charging profiles in conjunction with solution analysis that film growth accounts for but a minor component of the total anodic current. The majority of the current is consumed in the production of the divalent nickel ion in solution. After the passive film has formed, a residual film current persists and the electrode potential increases. Citing the x-ray data which indicate no film thickening, the author concludes that the residual current is being used to repair defects in the passive film which also accounts for the accompanying potential increase.

In yet another paper by MacDougall et al. [30], still more surface analytical techniques are used to study the passive film. In .15 N Na_2SO_4 solution (pH = 2.8), reflection high energy electron diffraction (RHEED) indicates that the film is stoichiometric NiO having a thickness of 9-12 Å, which agrees with the values as determined from both coulometry and $\text{O}_{K-\alpha}$ x-ray spectroscopy. A limiting thickness of 12 Å is noted even after 200 hour anodizations. In the transpassive region, the

film is no longer single crystal epitaxial but rather defective and polycrystalline, as indicated by RHEED. It must be remembered, however, that there was no way the authors could monitor changes that might occur in the film upon removal from solution and placement in vacuum.

In a unique approach, Siejka et al. [31] used a 1 N H_2SO_4 solution enriched with O^{18} to passivate a Ni electrode and then examined the film ex situ with nuclear microanalysis to determine the O^{18} content. They concluded that the first layer of oxygen fixed on the surface causes the anodic current to decrease by two orders of magnitude. After "unit cell thickness" is reached the current is limited by field-assisted ionic transfer. Current efficiency for film growth is low and growth seems to occur at the metal-oxide interface by in-diffusion of oxygen. Upon removal from solution the oxide layers are unstable and reoxidize. Although the authors draw no conclusions as to the composition of the passive film, the fact that the film is formed at the metal-oxide interface excludes precipitation as the passivation mechanism. Also, the evidence indicating that the ex situ film may not be in the same oxidation state as the in situ films confirms that conclusions drawn from ex situ film examinations may not be accurate.

Behavior of Nickel in Neutral Solutions

The behavior of Ni in neutral solutions has also been of considerable interest to a great number of researchers. Sato and Okomoto [15-17] are again responsible for the most often referenced work on this topic. They employed a solution of .5 M Na_2SO_4 + .1 M $(\text{KH}_2\text{PO}_4 + \text{K}_2\text{HPO}_4)$ (pH = 6.6) to obtain potential decay curves for a Ni electrode.

Comparison of the arrest potentials with calculated thermodynamic reversible potentials led the authors to conclude, just as they had in acid solutions, that three films are formed: NiO , Ni_3O_4 and Ni_2O_3 . The experimental arrest values are approximately $-.2$, $+.1$ and $+.1 \text{ V}_{\text{SHE}}$ which do not compare well with calculated values of $-.28$, $+.50$ and $+.91 \text{ V}_{\text{SHE}}$. As in the acid solution, they attribute passivation to the conversion reaction of NiO to Ni_3O_4 .

Cowan and Staehle [19] concluded that the passive film formed on Ni in $.1 \text{ N K}_2\text{SO}_4$ ($\text{pH} = 6.3$) is NiO . Their conclusion is also based on comparison of an experimentally obtained arrest potential ($-.204 \text{ V}_{\text{SHE}}$) with a calculated redox potential ($-.254 \text{ V}_{\text{SHE}}$). These values compare only slightly more favorably than those of Okomoto and Sato. However, in contrast to Okomoto and Sato, Cowan and Staehle do not observe any arrests at more anodic potentials.

Okuyama and Haruyama [32], using a boric acid-borate buffer solution ($\text{pH} = 8.39$), claimed to identify no less than three surface oxide films formed on a Ni electrode. By comparing plateaus on both anodic and cathodic charging curves with calculated redox potentials, the authors concluded that at low potentials NiO forms while at intermediate potentials Ni_3O_4 is formed. Both films are formed via a direct oxidation mechanism. At higher potentials Ni_3O_4 transforms completely to NiO_2 , which prohibits further divalent ion dissolution, i.e., this conversion reaction is responsible for Ni passivation.

Ord et al. [33] studied the passive behavior of Ni in $.15 \text{ N Na}_2\text{SO}_4$ solution ($\text{pH} = 6.1 - 9.1$) using ellipsometry. They reach the conclusion that NiO is the initial film formed on an anodic potential sweep but that this film converts to Ni(OH)_2 and eventually to NiOOH as the

potential progresses to more anodic values. Also concluded is that the film thickness is a direct function of electrode potential (contrary to the finding of MacDougall and Cohen in ref. 34) and that film growth is limited by the electric field within the film. The authors did not complement these data with electrochemical measurements; they are therefore unable to determine which film is responsible for passivation. Also not discussed is the effect that surface roughening may have on their results.

In a series of papers MacDougall et al. [27,30,34-37] arrive at several conclusions regarding the anodic oxidation of Ni in both sulfate and borate buffer solutions. The authors state that the film formed in .15 N Na_2SO_4 (pH = 8.4) solution at potentials cathodic to the oxygen evolution potential is NiO (determined by AES) having a maximum thickness of 12 Å. This film was said to be identical to the film they found in acid solutions. In borate buffer solutions the film is again determined by AES and RHEED to be NiO. At potentials anodic to the oxygen evolution potential, this film becomes polycrystalline and highly defective. However, at potentials anodic to oxygen evolution, a duplex film is found to be somewhat thicker--about 16 Å.

MacDougall et al. offer the following mechanism to explain the film formation process in the borate buffer solution. Initially, the clean Ni surface is oxidized to produce a passivating film of NiO. This film is formed by a direct oxidation mechanism rather than by precipitation. The NiO then begins to break down at defects with subsequent metal dissolution. The divalent Ni ions that result from this dissolution are oxidized at the oxygen evolution potential and precipitate out of solution as a NiOOH film. The NiOOH film converts to $\text{Ni}(\text{OH})_2$ upon

cathodic polarization. No experimental evidence is provided to confirm the existence of the $\text{Ni}(\text{OH})_2$. These authors propose that NiO cannot be converted to higher oxides--an assumption that ultimately necessitates the adoption of a comparatively complex reaction scheme, rather than the simple conversion process suggested by others [15,22].

In a clever attempt to characterize the passive film on Ni in neutral solution, Wilhelm and Hackerman [38] measured its photoelectrochemical response. Because the absorption edge of the film (3.7 eV) is the same as the known band gap of NiO (3.7 eV) the authors conclude that the passive film is indeed NiO . From integration of the anodic charging profiles it was also concluded that this passivating film is 10 \AA thick. No higher oxides were detected by this technique.

The Behavior of Ni in Alkali Solutions

Sato and Okamoto [15] note three arrests on a potential decay curve for a Ni electrode in $.05 \text{ M Na}_2\text{SO}_4 + .01 \text{ NaOH}$ solution ($\text{pH} = 11.7$). As in the acid and neutral solutions, the authors conclude that these arrests are due to the formation of NiO , Ni_3O_4 , and Ni_2O_3 . Unfortunately, the agreement between the experimental and calculated potentials for these films is not convincing. In fact, a potential arrest is not reported for the Ni/NiO reaction but nevertheless the authors state that this reaction still occurs.

Davies and Barker [39] examined the behavior of Ni in $.1 \text{ N NaOH}$ solution ($\text{pH} = 13$). By comparing the galvanostatic charging plateaus with thermodynamic redox potentials, the authors conclude that $\text{Ni}(\text{OH})_2$ is formed. The $\text{Ni}(\text{OH})_2$ is subsequently converted to Ni_2O_3 and finally partial conversion of the Ni_2O_3 to NiO_2 results in a final composition

of $\text{NiO}_{1.8}$. Based on current measurements, the Ni(OH) is determined to be one monolayer in thickness while the Ni_2O_3 has a three monolayer thickness. However, it is not considered that a component of the current must be attributed to metal dissolution prior to passivation. The final composition of $\text{NiO}_{1.8}$ is determined by coulometry based on the assumption that all current passed is used in the conversion of Ni_2O_3 to NiO_2 --the possibility of new film growth is not discussed.

Using only a potentiodynamic polarization curve, Schrebler-Guzman et al. [40] attempt to explain the behavior of Ni in .2 N KOH solution. They note two peaks on this curve. The first peak (the common passivation peak) is attributed to the formation of Ni(OH)_2 through a complex adsorption process. The second peak occurs just prior to oxygen evolution and results from the conversion of Ni(OH)_2 to $\beta\text{-NiOOH}$. The compositions of these films are assumed without explanation.

T. S. Lee [41] used polarization curves as the basis for the construction of an experimental $\text{Ni-H}_2\text{O}$ Pourbaix diagram. Agreement between the experimentally determined and equilibrium (calculated) diagrams is not generally obtained. The only good correspondence between the kinetic studies of Lee and the original calculated diagram of Pourbaix is between the zero current potential and the predicted Ni/Ni(OH)_2 equilibrium potential. There exists an obvious discrepancy between the actual passivation potential and that predicted from thermodynamic considerations. Also, the region of general corrosion is found restricted to much lower values of pH and somewhat higher potentials than predicted by Pourbaix. Lee was not successful in identifying the films using x-ray techniques.

Hopper and Ord [42] used ellipsometry in an attempt to characterize the film in 5 N KOH solution. They conclude that the film is β -NiOOH and is formed by a direct oxidation mechanism. The authors state candidly that unambiguous interpretation of ellipsometry data, including their own, is generally impossible.

Ellipsometry was also the basis for a study by Lu and Srinivasan [43] concerning the behavior of a Ni electrode in 1 N KOH electrolyte. They concluded that a 190 Å film of β -NiOOH is formed upon anodization above the oxygen evolution potential. The authors note, however, that it was necessary to lower the electrode potential below the oxygen evolution potential in order to obtain their data. Therefore, if a reversible conversion process is occurring at or near this potential it may not be detectable because of this procedure.

The Transpassive Behavior of Nickel

At potentials anodic to the passive region, the protective film on Ni often breaks down. This phenomenon is referred to as transpassivation and usually occurs concurrently with oxygen evolution. Although there is not general agreement as to the composition and formation mechanisms of the passivation film, several studies have been conducted in an attempt to understand the processes leading to the demise of this film in the transpassive region.

Expanding upon an earlier paper, MacDougall and Cohen [44] discuss the results of a cathodic charging profile for a Ni electrode in .15 N Na_2SO_4 solution (pH = 2.8). After the potential has decayed through two plateaus, a potential spike in the cathodic direction is observed. Noting that the surface activity of the electrode increases from less

than 2% before the spike to 10% afterwards and that scanning electron micrographs indicate the onset of pitting at this same potential, the authors conclude that the spike results from localized breakdown of highly defective sites within a NiO film. Once the breakdown has occurred the dissolution of the Ni substrate proceeds, leading to the undermining and eventual spalling of the remaining NiO layer. The authors preference for this undermining and spalling scenario as opposed to simple film thinning via dissolution and/or conversion is based on the behavior of two electrodes upon different cathodic treatments. Both samples were anodized under identical conditions. The first sample underwent a 20-minute galvanostatic cathodic charging ($20 \mu\text{A cm}^2$) treatment immediately after anodization while the second sample received this same cathodic treatment but only after it had decayed on open circuit up to the point of the spike (ca. 30 min.). Since the final recovered surface activities of the two electrodes differ by only 10%, the authors conclude that the film thicknesses are identical, i.e., no thinning of the film occurs on open circuit. An alternate explanation may be that the processes that occur during the relatively severe cathodic treatment predominate over those processes that may occur during the relatively gentle open circuit treatment. No interpretation is given by MacDougall and Cohen regarding the two potential plateaus also present on the reduction curve.

From optical and electron microscopy studies on Ni electrodes in sodium nitrate solutions, Datta and Landolt [45] also conclude that transpassive behavior is attributable to localized breakdown of the passive film. The breakdown is initiated at defects within the film (e.g., grain boundaries and dislocations) resulting in a pit-like

appearance in the early stages of the process. Once local breakdown is achieved the pit-like perforations expand allowing high rates of metal dissolution. This overall process yields a severely etched metal surface. The authors also conclude that dissolution occurs much more rapidly at higher current densities and is a function of grain orientations, and the process is virtually pH independent. Nickel 200 was used as the working electrode in these experiments. The authors do not discuss the possible impurity effects on film breakdown.

In a subsequent study Landolt [46] employed AES to analyze the film at various stages of transpassive breakdown. As in the case of iron and chromium, the apparent anodic film thickness reaches a maximum at the beginning of the transpassive region. The film thickness then decreases as the potential progresses to more anodic values. Nitrogen is detected within the transpassive film and its abundance is found to be a direct function of increasing potential. The nitrogen is always found in its highest concentrations at the metal-film interface. It is speculated by the author that the nitrates diffuse through the film via micropores or other defects and adsorb onto the metal surface. This process occurs to a greater extent at higher potentials and eventually leads to the destruction of the passive state. Neither thinning nor how the adsorbed nitrates destroy the film is discussed.

Sato [47] presents an energetics approach to study transpassive film behavior. This model is based on the formation of a cylindrical pore of radius r . The work required to form such a breakthrough pore in a passive film has two components as represented in the equation

$$A_b = \{2\pi r h \sigma + \pi r^2 (\sigma_m - \sigma)\} - .5\pi r^2 C_d \Delta E^2 \quad (1)$$

where A = pore formation energy

h = film thickness

σ = surface tension of the film-electrolyte interface

σ_m = surface tension of the metal-electrolyte interface

C_d = difference in capacitance between the passivated metal and metal with a porous film

ΔE = electrical potential difference between the metal and electrolyte.

The first term on the right side of the equation represents the variation in capillary energy which is dependent on surface tension while the second term represents the variation of electrical energy due to the potential field across the film. From equation (1) the author derives

$$\Delta E_b = \frac{\sigma_m - \sigma}{.5 C_d} \quad (2)$$

where ΔE_b is the lowest possible film breakdown potential. Based on an analysis of this model Sato arrives at two major conclusions. First, it is suggested that a potential range exists between the film formation potential (i.e., passivation potential) and the lowest possible breakdown potential (ΔE_b) where the film is stable against electrocapillarity breakdown. Secondly, from the viewpoint of film dissolution kinetics, this model predicts that a critical potential exists above which the passive film is electrochemically unstable (i.e., the transpassive potential). However, actual values are never determined for ΔE_b so that a comparison can be made directly with experimental values.

The Effect of Chloride Ions on the Passive Behavior of Nickel

As just discussed, if the electrode potential is made too anodic passive behavior can be lost resulting in extremely high rates of metal dissolution. Passivity can also be destroyed by the addition of aggressive anions to the electrolyte, most notably Cl^- ions. This loss of passivity can occur even though the electrode potential is well within the normal passive range. Just as there is much confusion regarding the nature of the passive film itself, there is again considerable disagreement regarding the processes leading to chloride-induced film instability.

T. S. Lee [41] reported that the presence of Cl^- ions in solution produces an enlargement of the corrosion region to higher pH values and more active potentials. The effect of the Cl^- is also manifested by continued corrosion at quite noble potentials due to the absence of a passivating film. Lee was not able, however, to identify the mechanism by which the Cl^- ions alter the corrosion process.

Kronenberg et al. [48] studied the behavior of a 99% pure Ni wire in 1 N NaClO_4 , 1 N NiSO_4 and 1 KCl solutions. From the Tafel slopes of the experimental polarization curves the authors conclude that Cl^- ions adsorb onto the surface and enhance the transfer of Ni from the metallic state to an adsorbed state from which dissolution occurs more readily. No further justification is given for this theory.

Based on stationary potentiostatic methods, potentiodynamic single sweeps and triangular cyclic voltammetry, Vilche and Arvia [49] also conclude that Cl^- ions adsorb onto the surface at low potentials within the active dissolution range. Then, at more anodic potentials within the active range, the surface becomes saturated with Cl^- ions resulting

in the formation of a layer of NiCl_2 . No analytical confirmation of such a NiCl_2 layer is provided, however.

Zamin and Ives [50] obtained polarization curves for a Ni electrode in 1 N H_2SO_4 solution containing various amounts of 1 N NaCl. They discovered that as the Cl^- ion concentration increased the passive region on the polarization curve decreased and that in solutions with a high enough Cl^- ion concentration passivity was altogether unobtainable. From accompanying metallographic observations, it was further shown that in solutions of low Cl^- ion concentration the passive film breakdown is initiated at the grain boundaries. However, at moderate concentrations the attack is no longer localized at grain boundaries but rather occurs in the interior of the grains as well. The authors conclude that passivity is governed by two competing processes. The process of film formation which occurs unhindered in Cl^- free environments is opposed by film breakdown when Cl^- ions are present. In low concentrations film formation is the predominant process and passivation proceeds, while at higher Cl^- ion concentrations film breakdown occurs rapidly and passivity is precarious. Once a critical Cl^- ion concentration is reached film breakdown occurs more easily than film formation at all potentials and, as Lee [41] found, passivity is unobtainable. Although this analysis is coherent and agrees well with their experimental data, a mechanistic explanation is still lacking.

In a subsequent paper, Zamin and Ives [51] again utilize polarization data along with microscopy studies to conclude that the variation in grain size, amount of cold work and annealing atmosphere have no effect on the critical pitting potential of a Ni electrode. However, they did find that pitting occurs only along grain boundaries

in small grain samples while in larger grain size electrodes pitting occurs both at the grain boundary and interior of the grain. It also seems that pit nucleation occurs during active dissolution before passivation and that these sites are merely reactivated when the potential of the electrode becomes more anodic than the critical potential.

Based on the Tafel behavior of a Ni electrode, Bengali and Nobe [52] concluded that the kinetics and mechanism of anodic dissolution are strongly dependent on the concentration of both the H^+ and Cl^- ions. At low concentrations of these ions the dissolution proceeds via an adsorbed $NiClOH^-$ complex while at higher concentrations dissolution is dependent on the formation of a $NiClH^+$ intermediate. Again, no analytical evidence is provided to substantiate the existence of these intermediates. Rather, the assumed existence of these species is predicated solely upon analogy to the iron-chloride system.

Contrary to the papers just discussed, MacDougall [53] concludes that Cl^- ions have no effect on the dissolution mechanisms of Ni. This is based on the observation that polarization curves are identical in the active region of Ni electrodes in .15 N Na_2SO_4 solutions ($pH = 2.8$) with and without Cl^- additions. However, the passivation current and total dissolution current are several times greater in the Cl^- containing solution which suggests that the role of the Cl^- is to hinder passive film formation. The author speculates that there is a competition between adsorption of Cl^- ions and the oxygen containing species necessary for passive film formation.

Also, in solutions containing Cl^- ions, transpassive behavior is initiated at substantially lower potentials. MacDougall explains this

by postulating that a dynamic equilibrium exists in the passive state between film breakdown at defects and subsequent film repair. The role of the Cl^- ion then is not to accelerate breakdown but rather to physically interfere with film repair. This idea is consistent with the already mentioned fact that passivation occurs at much greater current densities while at only slightly higher potentials.

In a second series of experiments described in this same paper, Ni electrodes were passivated in solutions with and without Cl^- ions and the subsequent open circuit behavior observed in solutions containing Cl^- ions. It was found that breakdown occurs much more rapidly for those films grown in the Cl^- containing solutions. This suggests that the presence of Cl^- ions in the formation solution substantially decreases the stability of the passivating oxide. This decreased stability is attributed by MacDougall to a more highly defective film structure rather than by direct incorporation into the film. X-ray emission spectroscopy indicates that the Cl^- ions in solution affected neither film thickness (still 9-12 Å) nor film composition (still NiO). No Cl^- ions were detected in the film but as MacDougall points out the detection limit for Cl^- is about 10%.

Sato [47] expands the energetics approach of transpassivity described in detail above to also explain the effects of Cl^- ions on the loss of passivity. He suggests that the adsorption of anions, in particular Cl^- , introduces new electron acceptance levels into the band structure of the passive oxide film which tends to lower the transpassive potential. Thus, the dissolution rate is faster at the anion adsorption sites.

Although there is no general agreement regarding the mechanism, all authors do at least agree that the presence of Cl^- ions in solution has a deleterious effect on the passivation process.

The Corrosion Behavior of Pure Copper

The nature of the protective film that forms on copper is much better understood than the film on nickel. It appears that only three films form on a Cu electrode and each is formed in a fairly well defined potential-pH regime.

In dilute acid solutions Cu dissolves to yield soluble salts and does not develop a protective passive film [54]. However, in strongly concentrated acid solutions, Leckie [55] has shown that a passive film does indeed form. In 10 M H_2SO_4 solution the passivation potential was observed to be .21 V_{SCE} which agrees quite well with the thermodynamically predicted reversible potential of .23 V_{SCE} for the $\text{Cu}/\text{Cu}_2\text{O}$ reaction.

T. S. Lee [41] employed a potentiokinetic technique to obtain polarization curves which he used in the construction of experimental Pourbaix diagrams. The experimental diagrams turned out to be quite similar to the equilibrium (calculated) Pourbaix diagrams. In addition, it was found that primary passivation occurred at potentials very close to the $\text{Cu}_2\text{O}/\text{CuO}$ transition while secondary passivation occurred near the $\text{Cu}_2\text{O}/\text{Cu}(\text{OH})_2$ boundary.

Perhaps the most complete and coherent work published concerning Cu passivation was offered in a series of four papers by Shoesmith et al. [56-59]. By comparing open circuit potential-time transients with x-ray and electron diffraction data along with SEM micrographs, the authors

were able to make several well substantiated conclusions. First, they were able to determine the potential regions of stability for the various corrosion films for a Cu electrode in 1 M LiOH solution. For electrodes potentiostated between $-.330 \text{ V}_{\text{SCE}}$ and $-.280 \text{ V}_{\text{SCE}}$ the resulting film is pure Cu_2O . A mixed film of Cu_2O and $\text{Cu}(\text{OH})_2$ is formed at potentials from $-.280 \text{ V}_{\text{SCE}}$ to $-.265 \text{ mV}_{\text{SCE}}$ range while mixed $\text{Cu}(\text{OH})_2 + \text{CuO}$ forms up to $-.060 \text{ V}_{\text{SCE}}$. At potentials anodic to $-.060 \text{ V}_{\text{SCE}}$ a pure CuO film results.

Although the authors offer no conclusions concerning the mechanism of Cu_2O formation, they are able to determine the formation process of the intermediate $\text{Cu}(\text{OH})_2$ film. It appears that the initial $\text{Cu}(\text{OH})_2$ film is formed via direct oxidation of the metal surface while subsequent layers of $\text{Cu}(\text{OH})_2$ are the result of precipitation from solution. These conclusions are based on SEM micrographs which show that the initial film formed in the $\text{Cu}(\text{OH})_2$ region has a very smooth appearance. After sequentially longer polarization times, the micrographs indicate that a three dimensional network of crystals nucleates and grows on top of the initial film. Without explanation it is also concluded that the CuO layer formed at somewhat more anodic potentials occurs by the dissolution of the lower oxides(s) and subsequent precipitation of CuO .

Burstein and Newman [60] employ a scratch test in an attempt to understand the nature of the Cu film. After an anodic film developed on a potentiostated Cu electrode, the surface was scratched and the resulting current fluctuation monitored. By comparing current plateau values with the standard reversible potentials the authors were able to "determine" the composition and thickness of the film. The electrode behavior was the same in both neutral and alkaline solutions. It seems

that a monolayer of CuOH is first formed over the scratch while a second monolayer of Cu_2O eventually develops on top of that. It is stated that both monolayers are formed at potentials well cathodic to the $\text{Cu}/\text{Cu}_2\text{O}$ film ultimately responsible for passivation. No external analysis is made either of film composition or thickness and no explanation is offered as to why Cu_2O is formed below its equilibrium potential.

Shanley et al. [61,62] attempted to identify the corrosion product on copper using the DR. Ex situ reflectograms were obtained for a Cu electrode potentiostated in a borate buffer solution ($\text{pH} = 9.2$). When held in the Cu_2O region (as predicated by the Pourbaix diagram), the resultant reflectogram displayed a series of peaks which corresponded quite well with the peak energies predicted by the band structure of Cu_2O . From this correlation the authors made the reasonable assumption that this reflectogram was indeed that of Cu_2O . When the electrode was potentiostated at somewhat more anodic values a second, distinct reflectogram was obtained. Although the band diagram for CuO was not available, the optical constants of CuO were well known. From these constants a theoretical reflectogram was calculated which is practically identical to the experimental curve. Hence the conclusion that this second reflectogram is indicative of CuO . Attempts to verify film composition using x-ray techniques proved inconclusive, presumably due to the lack of sufficient film thickness.

It was also shown in this work that the DR is capable of not only detecting pure oxides but also of indicating when a mixed oxide is present. The reflectogram of a mixed oxide, e.g., Cu_2O and CuO , is merely the superposition of the reflectograms for the pure components.

This is an extremely fortunate circumstance in that it permits the detection and monitoring of the conversion of one oxide into a second oxide. This conversion may conceivably result from either a change in the electrode potential or a change in the electrode environment, e.g., the addition of Cl^- ions or even removal from solution.

Lastly, it was shown that peak height in a reflectogram is a direct function of film thickness. That is, as the corrosion film thickens the peaks on the reflectogram show a corresponding increase in magnitude.

It should be pointed out that all of the reflectograms presented in this work were obtained by covering one-half of the electrode face with collodion. This was necessary in order to maintain half of the sample at a constant reflectivity. Although experiments showed that the collodion itself has no spectral response within the wavelength range tested by the DR, its use nevertheless provides an undesirable variable in the interpretation of the reflectograms. This is particularly true for those reflectograms obtained after long polarization times when the collodion is no longer as protective. Also it should be recognized that although the in situ reflectograms for a specific oxide display the same general characteristics (e.g., peak positions) as do the ex situ reflectograms, the in situ curves invariably exhibit a noticable "noise" component. This, presumably, is also a direct result of the collodion which is usually stripped before an ex situ curve is executed.

The Corrosion Behavior of Nickel-Copper Alloys

The most widely used family of Ni-Cu alloys are the Monels. Since their introduction over half a century ago, the Monels have become widely used in heat exchanger tubing and general marine environments.

However, in spite of this prevalence there has been a conspicuous lack of basic research regarding Monel and particularly the parent Ni-Cu binary system. As a result little is actually known about the passivation process involved that makes these alloys so valuable. In addition, there is no general agreement regarding the ideal composition for optimum corrosion performance in many environments. In contrast to pure Ni, the basic research that has been conducted on the corrosion properties of the Ni-Cu system, although lacking in scope, is coherent and on many aspects there is even general agreement.

From his work on experimental Pourbaix diagrams, T. S. Lee [41] concluded that the binary alloy shifted from copper-like to nickel-like behavior in the 20-45% nickel range. Lee also pointed out that the Ni-80 Cu alloy had a zero current line near the Ni/Ni(OH)_2 equilibrium potential and that primary passivation occurred at nearly the same potential as for pure Ni while secondary passivation coincided with the passivation potential of pure copper. This of course suggests that primary passivation is attributable of the nickel component while copper oxide is responsible for any secondary passivation processes. However, the author's attempts at independent verification of film composition using x-ray diffraction techniques were unsuccessful because of the thinness of the films.

Mansfield and Uhlig [63] studied polarization curves for various Ni-Cu alloys in 1 N H_2SO_4 . They found that primary passive behavior is exhibited only by those combinations containing greater than 38% Ni which is in agreement with the findings of Lee. It was noted that as the nickel content is increased above this 38% threshold that primary passive behavior becomes more pronounced. The authors reason that since

the d-band is unfilled in the 38% Ni alloy, these compositions can more readily chemisorb oxygen which is in turn responsible for passivation. Although it is conceded that metal ions may also be present in the chemisorbed oxygen layer, it is concluded that they do not exist in stoichiometric proportions.

Mansfield and Uhlig also observed secondary passivation. However, it was shown that this behavior is independent of the Ni content and, like primary passivation, is the result of a chemisorbed film. Although both films are considered to be nonstoichiometric, the authors state that upon cathodic polarization the secondary film converts into the primary film which in turn decomposes at the Flade potential.

It was again found that passive behavior is lost in alloys containing more than 70% Cu by Osterwald and Uhlig [64]. By comparing the Flade potential with thermodynamic values, the authors reached the conclusion that passivation is attributable to a stoichiometric NiO surface film. The Flade potential is noted to increase to more noble potentials as the copper content of the alloy increases. This is explained in terms of the affinity for oxygen adsorption onto the surface decreasing as the result of the higher Cu content. Finally, at about 70% Cu, the stay time of the adsorbed oxygen is so short that it is unable to convert into a protective oxide and metal dissolution proceeds.

Due to the considerable cost of Cu and especially Ni, it has been desirable to maintain or even increase the corrosion resistance of this binary alloy through small third element additions. As noted by Lee [41], the corrosion characteristics of a Ni-30 Cu alloy can actually be

enhanced by small (.9 w/o) additions of iron. Advantage of this fortuitous improvement was taken in the development of Monels.

Kiyoshige and Yamane [65], however, reported that minor additions (ca. 2%) of Mn, Cr and Fe had very little effect on the anodic or cathodic polarization behavior of a Ni-30 Cu base alloy. On the other hand, it was found that a homogenization heat treatment resulted in a remarkable reduction in the corrosion current for all compositions. This effect is presumably the result of the elimination of coring which would essentially set up microscopic "galvanic" couples within the non-homogenized metal sample.

Several attempts have been made to identify the corrosion film present on Monel samples. However, without exception, these experiments are performed in a specialized solution or at high temperatures which makes the data difficult to relate to the basic corrosion processes. Hettiarachichi and Hoar [66] reported the formation of a uniform "brownish gray" film on a Monel 400 electrode potentiostated in the passive region. The electrolyte used was a chloride/bicarbonate solution (pH = 8.3). Microscopic examination revealed that the film was actually quite porous. No attempt was made to identify the composition of the film.

McIntyre et al. [67] examined the film formed at open circuit on a Monel 400 alloy in LiOH solution at 285°C. Using XPS it was determined that at a pH of ~ 10 the film was predominantly $\text{Ni}(\text{OH})_2$. At a somewhat higher pH (14), NiO was observed as the predominant film. Upon sputtering the outer oxide layers, it was determined that a copper oxide (valence not given) exists under the nickel oxide (hydroxide).

Ugiansky and Ellinger [68] studied a welded Monel screen that failed while in service in a well pipe. Electron microprobe analysis indicated that a copper-rich phase was present at the grain boundary which led the author to suggest corrosion via a dealloying mechanism. But as already pointed out by Kiyoshigea and Yamane [65], the heat treatment can produce profound effects on the corrosion behavior of Monel. Thus, an equally acceptable explanation is that the copper-rich phase near the grain boundaries is the result of coring subsequent to welding rather than dealloying or a solid state diffusion process.

Summary

As the result of extensive research, it has been "conclusively" determined that the passivating film that forms on a nickel electrode in acid solutions is $\text{Ni}(\text{OH})_2$, NiO , NiOOH , Ni_3O_4 , Ni_2O_3 , NiO_2 , $\text{NiO}_{1.5-1.7}$ or chemisorbed oxygen, which forms via the NiO_{ads} , NiOH^+ or NiOOH intermediates. Also, decisively shown is that the film is formed by the precipitation and/or direct oxidation mechanisms and has a thickness ranging from one monolayer to upwards of 90 \AA .

About 60% of the literature dealing with the passivation of nickel in neutral solutions states that NiO is the passivating film. However, other studies have suggested that NiOOH , Ni_3O_4 , NiO_2 or the interconversion of these compounds may be responsible.

Regarding Ni in alkaline electrolytes, most researchers have concluded that $\text{Ni}(\text{OH})_2$ causes passivity, but still others have attributed the phenomenon to the formation of Ni_3O_4 , Ni_2O_3 or NiOOH . So it seems clear that in spite of the numerous research efforts, the mechanism of nickel passivity is still a topic of much controversy.

In light of this controversy, it is somewhat surprising that the few papers dealing with transpassive behavior seem to agree on the general mechanism of film breakdown. Although no specific mechanisms are generally mentioned, it is believed that breakdown occurs via localized defects within the film. There is further agreement that Cl^- ions in solution are able to accelerate this process. Although the specific role of the Cl^- ions is still unclear, it is believed that they in some way cause a higher defect density within a passive film.

The behavior of copper in solution has been well documented with some degree of accord. Only three films have been observed to form anodically, CuOH , Cu_2O and CuO .

When copper is alloyed with nickel, the alloy behaves as pure copper if the copper content is greater than about 70%. If the copper content is lower than this threshold value, the alloy behavior is better approximated by the behavior of pure nickel. Small additions of iron are found to improve the corrosion performance of pure Ni-Cu alloys but detailed mechanisms have not been postulated.

In light of the controversy concerning the passivation of pure Ni and the absence of basic research regarding the behavior of Ni-Cu alloys, a concerted effort has been made in the present study to clarify many of these points. Specifically, traditional polarization techniques have been combined not only with dependable ex situ surface analytical techniques (ESCA, AES) but also with Differential Reflectometry utilizing a unique sample design which allows direct comparison of in situ and ex situ results. This combination of techniques results not only in positive in situ film identification but also provides much

valuable information which can be used to deduce much about the actual mechanisms of film formation.

CHAPTER 3 EXPERIMENTAL PROCEDURE

Sample Preparation

As discussed in the Introduction, the DR measures the normalized difference in reflectivity between two adjacent samples. For instance, in order to obtain a reflectogram indicative of a specific corrosion film it is necessary to compare a film free substrate to a second identical substrate that has this surface film. Thus it is clear that a special sample design is required to facilitate in situ reflectivity measurements.

The electrode design that was adopted to achieve this situation in situ is presented schematically in Figure 1. This electrode configuration is hereafter referred to as a split insulated disk or SID electrode. The "halves" of each SID electrode are identical in composition, e.g., pure Ni. However, when in solution, one electrode is cathodically protected, insuring no film growth while the adjacent sample is held at an anodic potential which may induce a corrosion film. In this manner an in situ reflectogram can be obtained for the given corrosion film.

Specifically, each SID is prepared by obtaining two small (typically 1 cm x .5 cm), flat pieces of a metal or alloy which is generally achieved by halving a single piece of the metal or alloy to be used with a diamond saw. Afterwards, an insulated wire (typically 18 gauge, copper multi-strand) is soldered to the back of each of the halves. The two halves are then electrically insulated from one

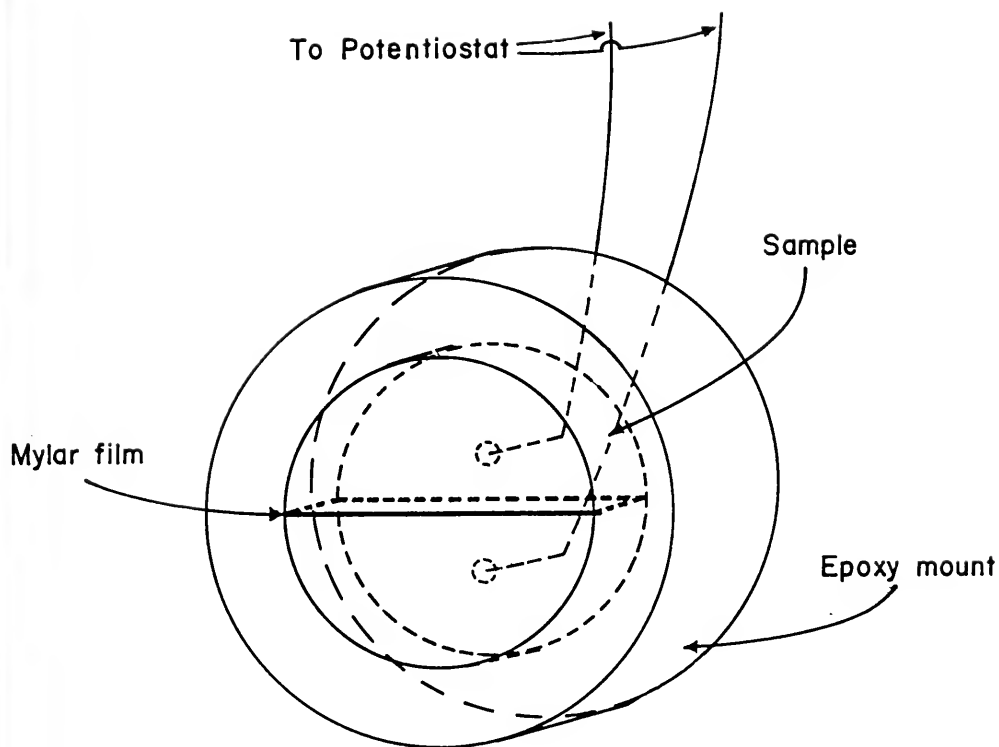


Figure 1. The Split Insulated Disk (SID) electrode used for in situ optical measurements.

another by a thin (1 mil) sheet of Mylar* film after which the whole assembly is set in Quickmount,** a self-setting acrylic epoxy.

Both the Ni and Cu used in the present work were obtained from McKay Corp., New York. The Ni is 99.95% pure while the Cu has a purity of 99.999%. The Ni-30 wt.% Cu alloy was produced by arc melting, in a gettered He atmosphere, the appropriate amounts of the Ni and Cu just described. The arc melting process was performed three times in all to ensure thorough mixing of the two components. The resulting button was then homogenized at 1000°C for three days in a He atmosphere.

After mounting, each SID was ground with a series of 240, 320, 400 and 600 grit SiC papers. Microcut*** paper was then used to further smooth the metal surface and, more importantly, remove any embedded SiC particles. After a satisfactory surface finish was obtained, the SID was polished with 6 μm and finally 1 μm diamond paste on Microcloth*** lubricated with Metadi*** fluid. The sample was subsequently washed in a soap solution, thoroughly rinsed in distilled water and finally dried in a gentle stream of dry air. All SID electrodes were inserted into the electrolyte within five minutes after polishing.

* Trademark of DuPont

** Trademark of Fulton Metallurgical Products, Inc.

*** Trademarks of Buehler, Ltd.

Solution Preparation

All solutions used were prepared from triply distilled, deionized water. Resistivity was typically greater than 10^6 ohms/cm. The electrolyte used in all experiments was 0.15 N Na_2SO_4 . The Cl^- solutions were produced by the addition of 5.84 g of NaCl to one liter of the sulfate solution producing 0.1 N concentration of the Cl^- ion. Reagent grade Na_2SO_4 and NaCl were used in all cases. The solution pH was adjusted by adding either 0.1 N NaOH or 0.3 N H_2SO_4 while deaeration of the solution was accomplished by purging for 18 hours with purified N_2 . The solutions not deaerated were simply left open to the atmosphere during the course of the experiments and are referred to in the remainder of this work as "open solutions."

The Corrosion Cell

The cell employed in these experiments was the same in situ cell used by Shanely et al. [61] and is shown in Figure 2. As will be discussed in the Results and Discussion, the quartz window is not transparent at wavelengths less than 220 nm. In order to expand the range over which data could be collected, the quartz was replaced by a Spectrosil window which is transparent to wavelengths down to about 180 nm. It was found, however, that the effects of the electrolyte must also be considered since, like quartz, it absorbs light of wavelengths shorter than 220 nm.

The counterelectrode was a one-inch square of platinum screen while a saturated calomel electrode was used as a reference. All potentials quoted are referred to this scale.

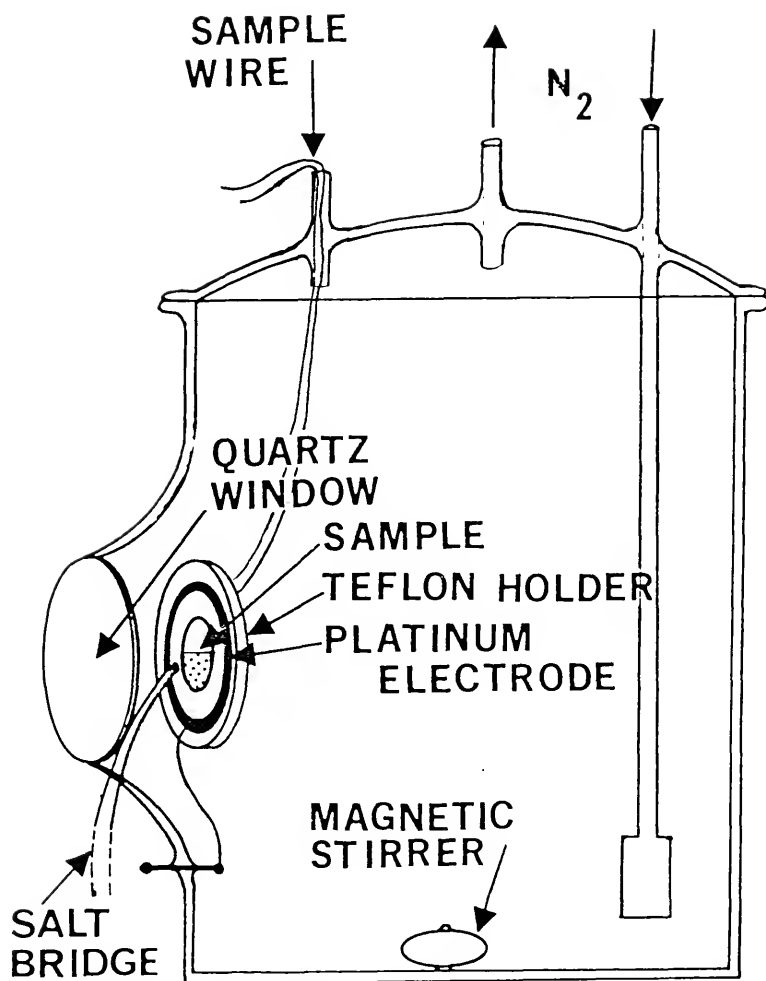


Figure 2. In situ corrosion cell [61].

Polarization Techniques

After final polishing and drying the SID electrode was placed, under potential control, into the electrolyte. The potential upon immersion in each case was approximately 50 mV anodic to the reversible hydrogen potential (i.e., -450 mV at pH = 4.0; -600 mV at pH = 8.0; -900 mV at pH = 12.0). Such a potential was found sufficiently cathodic to prohibit film formation prior to the start of the experiment while not being so cathodic as to induce H_2 evolution which severely alters the reflectivity of the electrodes.

The top electrode in the SID configuration was maintained at this initial cathodic potential throughout the experiments. The potential of the lower electrode on the other hand was increased by 50 mV increments every two minutes until the oxygen evolution potential was reached. Current measurements were taken at the end of each two minute interval and reflectograms were taken every 100 mV throughout the experiments. There was typically a ten minute interval between the insertion of the SID electrode into solution and the initial potential step.

All experiments were repeated at least once with little variation being observed (less than 10% in all cases) in either the polarization or reflectivity data.

Ex situ reflectograms were obtained by removing the electrode from solution, rinsing in distilled water and drying in a gentle stream of dry air. The electrode was subsequently remounted on the stage of the DR and a reflectogram obtained. The time elapsed between the removal from solution and the mounting on the stage was typically less than five minutes.

CHAPTER 4 RESULTS AND DISCUSSION

Identification of Anodic Surface Films

Anodic Films on a Copper Electrode

Two types of surface films were obtained by anodic polarization of a pure Cu electrode in 0.15 N Na_2SO_4 . The first film type was obtained at a potential of -250 mV in pH = 9.0 solution. The reflectogram corresponding to 18 hours of polarization under these conditions is shown in Figure 3a. This reflectogram displays a prominent maximum at 380 nm accompanied by two lesser maxima at 317 nm and 245 nm. In addition, two shoulders are observed; one at 550 nm and the other at 460 nm. Subsequent to obtaining this reflectogram the Cu electrode was removed from solution and a second, ex situ reflectogram obtained (Figure 3b). Since the peak positions and relative magnitudes are virtually identical, it can be concluded that the film undergoes no compositional alteration upon removal from solution. The sample was then promptly inserted into the vacuum chamber of a combination ESCA-AES system. Magnesium $\text{K}\alpha$ x-rays (1253.6 eV) were used to irradiate the sample and the resulting data were standardized by adjusting the energy scale so that the carbon peak would correspond to 285.0 eV. The resulting ESCA data (Figure 4) show the Cu $2p_{3/2}$ peak occurring at 936.9 eV. After the carbon correction factor of 4.1 eV is taken into account this peak value is adjusted to 932.8 eV which could belong to any of the following copper compounds:

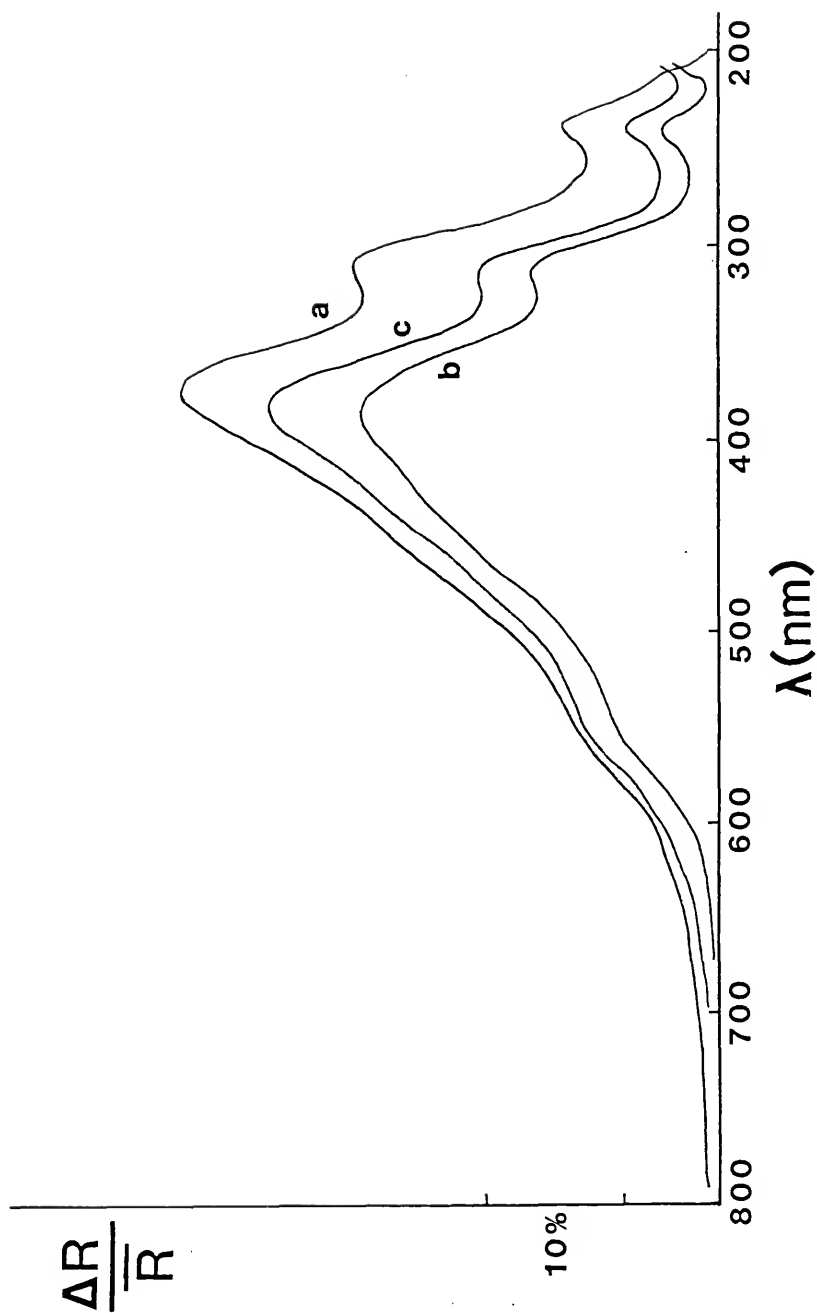


Figure 3. Reflectograms of Cu_2O obtained (a) in situ [pH = 9.0, -250 mV_{SCE}, 18 hr.], (b) ex situ and (c) after ESCA.

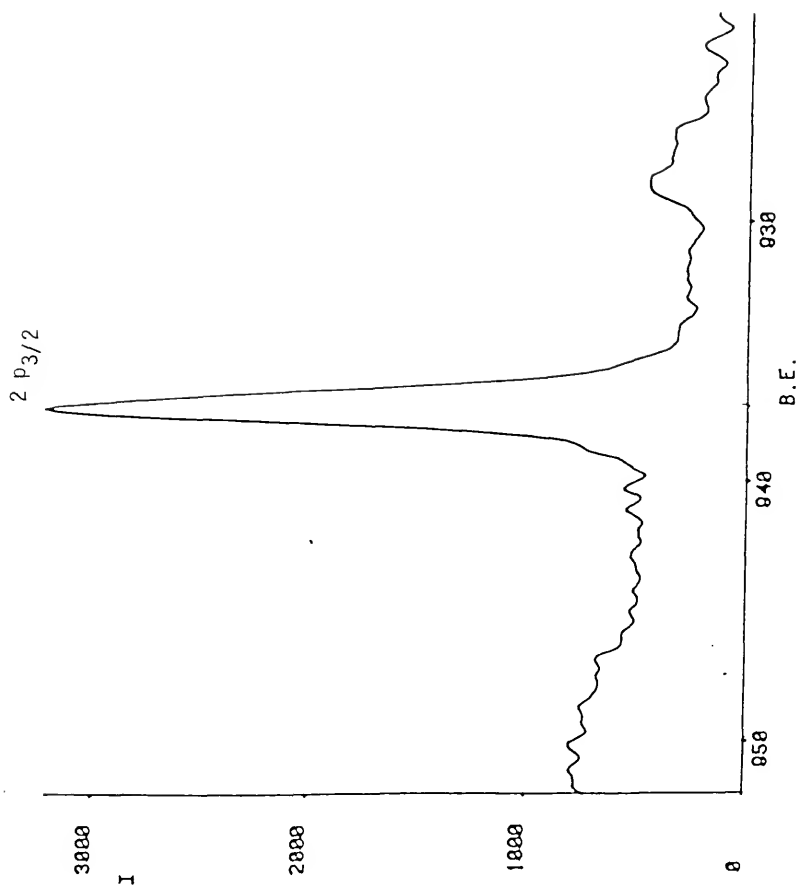


Figure 4. The Cu $2p_{3/2}$ peak from ESCA for a Cu SID potentiostated for 18 hours at $-250 \text{ mV}_{\text{SCE}}$ in pH = 9.0 solution.

Cu (metallic), BE = 932.4 eV;

Cu_2O , BE = 932.5 eV;

CuO , BE = 933.7 eV;

$\text{Cu}(\text{OH})_2$, BE = 934.7 [69].

However, it is observed that the shake-up peaks which normally accompany the principle Cu $2p_{3/2}$ peak (15-20 eV higher) for both CuO and $\text{Cu}(\text{OH})_2$ are absent. This indicates that this peak results from either Cu_2O or metallic Cu. When the Cu $L_{3M_{4,5}M_{4,5}}$ AES peak is considered, however, a positive identification of this film can be made. The corrected AES peak for this film occurs at 916.1 eV (Figure 5) which agrees quite well with the accepted value of 916.3 eV for Cu_2O [70]. (The $L_{3M_{4,5}M_{4,5}}$ AES peak occurs at 919.0 eV for pure copper metal.) The combined ESCA-AES data indicate, therefore, that the film represented in the reflectogram of Figure 3a is Cu_2O . A third reflectogram obtained from this sample after removal from the vacuum chamber indicates that neither the vacuum nor x-ray radiation altered the film composition (Figure 3c).

The second type of film observed to form on the Cu electrode can be obtained at a potential of +450 mV in a solution of pH = 4.3. The series of reflectograms obtained for this film appear in Figure 6. Only two features are distinguishable on the in situ reflectogram--a shoulder at 575 nm and a "peak" at 225 nm. Comparison of the ex situ curves for this sample mounted within and without (Figures 7a and b) the dry corrosion cell indicate that this 225 nm "peak" is an artifact which results from the absorption by the quartz window at wavelengths shorter than 225 nm. This result is an indication that any true peak must be off scale, i.e., at a wavelength shorter than 200 nm.

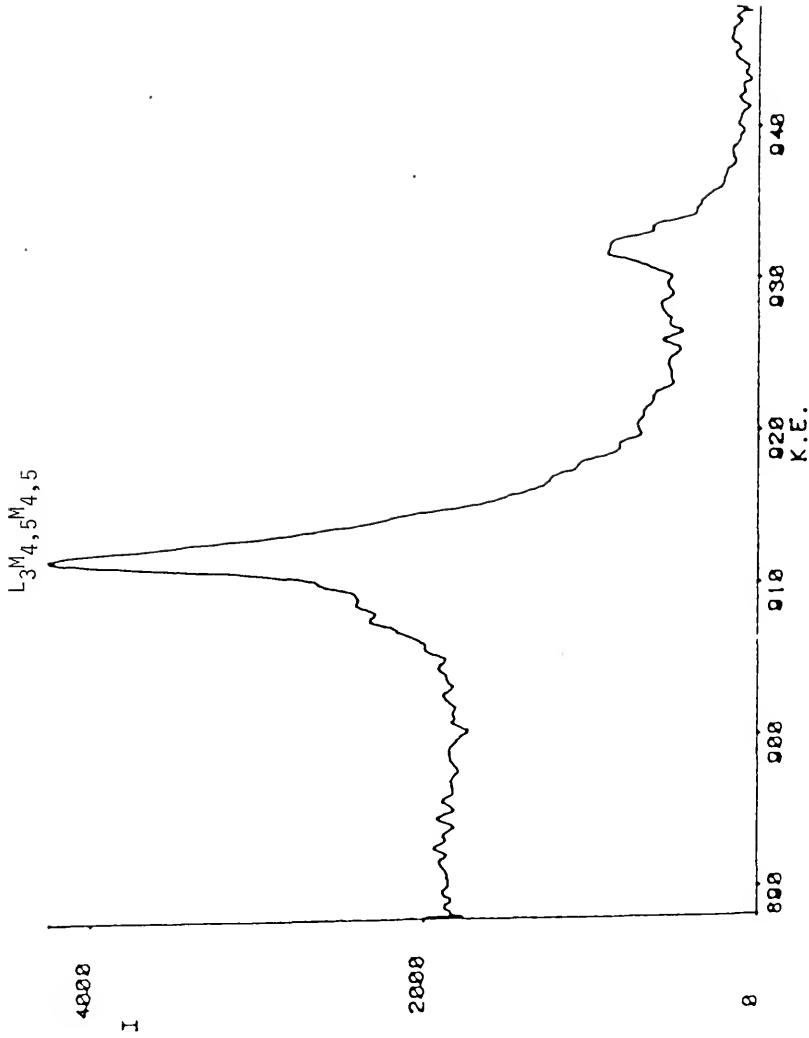


Figure 5. The AES $L_{3M_{4,5}}M_{4,5}$ peak from the Cu SID potentiostated for 18 hours at $-250 \text{ mV}_{\text{SCE}}$ in $\text{pH} = 9.0$ solution.

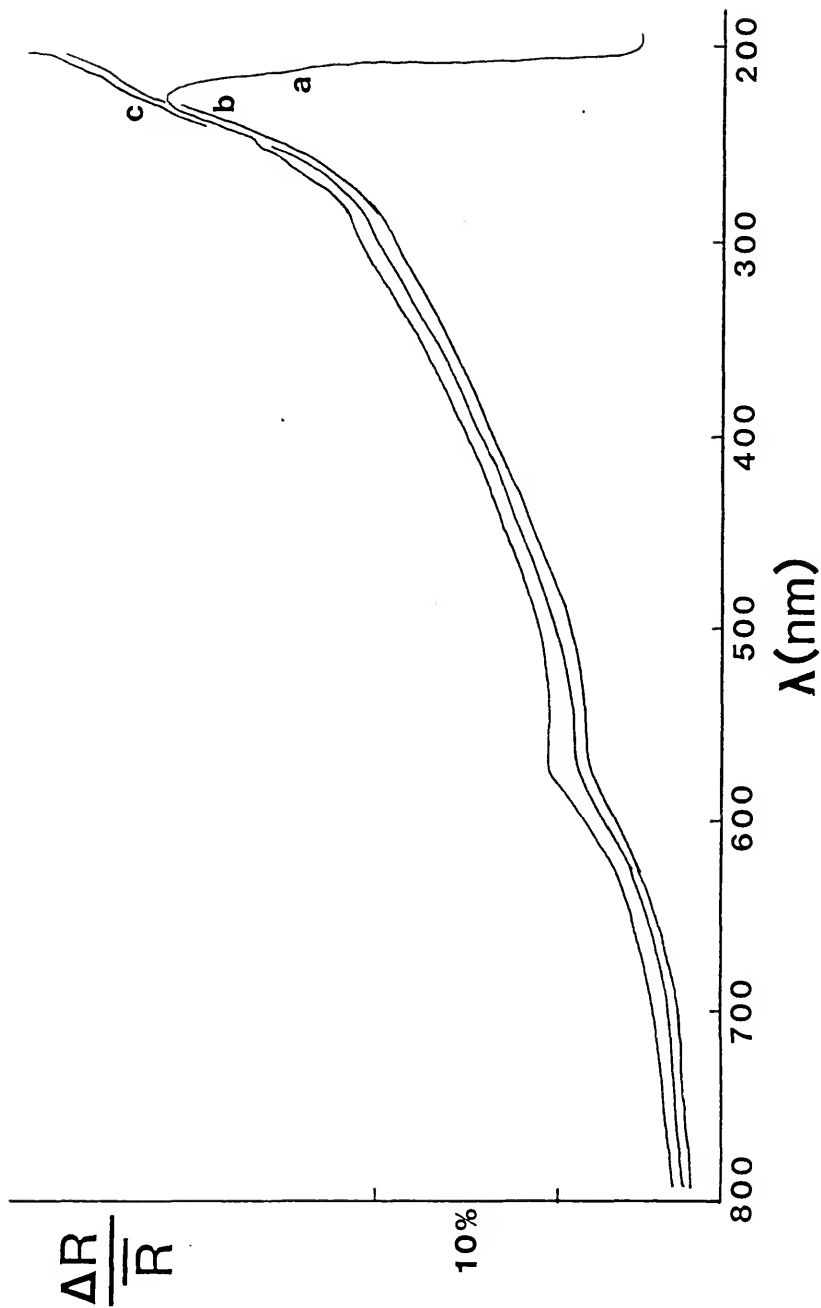


Figure 6. Reflectograms of CuO obtained (a) in situ [pH = 4.3, +450 mV_{SCE}, 2 sec], (b) ex situ and (c) after ESCA.

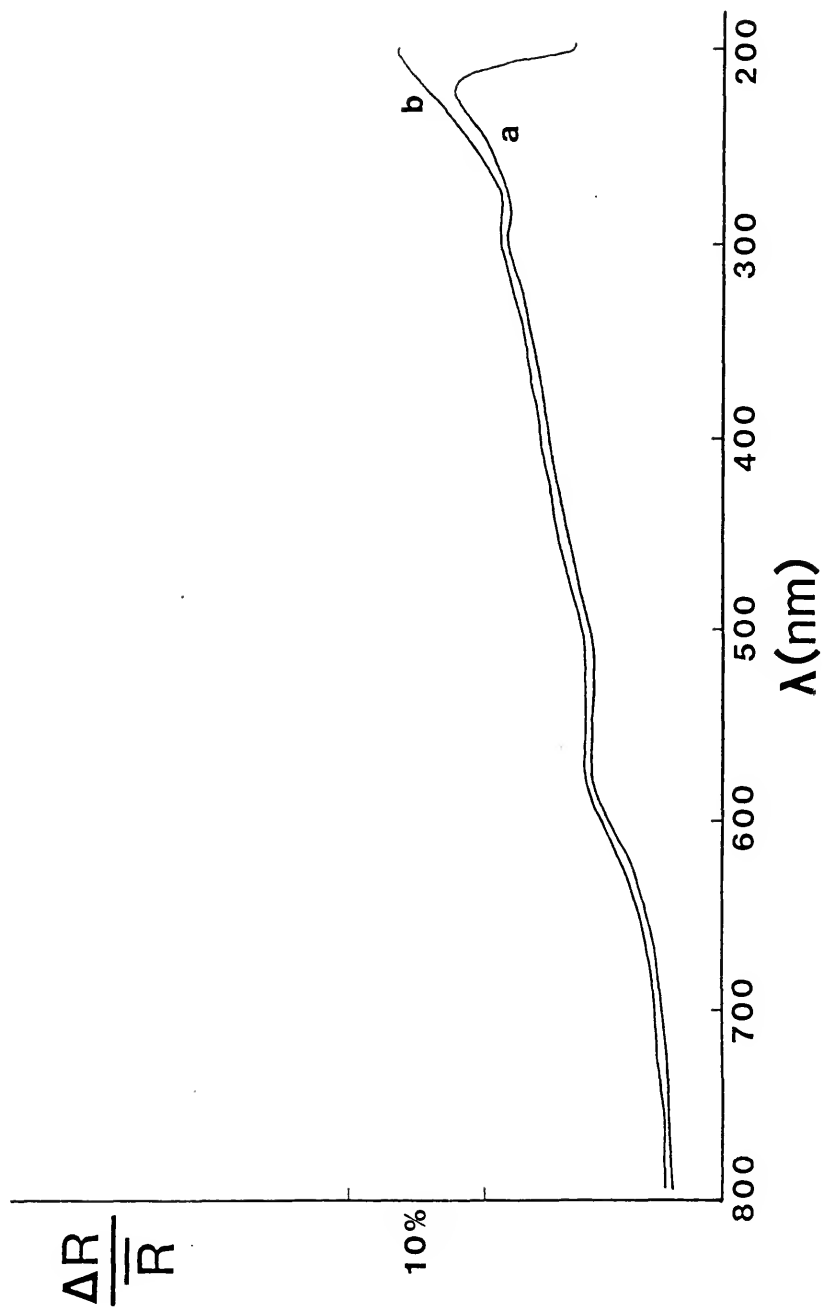


Figure 7. Ex situ reflectograms of CuO (a) in dry corrosion cell, and (b) on the DR stage.

The data obtained from ESCA analysis of this film are presented in Figure 8. The binding energy of the major peak (corrected value of 933.7 eV) agrees well with the accepted value for CuO [69]. The presence of the shake-up peaks is also a clear indication that the film is indeed CuO [69]. Again, comparison of the in situ, ex situ and post-ESCA film shows that this film is also unaffected by removal from solution and vacuum treatment. The correspondence of the reflectograms of Figures 3 and 6 with Cu₂O and CuO agree with the results of Shanley [61] who used band structures and optical constants to arrive at the same correlation.

Anodic Films on a Nickel Electrode

Three corrosion films are observed to form on a Ni electrode in 0.15 N Na₂SO₄ solution. A typical reflectogram corresponding to the film most commonly formed appears in Figure 9. The only striking feature is the "peak" (again artificial) at 225 nm. The curve drops off smoothly from this "peak" to the upper limit of 800 nm. The O 1s and Ni 2p_{3/2} peaks from ESCA analysis of this film are displayed in Figures 10 and 11. The Ni 2p_{3/2} peak occurs at 856.1 eV (corrected) which falls in the middle of the range of values for Ni(OH)₂ reported in the literature (e.g., 855.6 eV [71], 855.9 eV [67], 856.1 eV [72], 856.45 eV [69]). Also, see Table 1. The O 1s value of 532.2 eV from Figure 10 also agrees quite well with values reported for Ni(OH)₂ by Barr [69] (531.95), McIntyre et al. [67] (531.7 eV) and Ali [72] (532.1 eV). Several researchers [73-75] have obtained ESCA structures very similar to the ones in Figures 10 and 11 by bombarding a clean nickel surface with oxygen in a vacuum system. They speculate that the resulting compound

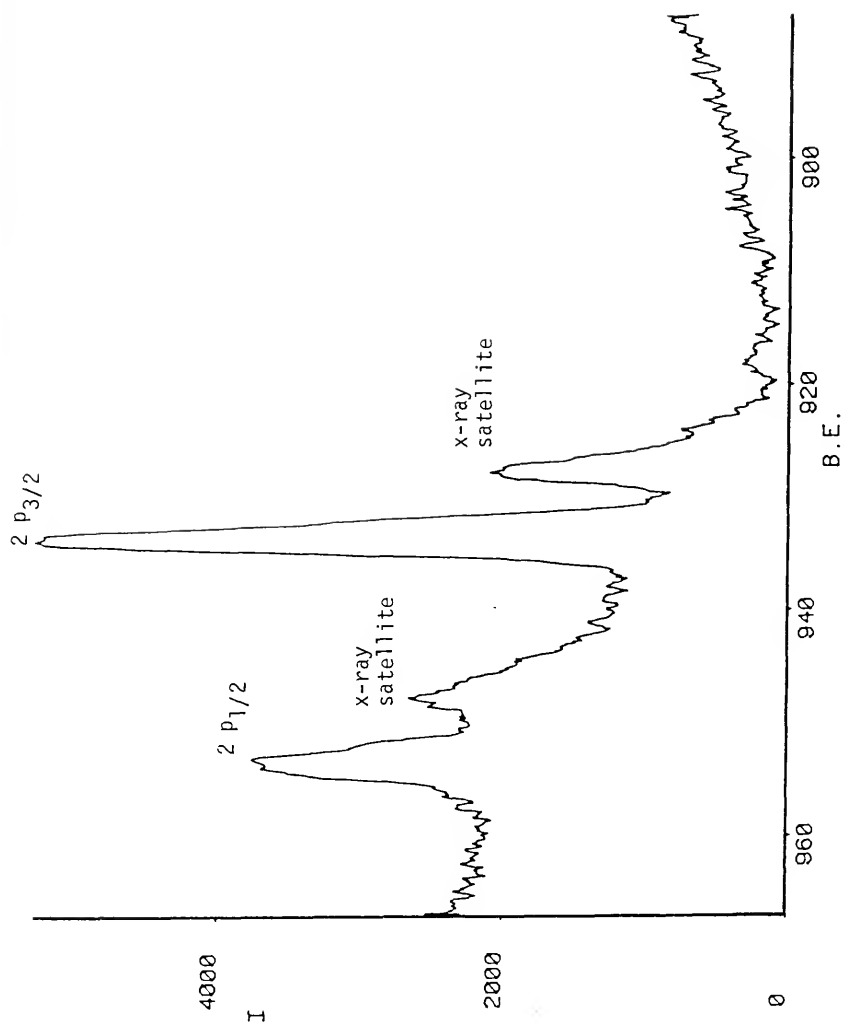


Figure 8. The ESCA Cu $2p_{3/2}$ peak that results from potentiostating at +450 mV_{SCE} for 2 seconds at $pH = 9.0$.

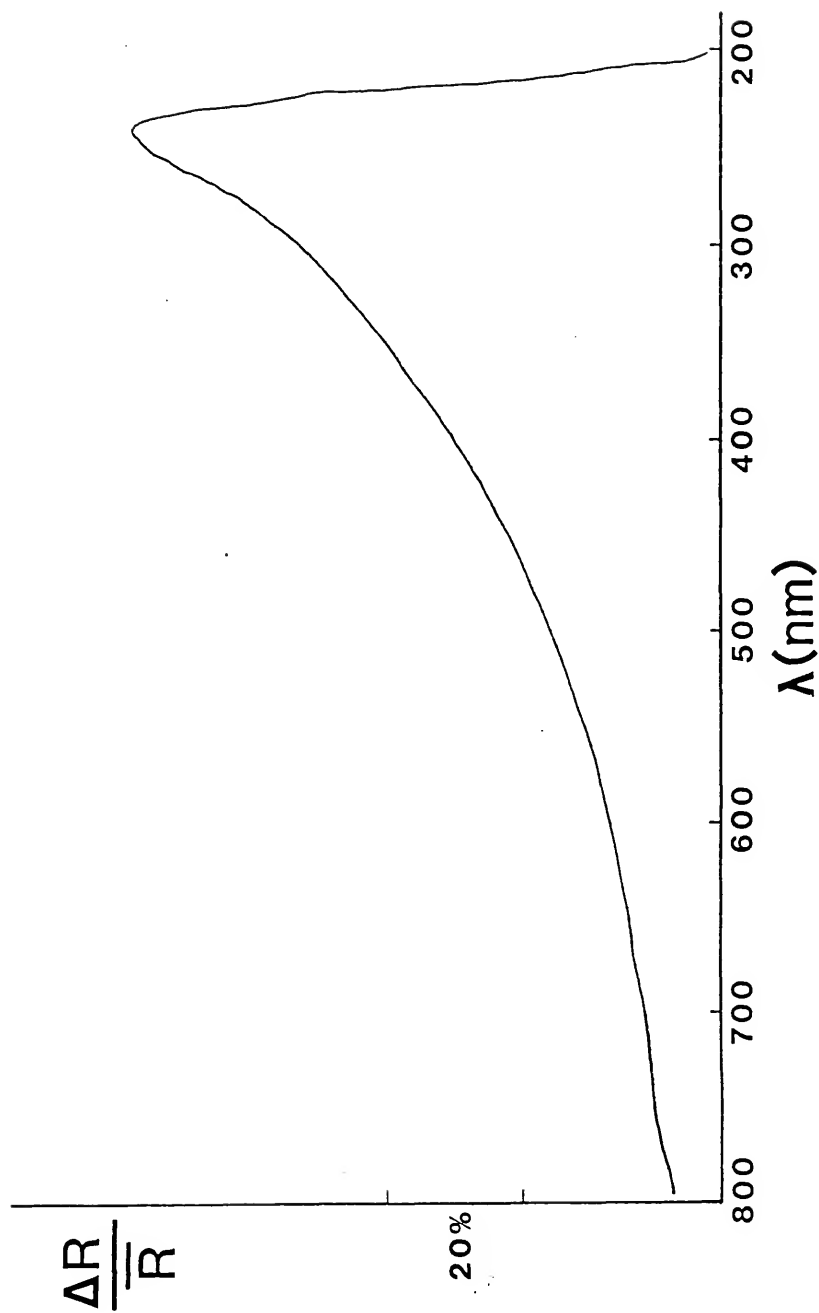


Figure 9. In situ reflectogram of Ni(OH)_2 [$+50 \text{ mV}_{\text{SCE}}$, $\text{pH} = 4.0$, 10 minutes].

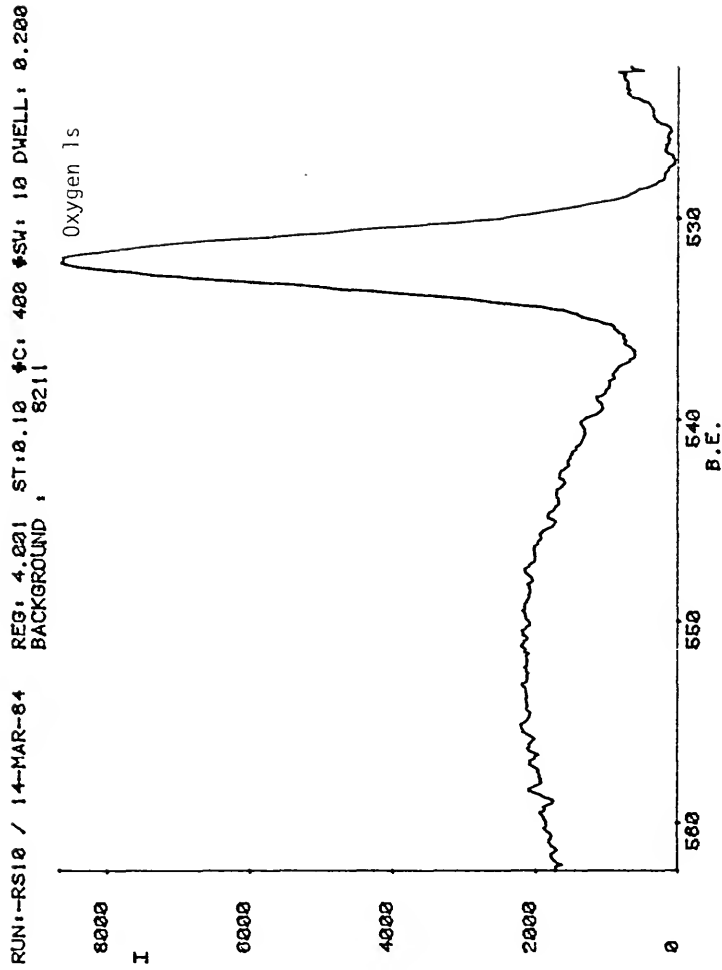


Figure 10. The ESCA oxygen 1s peak from a Ni electrode [$+50 \text{ mV}_{\text{SCE}}$, $\text{pH} = 4.0$, 10 minutes].

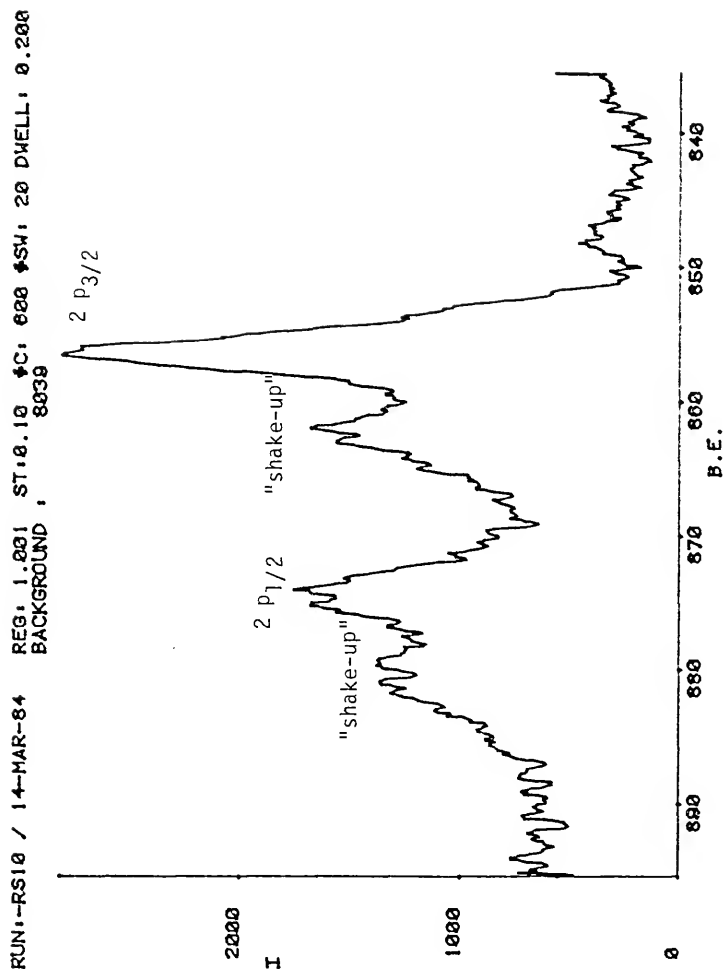


Figure 11. The ESCA $\text{Ni} p_{3/2}$ peak from a Ni electrode [$+50 \text{ mV}_{\text{SCE}}$, $\text{pH} = 4.0$, 10 minutes].

TABLE 1
 BINDING ENERGY DATA FOR NICKEL AND NICKEL COMPOUNDS*

Binding Energy, (eV)					
Ni	NiO	Ni ₃ O ₄	Ni ₂ O ₃	NiO ₂	Ni(OH) ₂
852.60	--	--	--	--	856.10
852.50	854.00	--	--	--	855.90
852.50	854.00	--	--	--	855.60
852.75	854.60	--	855.70	--	856.45
852.90	854.50	--	855.80	--	--
852.00	855.00	--	--	--	--
--	854.00	--	--	--	--

* [reference 72]

is Ni_2O_3 rather than $\text{Ni}(\text{OH})_2$. There is, however, no reason to conclude that the film formed in the present work in aqueous solution would be similar to that formed under these extreme conditions, rather than the more commonly formed $\text{Ni}(\text{OH})_2$. It is reasonably concluded, therefore, that the film discussed above is indeed $\text{Ni}(\text{OH})_2$.

The second film type observed to form on a Ni electrode always occurs as a minor constituent in a mix with $\text{Ni}(\text{OH})_2$. A typical reflectogram indicating such a mix is displayed in Figure 12. Notice that a prominent shoulder occurs at about 320 nm on a curve that would otherwise be indicative of $\text{Ni}(\text{OH})_2$. The fact that the relative height of the peak at 225 and this shoulder at 320 nm varies as a function of solution pH and electrode potential is a clear indication that this is a mixed film. Although the relative amplitude can be varied somewhat, it is interesting to note, when grown in solution, this shoulder never develops into a true peak but rather is always a minor component of the $\text{Ni}(\text{OH})_2$ peak. An ESCA analysis of two films that displayed a prominent shoulder on a reflectogram indicated in both cases that the film was still pure $\text{Ni}(\text{OH})_2$. Two possible explanations can be offered to explain this result. First, it could be that the amount of the compound responsible for the shoulder is present in an insufficient amount to be detected by ESCA. Alternatively, it could be that this second compound is present at the metal/ $\text{Ni}(\text{OH})_2$ interface in which case the ejected electrons needed for the analysis could well be completely attenuated by the $\text{Ni}(\text{OH})_2$ overlayer, which is, in fact, sufficiently thick to prevent detection of the underlying Ni substrate.

In order to identify this second Ni compound, a somewhat different method of film preparation was attempted. Instead of growing the film

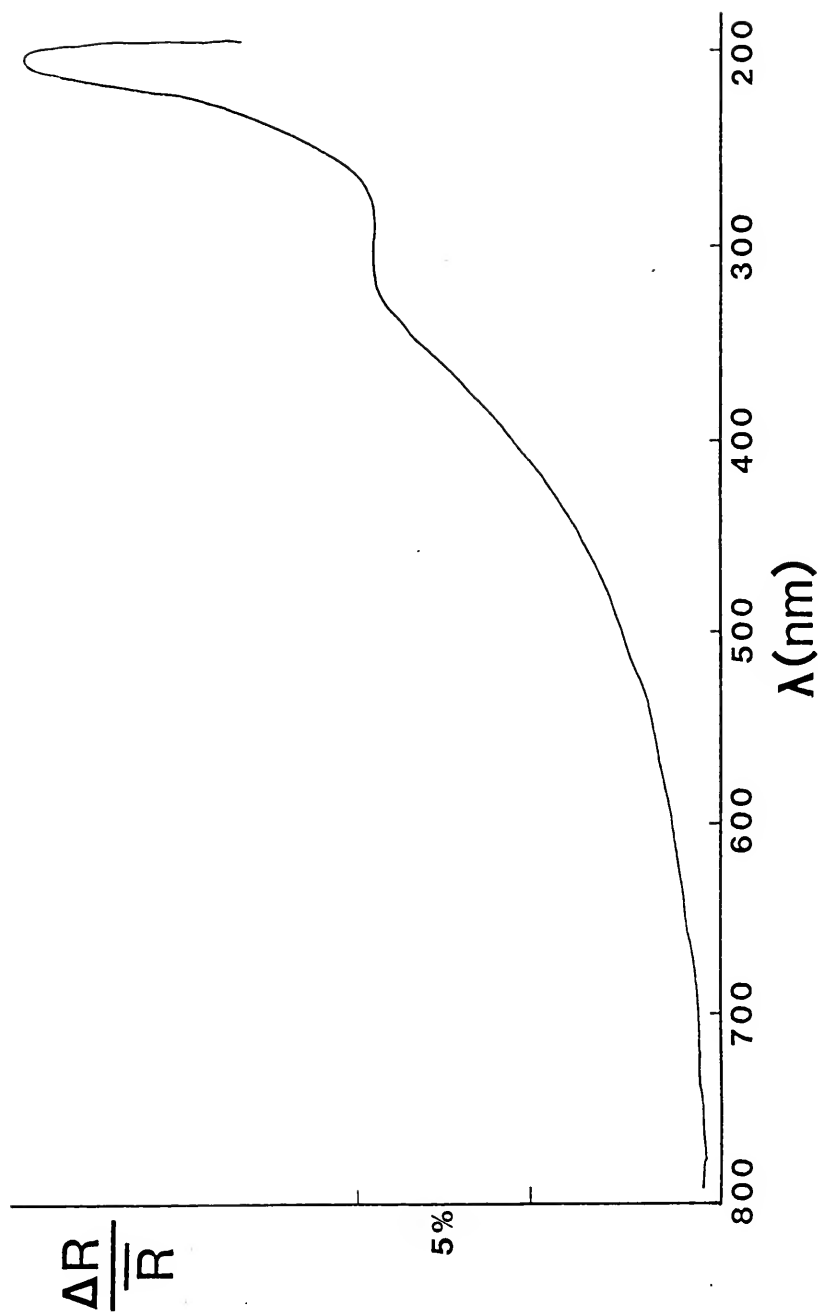


Figure 12. In situ reflectogram indicating a mix of $\text{Ni}(\text{OH})_2$ and NiO [$+300 \text{ mV}_{\text{SCE}}$, $\text{pH} = 13.0$, 20 minutes].

under anodic polarization in an aqueous solution, half of the nickel SID was removed from the epoxy mount after polishing and heated for three minutes in a pure oxygen atmosphere. The final temperature was about 460°C after which this half sample was left to cool to room temperature in the passing oxygen (about 10 minutes). This sample was then remounted with the as-polished specimen, which had been stored in room temperature air, and the reflectogram in Figure 13 obtained. The Ni(OH)_2 peak at 225 nm is again present just as in the solution grown film. However, instead of just a shoulder, a well defined peak now exists at 330 nm and is actually greater in magnitude than the Ni(OH)_2 peak. The $\text{Ni } 2p_{3/2}$ and $0 \text{ } 1s$ peaks obtained from the subsequent ESCA analysis are presented in Figures 14 and 15. Close examination of both peaks reveals that each is actually a doublet. A computer resolution of the doublets appears in Figure 16 and 17. The Ni doublet deconvolutes into peaks positioned at corrected energies of 854.1 eV and 856.0 eV while the oxygen doublet yields peaks at 529.7 eV and 531.9 eV. The 856.0 eV nickel peak and 531.9 eV oxygen peak agree well with the values of 856.1 eV and 532.2 eV already obtained in this study for pure Ni(OH)_2 . The remaining nickel peak at 854.1 eV agrees quite well with the published value of 854.0 eV [67,71,76] for NiO while the oxygen peak at 529.7 eV agrees exactly with published values [73] for NiO. This confirms that a mixed film, namely Ni(OH)_2 and NiO, is responsible for the reflectograms in Figures 12 and 13. Moreover, since the "peak" at 225 nm has already been identified as Ni(OH)_2 it can then be concluded that the second peak (or shoulder, depending on relative film composition) at 330 nm results from NiO.

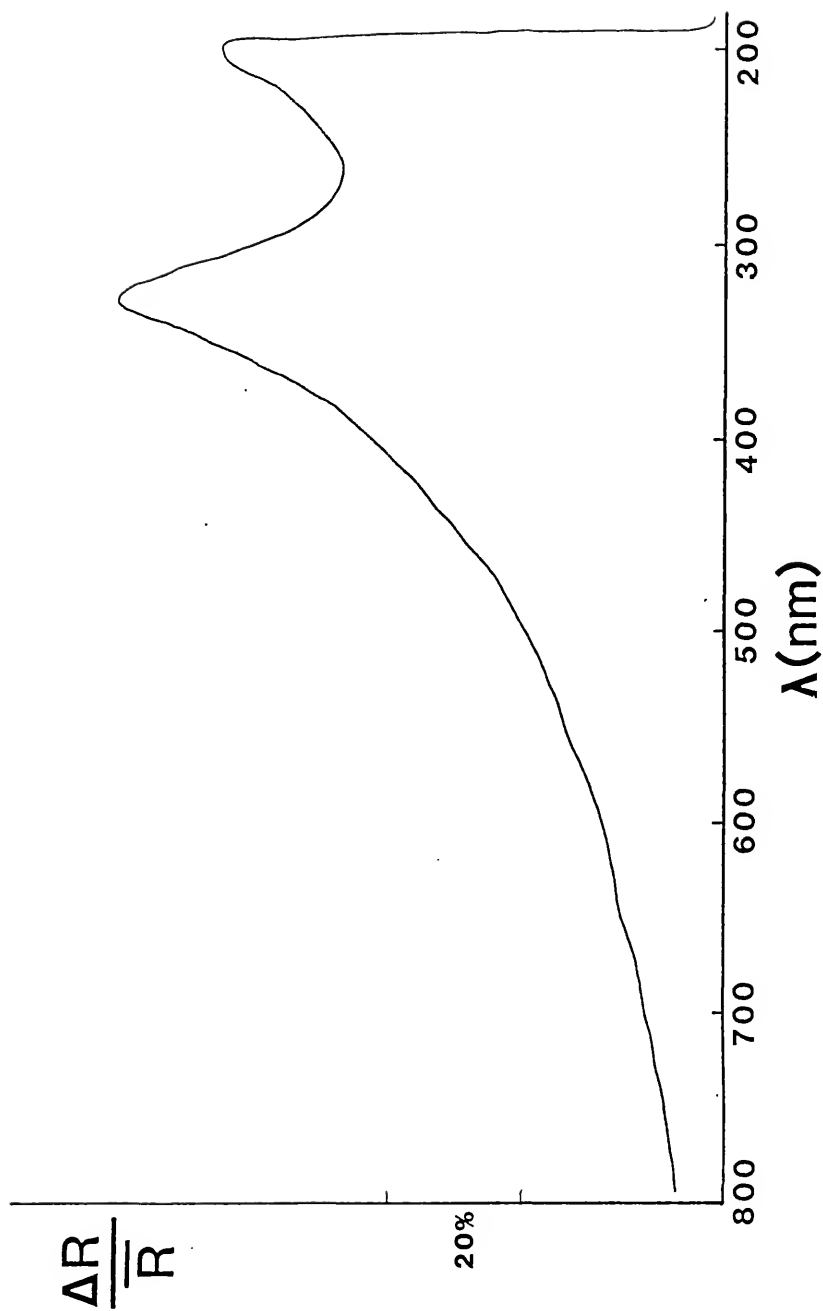


Figure 13. Reflectogram of $\text{Ni}(\text{OH})_2 + \text{NiO}$ prepared in an O_2 atmosphere at 460°C for 3 minutes.

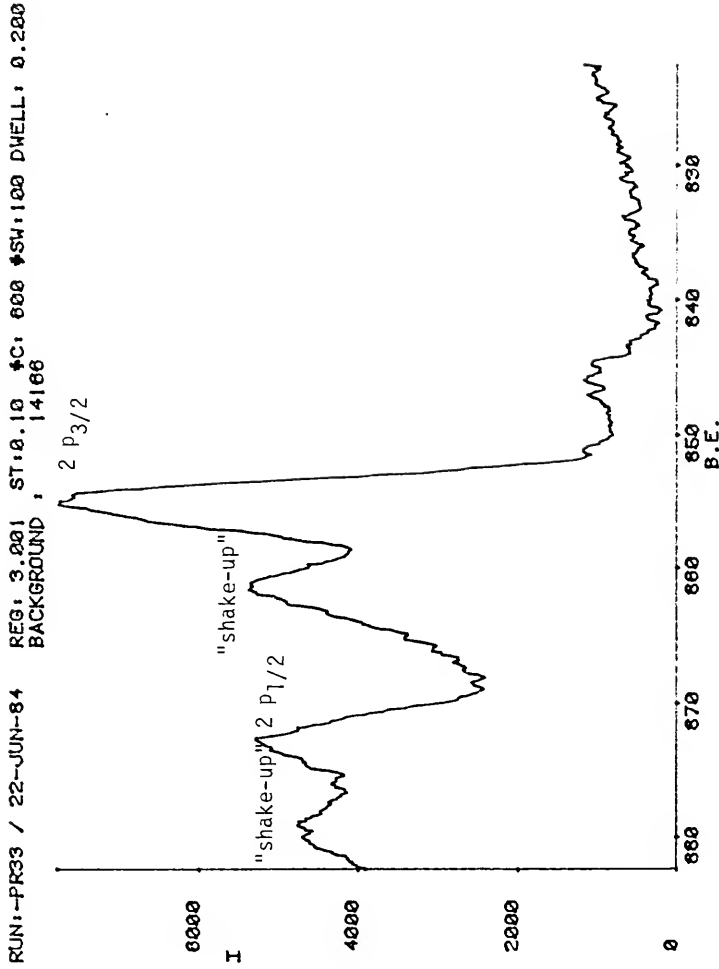


Figure 14. The ESCA Ni 2p_{3/2} peak obtained from a Ni sample oxidized at 460°C in an O₂ atmosphere for 3 minutes.

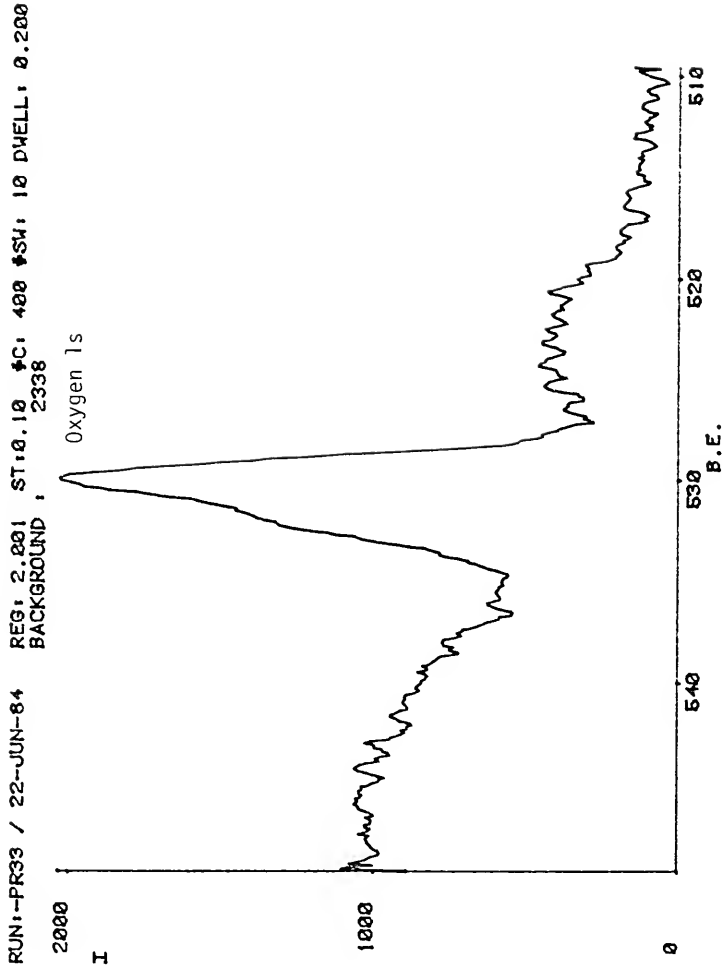


Figure 15. The ESCA oxygen 1s peak obtained from a Ni sample oxidized at 460°C in an O_2 atmosphere for 3 minutes.

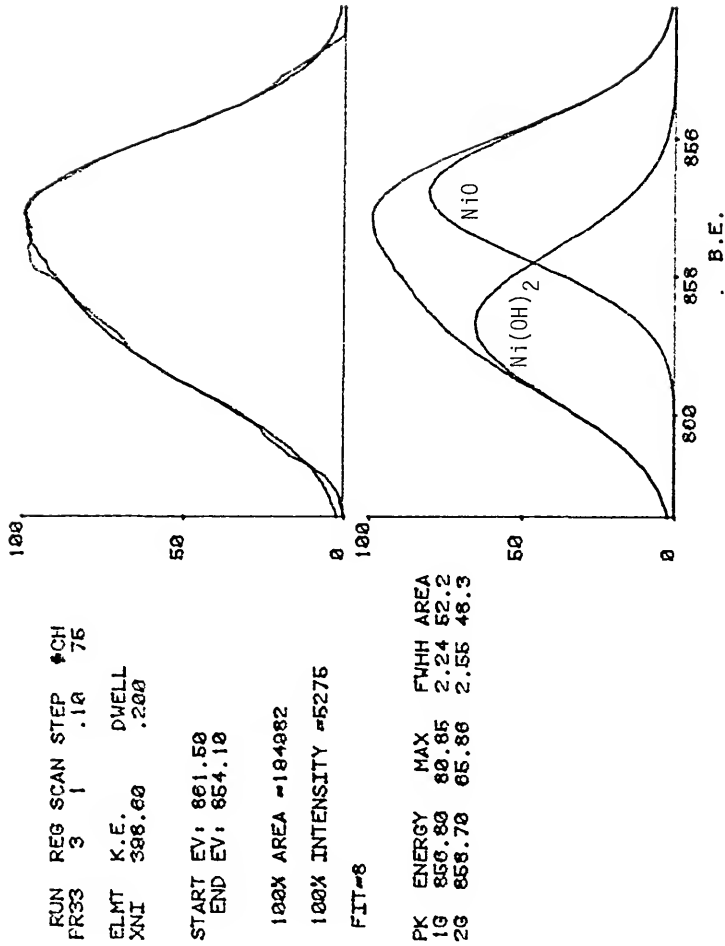


Figure 16. Deconvolution of the Ni 2p_{3/2} peak of Figure 14. [The carbon correction factor of 2.5 eV must be subtracted from the energy scale.]

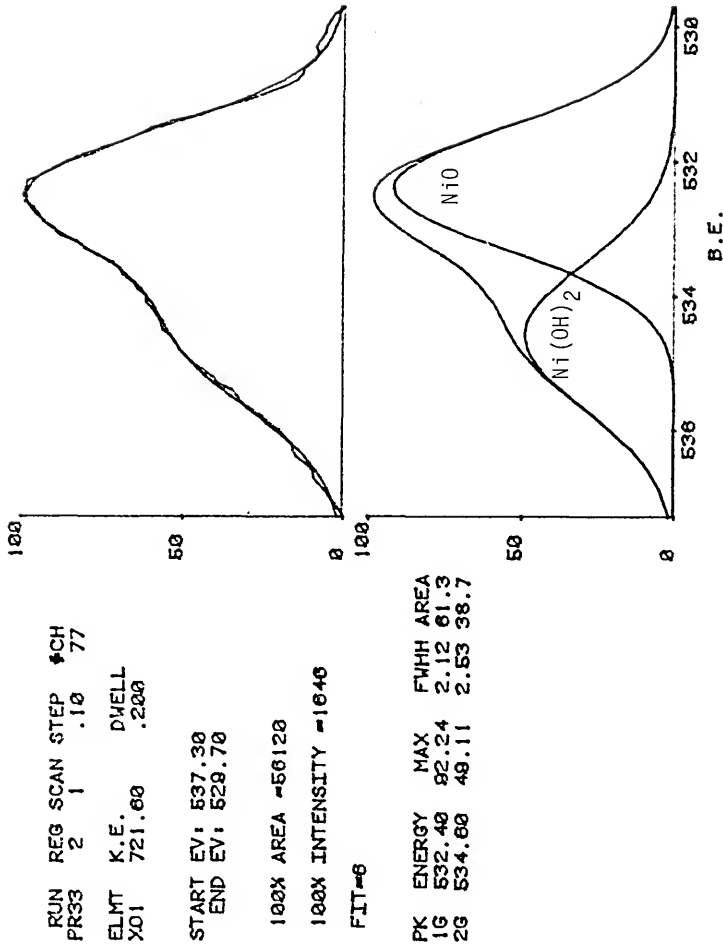
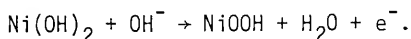


Figure 17. Deconvolution of the oxygen 1s peak of Figure 15. [The carbon correction factor of 2.5 eV must be subtracted from the energy scale.]

Based on calculations [77] involving the relative areas of the Ni $2p_{3/2}$ peaks it is determined that the oxidation film is approximately 52% NiO--the balance being $Ni(OH)_2$. Comparison of the reflectogram peak heights in Figures 12 and 13 indicates that the anodically formed film is roughly 10% NiO, 90% $Ni(OH)_2$. Since the detection limit of NiO in $Ni(OH)_2$ for ESCA is on the order of 10%, it is not surprising that the anodic film was analyzed as being pure $Ni(OH)_2$.

The third film type observed to form on a Ni electrode in sulfate solution occurs only at a pH = 8 or greater and only on those electrodes which have not experienced an active-passive transition. A rather intriguing characteristic of this film is that it seems to form only by conversion of $Ni(OH)_2$. In fact, formation will not occur at all unless a $Ni(OH)_2$ layer is first grown on the electrode. A reflectogram indicating the presence of this third film type is presented in Figure 18. Notice that as the peak at 625 nm increases, the $Ni(OH)_2$ "peak" at 225 nm diminishes, which indicates clearly that a conversion reaction is occurring. The magnitude of the NiO peak at 330 nm seems unaffected, however. If the electrode potential is subsequently reduced to any value cathodic to the oxygen evolution potential, the 625 nm peak disappears within seconds while the $Ni(OH)_2$ "peak" sharply increases. This reverse conversion reaction also occurs if the electrode is removed from solution. Since this type of film cannot be isolated ex situ, positive identification is not possible.

It has been suggested by Jones and Wynne-Jones [78] and by Lukovtsev [79] that $Ni(OH)_2$ can be oxidized to $NiOOH$ at higher potentials via a deprotonation reaction:



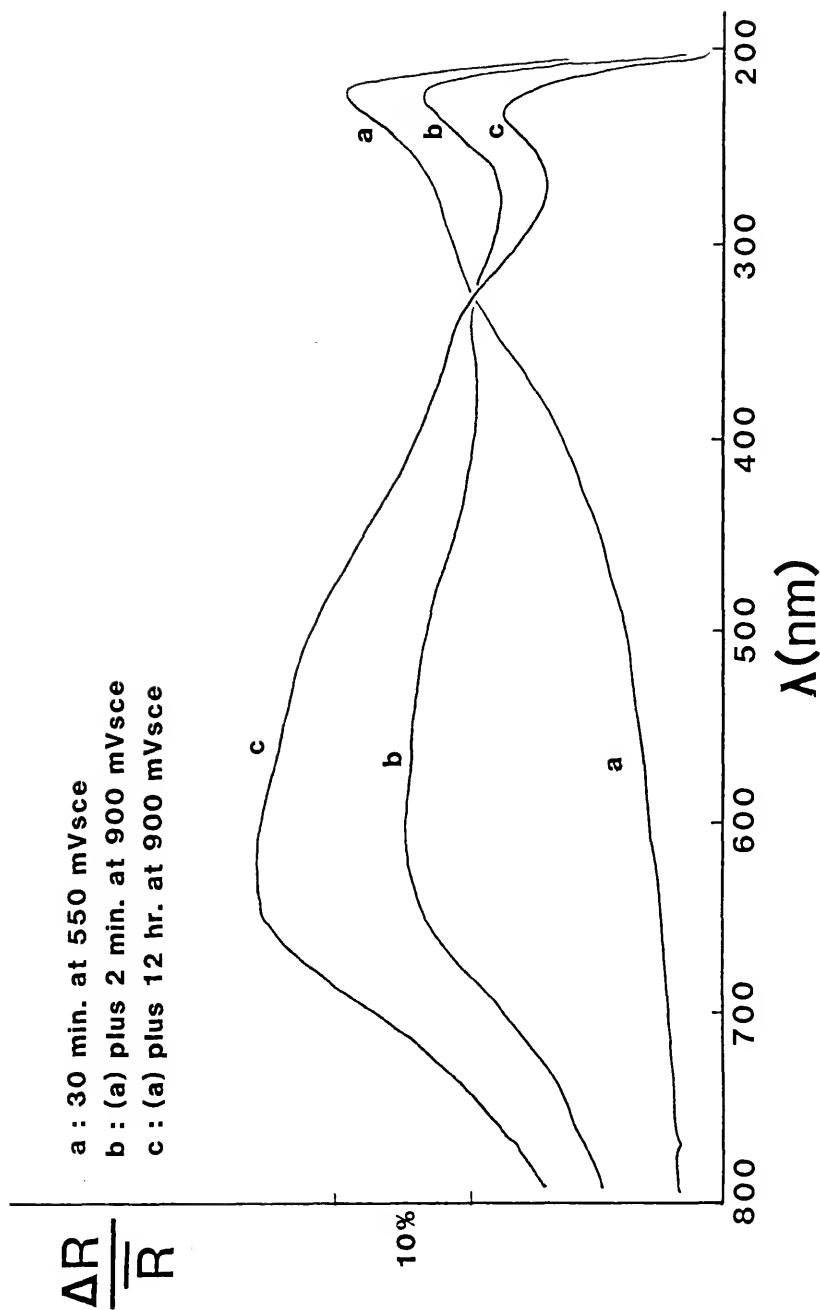


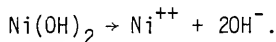
Figure 18. In situ reflectogram indicating the conversion of $\text{Ni}(\text{OH})_2$ to NiOOH as a function of potential.

Confirmation of this reaction in a nickel-cadmium cell was made by Uno [80] who showed by x-ray measurements that Ni(OH)_2 does indeed convert to the oxyhydroxide upon charging. He further noted the reverse reaction to occur upon discharge of the cell. Based on the agreement of the present observations with those in the literature, it is assumed that the peak at 625 nm on the reflectograms of Figure 18 is characteristic of NiOOH .

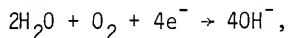
Anodic Behavior of Nickel in 0.15 N Na_2SO_4

Anodic Behavior at pH = 4.0

When a freshly polished Ni SID electrode is potentiostated between -300 mV and -100 mV in .15 N Na_2SO_4 solution of pH = 4.0 in an open corrosion cell, a negative peak appears on the resulting reflectogram (Figure 19a and b). This negative peak is the mirror image of the curve obtained for Ni(OH)_2 growth which indicates that a Ni(OH)_2 film is dissolving from the surface of the working electrode, perhaps according to the simple dissolution reaction:



However, if oxygen reduction is occurring at the electrode surface,



the surface pH will no longer be that of the bulk solution but substantially higher. This higher pH results in the stabilization of the Ni(OH)_2 film which, as shown in this study, is virtually insoluble at pH values as low as 7.1 (Figure 20). Although oxygen reduction is

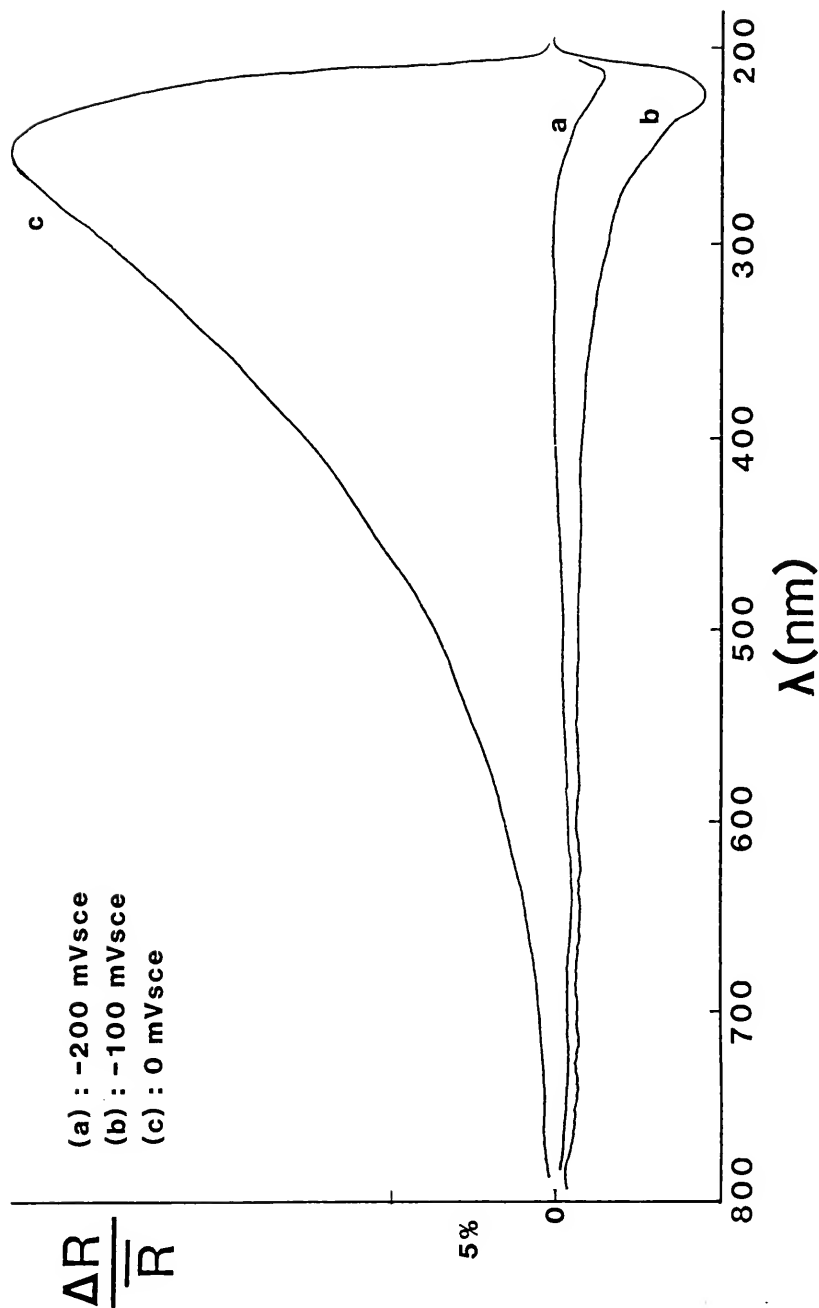


Figure 19. Reflectograms corresponding to the indicated potentials for a Ni SID (pH = 4.0, open solution).

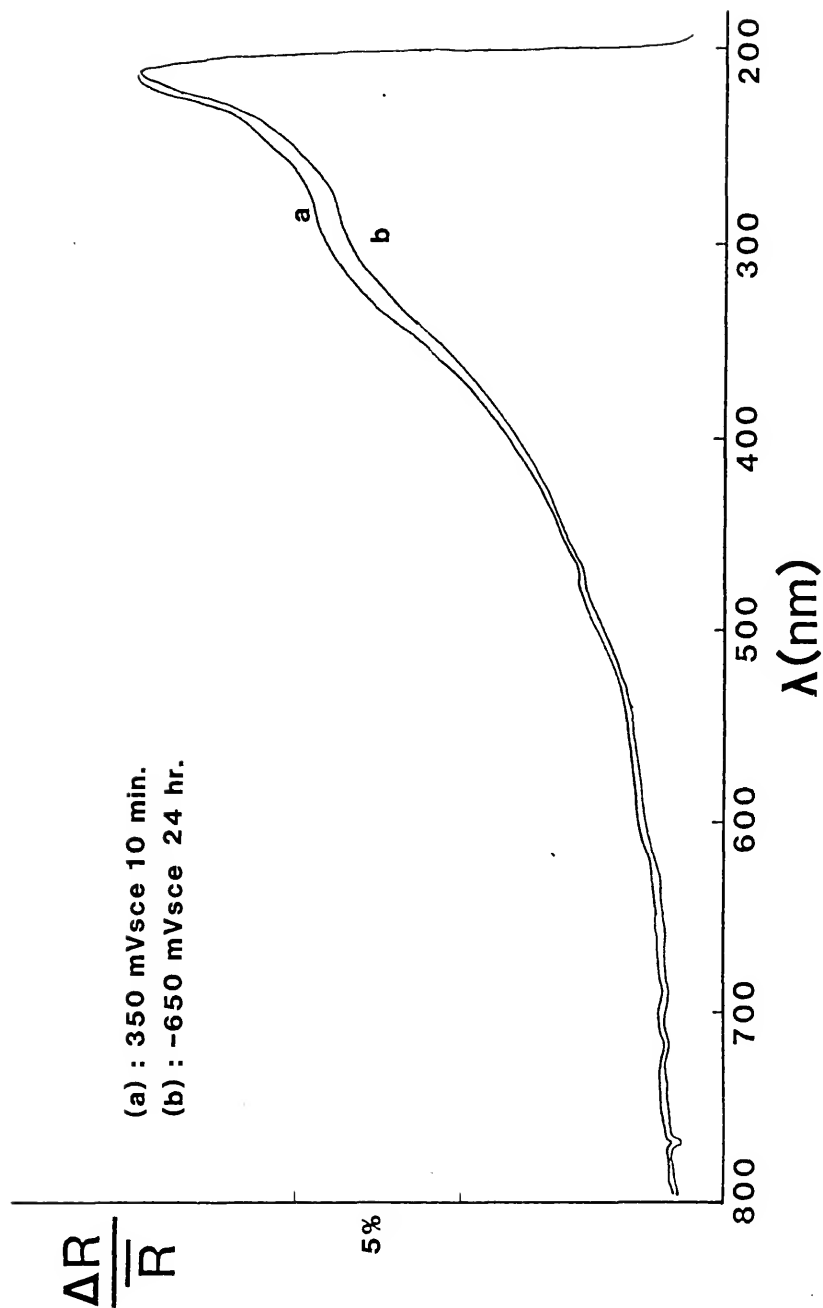


Figure 20. Reflectograms which indicate that $\text{Ni}(\text{OH})_2$ is virtually insoluble at a pH of 7.1 (open solution).

thermodynamically possible at any potential cathodic to +750 mV, it may actually only occur at potentials substantially more cathodic to this value due to the large overpotential required and the small exchange current density for this process on nickel. If oxygen reduction ceases at about -300 mV on the anodic scan, the surface pH of the working electrode will begin to approach that of the bulk (4.0) and Ni(OH)_2 reduction can proceed. However, the optical reference electrode is still being maintained at a potential of -450 mV where oxygen reduction easily occurs. This results in the continued stabilization of the "as polished" Ni(OH)_2 film on the optical reference electrode; hence, a negative peak occurs on the reflectogram.

This explanation of film stability is supported further by the results of the following experiment. After a thick Ni(OH)_2 film (relative to the "as polished" thickness) was grown on the working electrode by potentiostating in the passive region, the electrode potential was switched to -100 mV. As expected, the peak height diminishes as a function of time indicating that the Ni(OH)_2 film is dissolving (Figure 21). If this same experiment is performed in a pH = 7.1 solution no film dissolution occurs even after 24 hours at this reduction potential. These dissolution results are consistent with those of MacDougall [29].

In the deaerated solution, pH = 4.0, no negative peaks are observed on the reflectograms (Figure 22). This behavior can be attributed to the "as polished" Ni(OH)_2 film dissolving simultaneously on both halves of the electrode. This would be expected since the surface pH would be that of the bulk solution (4.0) in the absence of oxygen reduction.

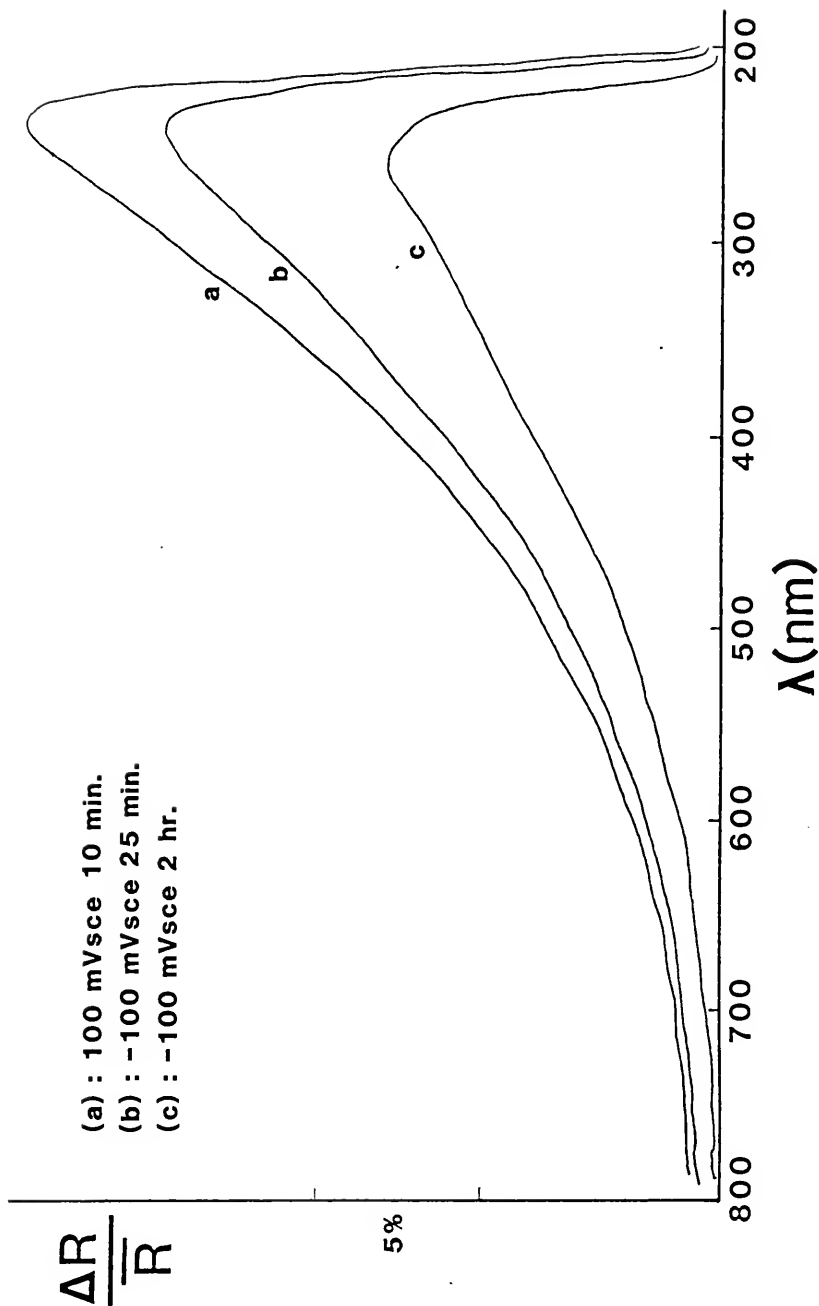


Figure 21. Reflectograms which indicate the solubility of $\text{Ni}(\text{OH})_2$ at a pH of 4.0 (open solution).

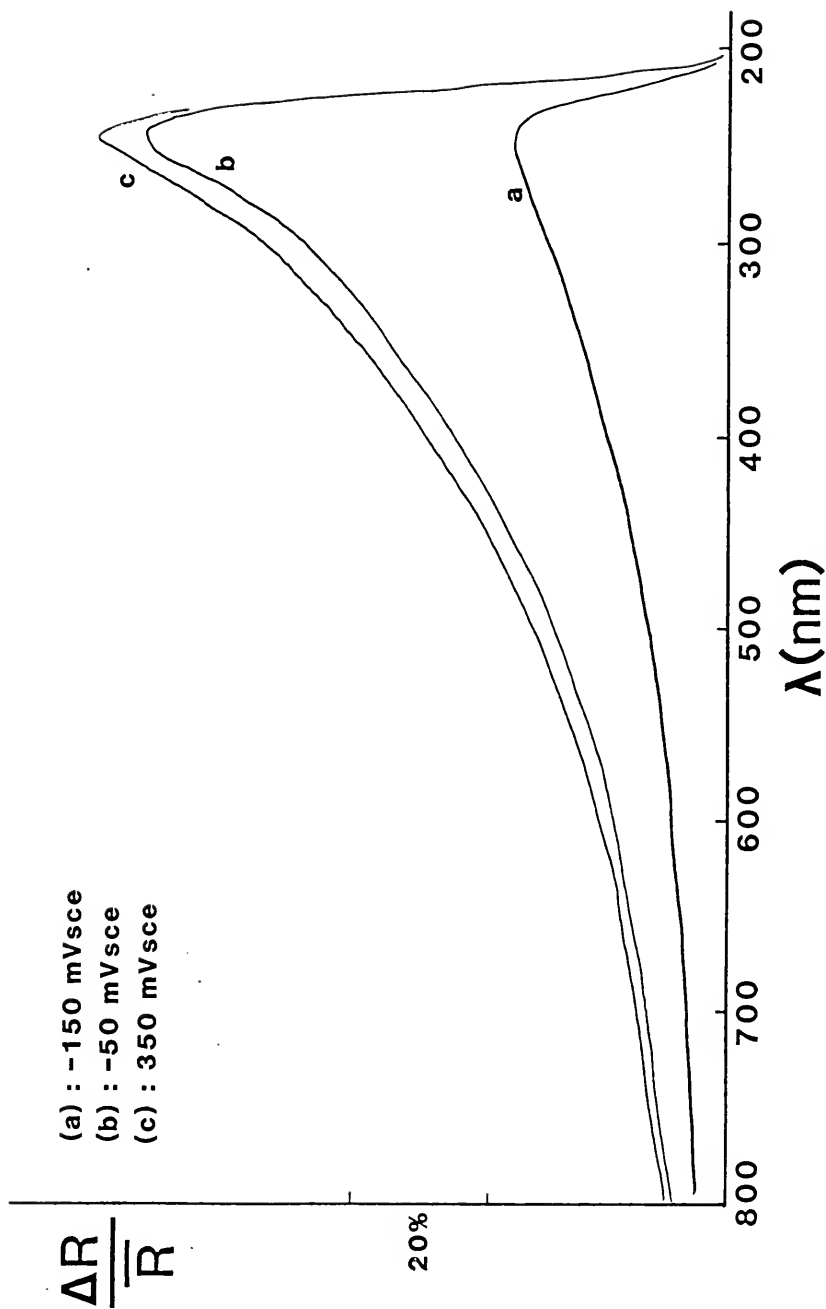
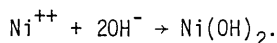


Figure 22. Reflectograms indicating Ni(OH)_2 film growth in pH = 4.0, deaerated solution.

Since the working electrode is free from surface films prior to passivation, metal dissolution proceeds uninhibited. At about -150 mV the current reaches a maximum and the Ni(OH)_2 film has grown to a substantial thickness (Figure 23). By + 50 mV the film has attained maximum thickness and passivation is complete, the passivation process occurring over a rather broad 400 mV span. The passivation reaction is presumably



In contrast, the passivation of the Ni electrode in the open solution occurs over a narrower potential range of only 150 mV (Figure 24). Although the passivation current density is similar in the two cases the passivation potential is approximately 100 mV more anodic in the case of the open solution. These observations can be explained by recalling that the surface film present on the working electrode in the open solution is not completely dissolved until a potential of -100 mV is reached on the anodic scan. The presence of this film retards metallic dissolution as evidenced by the very low current values in the potential range -450 mV to -100 mV. (Note that the absence of such a film in the deaerated solution results in a substantially greater current in this potential range.)

Finally, when the film is completely reduced, the working electrode is at a potential well into the metal dissolution region. This results in rapid Ni^{++} ion dissolution as evidenced by the accompanying sharp increase in anodic current at -80 mV (Figure 24). Recall that the optical reference electrode is still at a potential where oxygen reduction occurs resulting in the production of hydroxide ions. The

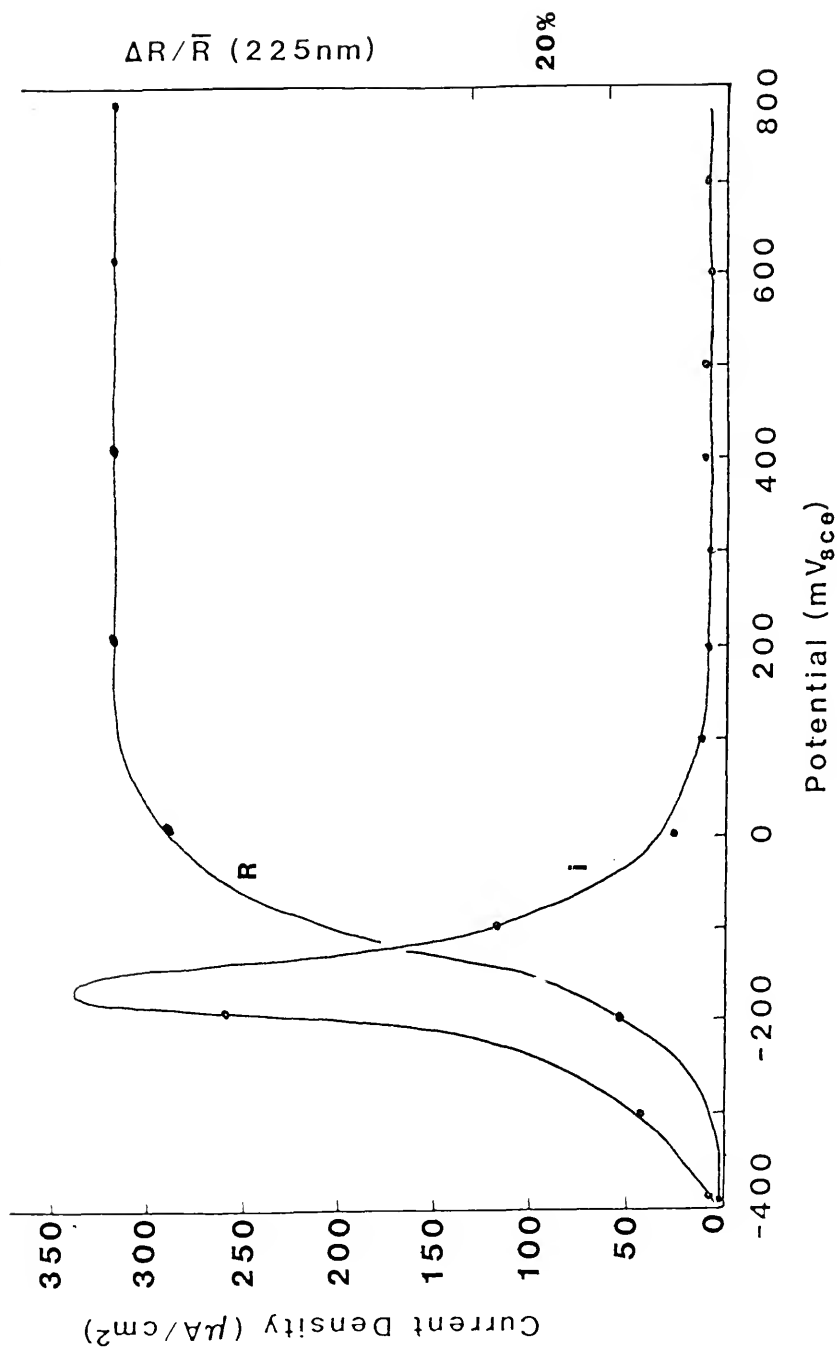


Figure 23. Polarization and reflectivity data for Ni in pH = 4.0, deaerated solution.

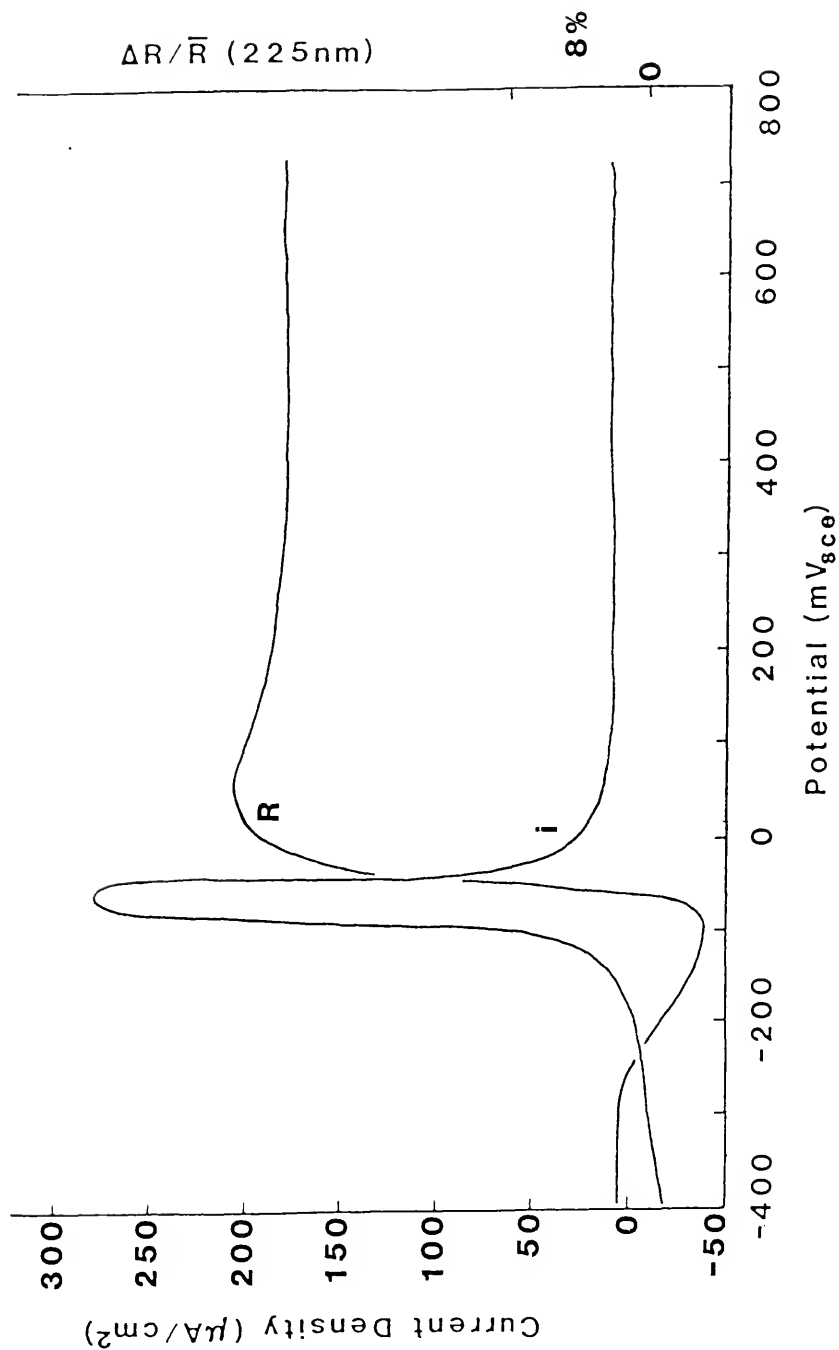


Figure 24. Polarization and reflectivity data for Ni in pH = 4.0, open solution.

high concentration of Ni^{++} ions coupled with the relatively high concentration of OH^- ions results in the rapid (as evidenced by the sharp increase in $\Delta R/\bar{R}$) and uniform (as evidenced by the sharp decrease in current) formation of the passivating $\text{Ni}(\text{OH})_2$ film. It is interesting to note that the passive film in deaerated solution is five times thicker than the same passivating film formed in open solution (c.f. reflectivity data of Figures 23 and 24). A possible explanation for this lies in the fact that in the deaerated solution Ni anodically dissolves into solution at potentials between -400 mV and the passivation potential. It could well be that in this potential region $\text{Ni}(\text{OH})_2$ nucleates on those grains more favorably oriented for film growth (c.f. references 23 and 24) and attains an appreciable thickness on these grains prior to the passivation of the remaining surface. Reflectivity measurements, in fact, show that $\text{Ni}(\text{OH})_2$ is indeed forming even at potentials 150 mV cathodic to the passive potential. After the passive potential is reached, the current drops off relatively slowly--the passive current density not being attained for yet another 200 mV. During this interim the reflectivity data indicate that the film continues to thicken. This rather sluggish passivation behavior is consistent with the suggestion that the film thickness varies over the surface and explains why the average film thickness, as indicated by the reflectivity data, is so great. Based on calculations involving optical constants, this film appears to be approximately 130 \AA thick.

Once the passive plateau is reached the film is very stable and there is no indication of any further thickening throughout the balance of the experiment. The film formed in the open solution, however, appears to thin, i.e., the peak height diminishes somewhat. An alternative interpretation is that the film does not actually thin but

instead small amounts of Ni(OH)_2 precipitate on the optical reference electrode. This is quite possible because of the high hydroxide concentration maintained at surface combined with Ni^{++} ions that could easily diffuse to this surface from the adjacent working electrode.

Although the mechanism of film formation cannot be absolutely determined from the present data several revealing observations can, nevertheless, be made. Firstly, in the open solution the film is observed to be rapidly formed at a potential of -50 mV while, as already pointed out, the same type of surface film is unstable and dissolves at a potential just 50 mV cathodic to this value. Secondly, film formation is accompanied by very large anodic currents which would result in extremely high Ni^{++} ion concentrations near the surface of the electrode. Thirdly, although the magnitudes of the passive currents are the same for the electrode in the deaerated and open solutions, the film is five times as thick in the deaerated case. Moreover, the film in both cases is observed to maintain a constant thickness (disregarding the anomalous effect in the open solution) after formation, i.e., the film thickness is not a function of electrode potential. All four observations indicate clearly that the passivation film forms via a precipitation mechanism.

Anodic Behavior at pH = 8.0

The behavior of the Ni electrode in pH = 8.0, deaerated solution (Figure 25) is quite similar to the behavior already discussed for this electrode in the pH = 4.0 deaerated solution. The similarities include the magnitude of passivating current density ($400 \mu\text{A}/\text{cm}^2$ at pH = 8.0 versus $350 \mu\text{A}/\text{cm}^2$ at pH = 4.0) and the passivation potential (-200 mV

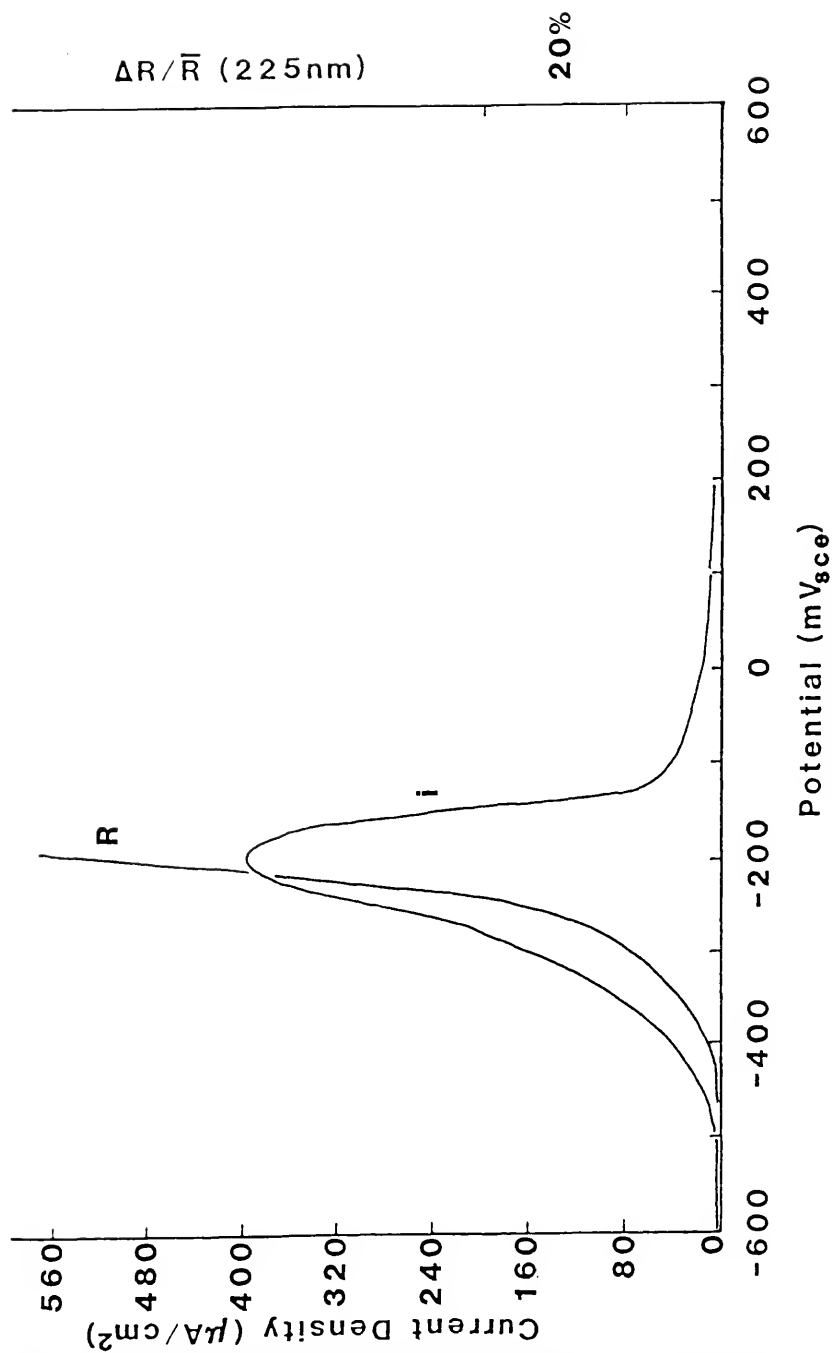


Figure 25. Polarization and reflectivity data for Ni in pH = 8.0 deaerated solution.

versus -170 mV). A third striking similarity is the broad potential range over which passivation occurs (400 mV in both solutions). However, although the passivation film is Ni(OH)_2 in both instances, it is approximately twice as thick in the pH = 8.0 solution. Furthermore, upon removal from the pH = 8.0 deaerated solution the working electrode is observed to be partially covered with a milky-white film; the balance of the surface film appearing clear as usual. (Both reflectivity (Figure 26) and ESCA data indicate that this thicker film is still Ni(OH)_2 .)

Once into the passive plateau the current density is nearly the same for the nickel electrode in the pH = 8.0 deaerated solution as it was in both the deaerated and open solutions of pH = 4.0. This similarity is notable especially since the film thickness varies by a factor of ten among these surfaces. This, of course, suggests that only a relatively thin film is required to achieve passivity. Also note that the current in all three cases (pH = 4.0 deaerated and open, pH = 8.0 deaerated) is constant throughout the passive plateau (a range of about 700 mV) and that there is no increase in film thickness. This indicates that ionic transport through the film is not field dependent but perhaps more a function of the gross structural characteristics, e.g., porosity.

In pH = 8.0, open solution, oxygen reduction is again evidenced by a cathodic current below a potential of about -200 mV (Figure 27, c.f. pH = 4.0, open cell). Above -200 mV the current density is quite low and constant; apparently the electrode was passivated without experiencing active dissolution. Reflectivity data shows that the film grows steadily from the start of the experiment and, as expected, no

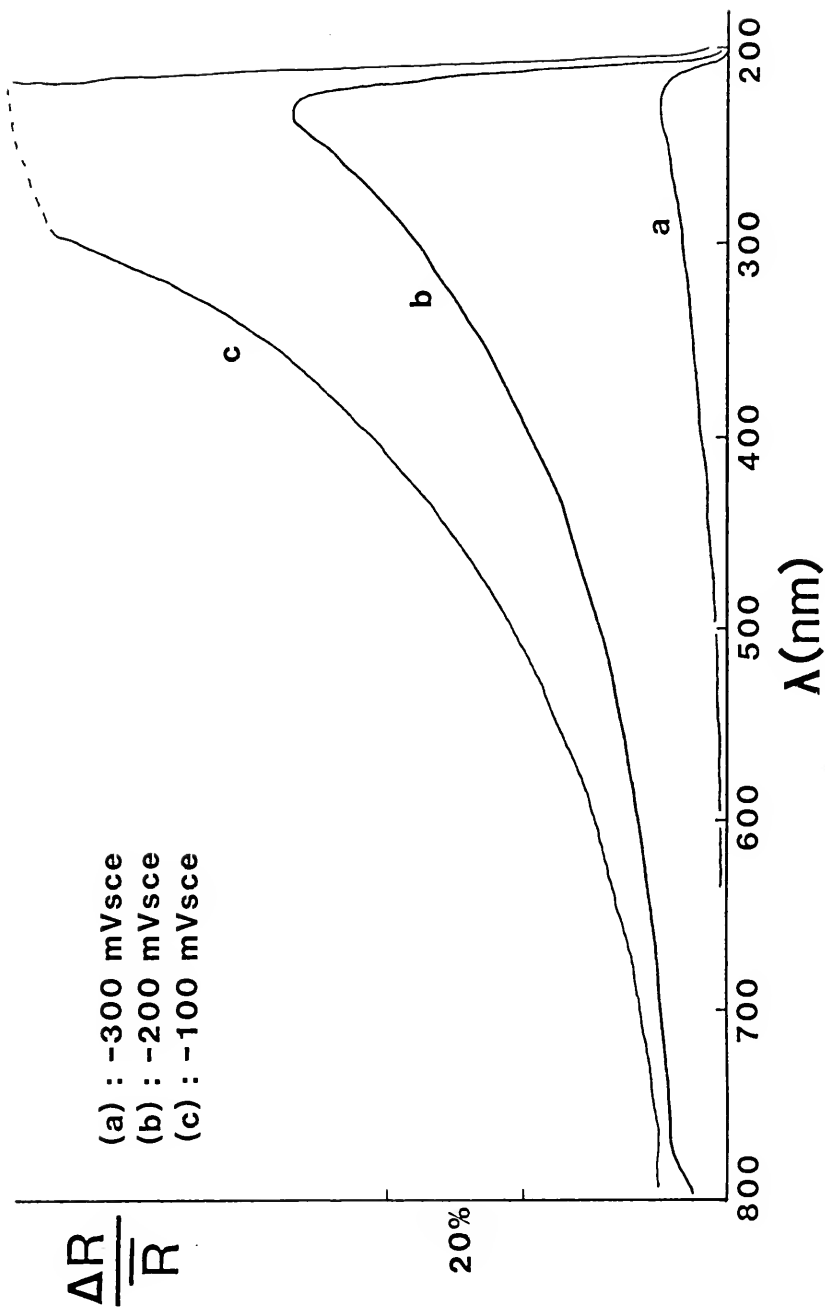


Figure 26. Reflectograms indicating the formation of a thick $\text{Ni}(\text{OH})_2$ film in $\text{pH} = 8.0$, deaerated solution.

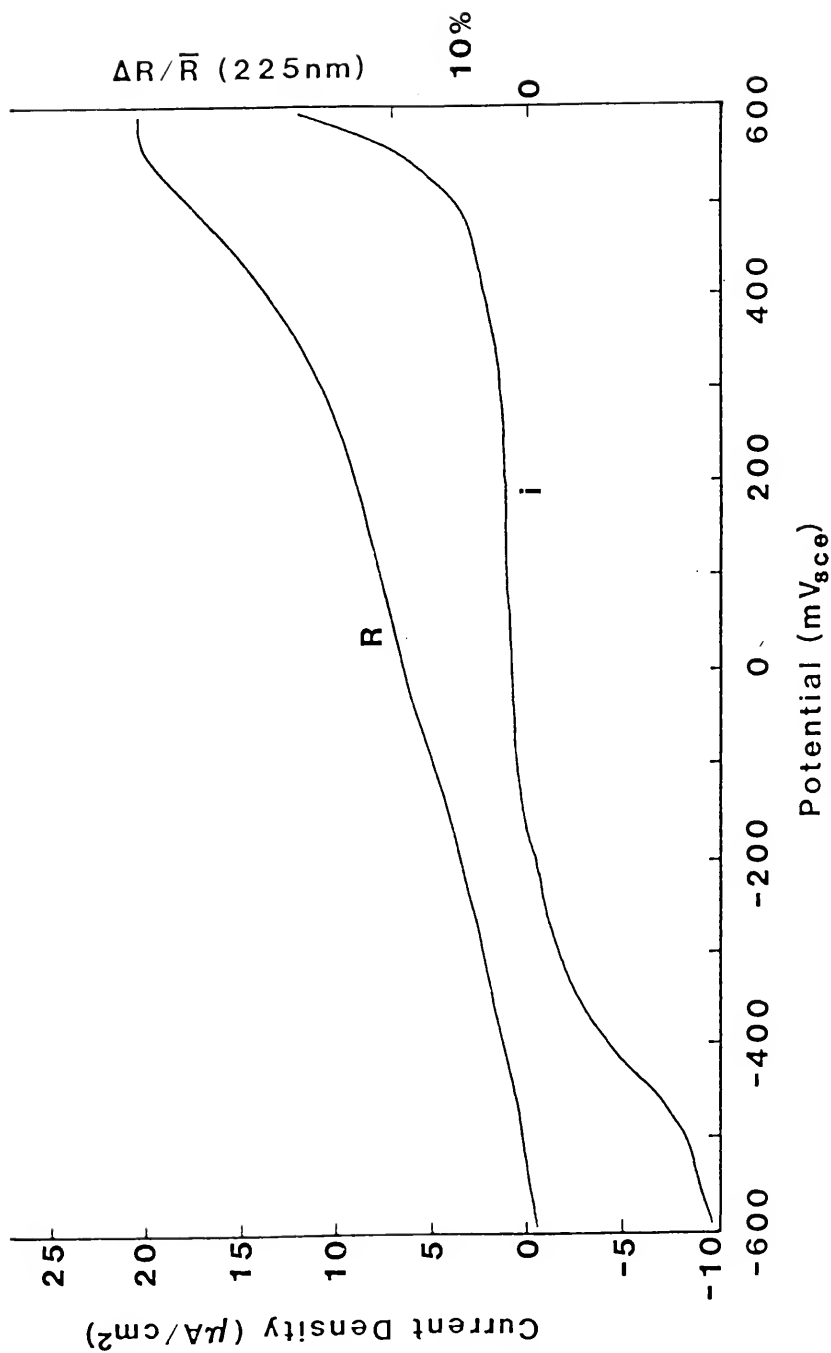


Figure 27. Polarization and reflectivity data for Ni in pH = 8.0, open solution.

reduction of the "as-polished" film occurs as it did in the pH = 4.0 open solution.

Near -100 mV a small NiO component in the film develops (Figure 28). As the potential is increased this component becomes somewhat more prominent although it never appears as more than a shoulder on the Ni(OH)_2 reflectivity structure.

The overall film thickness throughout the experiment appears to be a linear function of potential. This linear dependency indicates that field assisted ionic conduction through the film is likely responsible for the passive current which is in contrast to the films already discussed. Reflectivity data indicate that the film under present consideration is some 60 times thinner than the film formed in the deaerated solution. Both observations support the suggestion that the conduction mechanism in the two films is quite different.

Also in contrast to the three films previously discussed is the fact that this thin film converts to NiOOH at potentials near the oxygen evolution potential. Since the composition of all the films in the passive regions is virtually identical, the only explanation is that the field across the thinner, more coherent film is large enough for the transforming deprotonation reaction to occur. The field across a bulkier film at a similar potential would, of course, be considerably less.

Anodic Behavior at pH = 12.0

The general behavior of the nickel electrode in pH = 12.0, open and deaerated, is similar to that just discussed for pH = 8.0 solution. In the pH = 12.0 open solution oxygen reduction is again indicated at

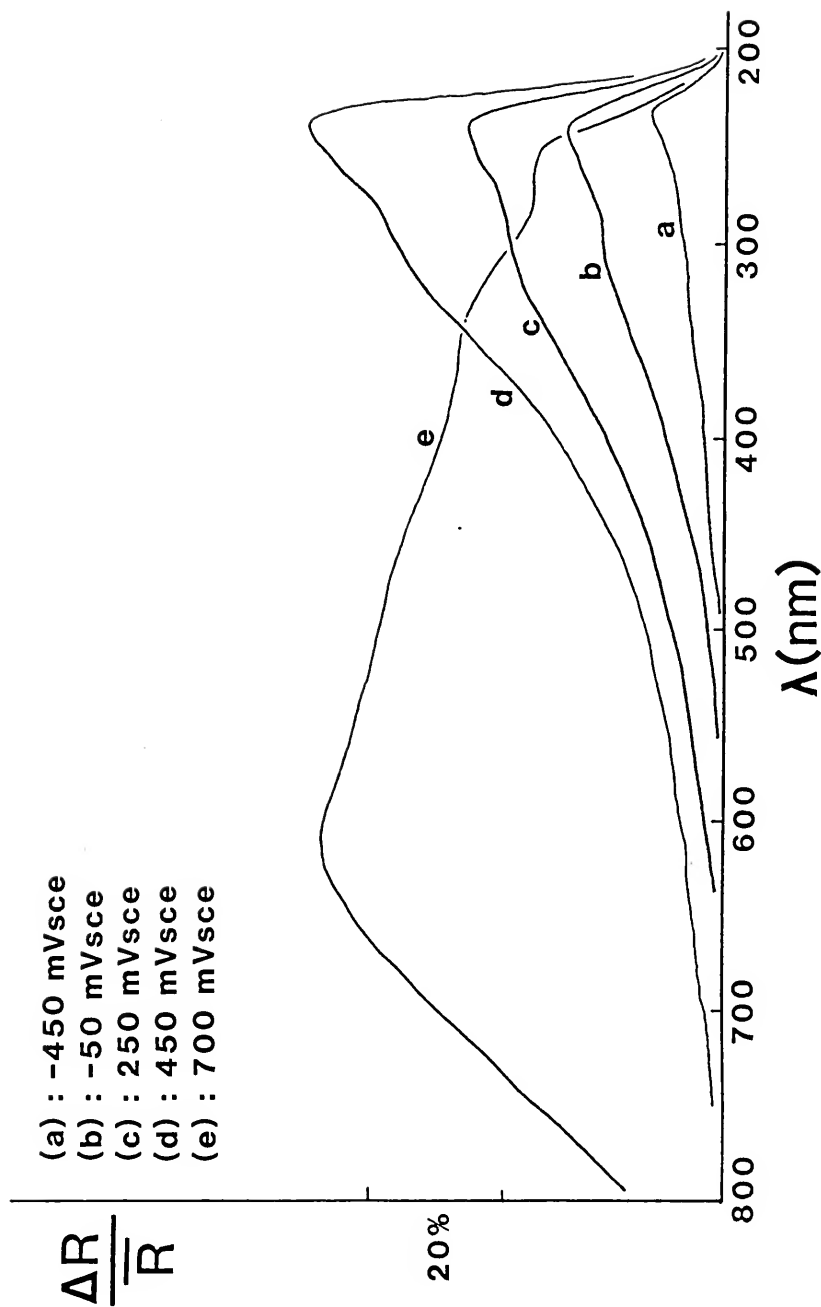


Figure 28. Reflectograms indicating $\text{Ni}(\text{OH})_2$, NiO and NiOOH as formed in $\text{pH} = 8.0$, open solution.

potentials near the start of the experiment (Figure 29). Once oxygen reduction has ceased (-600 mV), the current becomes slightly anodic and maintains a rather modest current density of $4 \mu\text{A}/\text{cm}^2$ until the oxygen evolution potential is reached. As was the case for the pH = 8.0 open solution, passivation occurs without active dissolution. The film thickness is again a linear function of electrode potential with the NiO shoulder appearing at a potential of approximately 0 mV (Figure 30).

In the pH = 12.0 deaerated electrolyte, the film growth is again a linear function of potential (Figure 31) but thickness is approximately half that obtained in the open solution. The NiO shoulder again appears near 0 mV (Figure 32). Transformation of $\text{Ni}(\text{OH})_2$ into NiOOH is observed for both the open and deaerated solutions at a potential of about +450 mV.

In summary, the behavior of Ni in 0.15 N Na_2SO_4 can be divided into two distinct categories. In solutions of low pH (pH = 4.0 open and deaerated, pH = 8.0 deaerated) a very thick passivating $\text{Ni}(\text{OH})_2$ film forms apparently by a precipitation mechanism. This film, once formed, does not thicken throughout the balance of the experiment. It has also been noted that neither NiO nor NiOOH is observed in these solutions. Also, the current density throughout the passive plateau is relatively high ($8\text{--}10 \mu\text{A}/\text{cm}^2$).

These conclusions concerning film composition are quite different than those reached by Okamoto and Sato [15-17] who stated that NiO , Ni_2O_3 and Ni_3O_4 are all formed in low pH solution (4.5). Although Bockris and Reddy did identify $\text{Ni}(\text{OH})_2$ on a nickel electrode in a solution of pH = 3.15, they stated that it was merely a precursor film rather than the film actually responsible for passivation. This of course is in direct

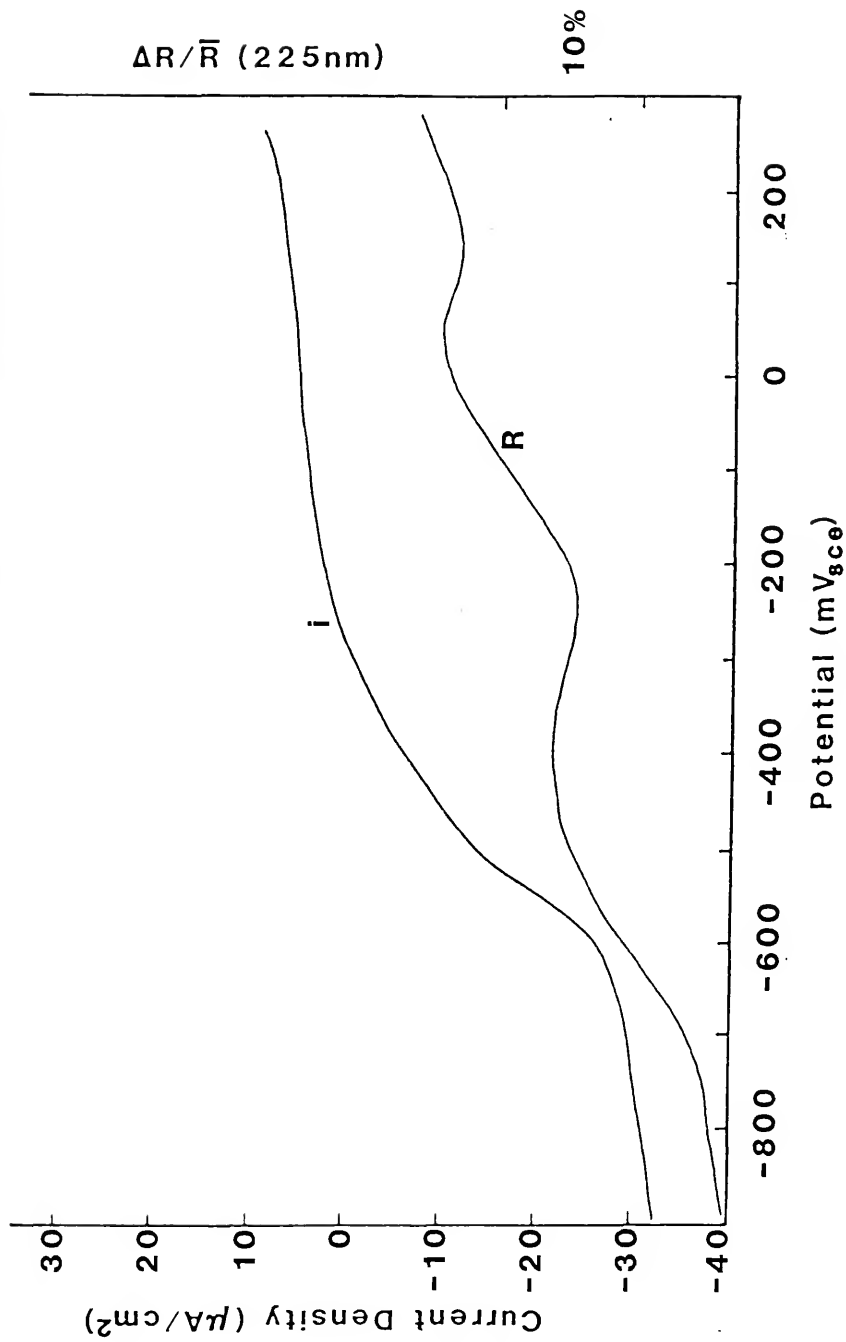


Figure 29. Polarization and reflectivity data for Ni in pH = 12.0, open solution.

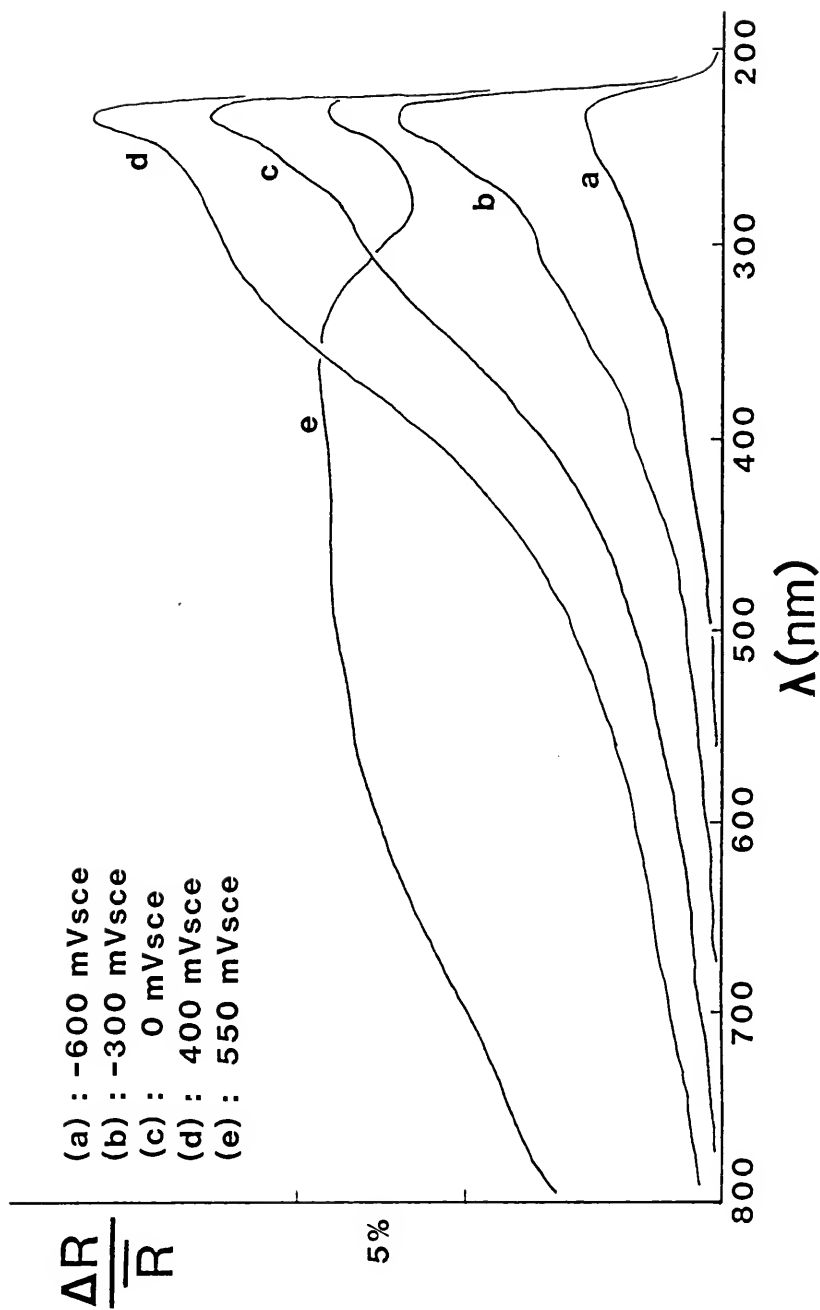


Figure 30. Reflectograms indicating Ni(OH)_2 , NiO and Ni(OH)_2 in pH = 12.0, open solution.

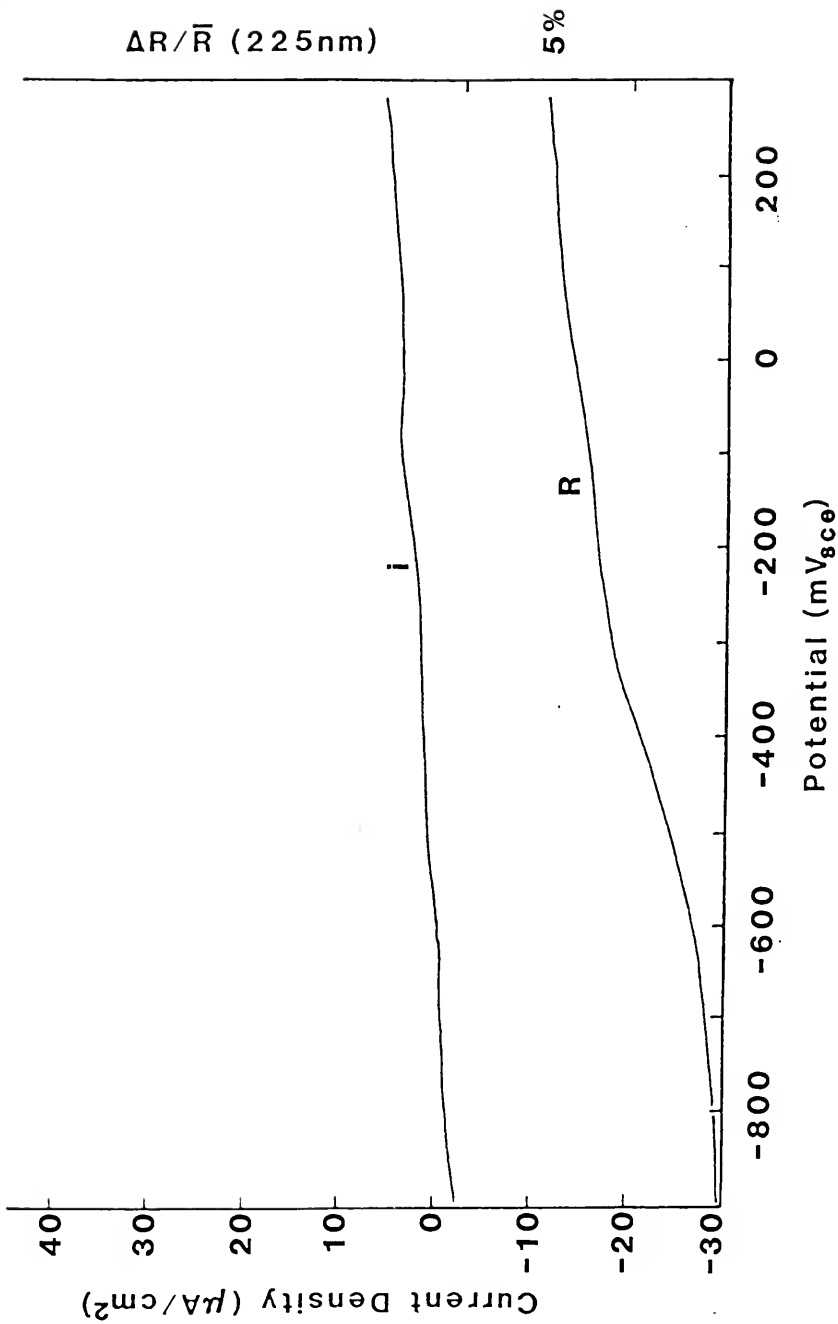


Figure 31. Polarization and reflectivity data for Ni in pH = 12.0, deaerated solution.

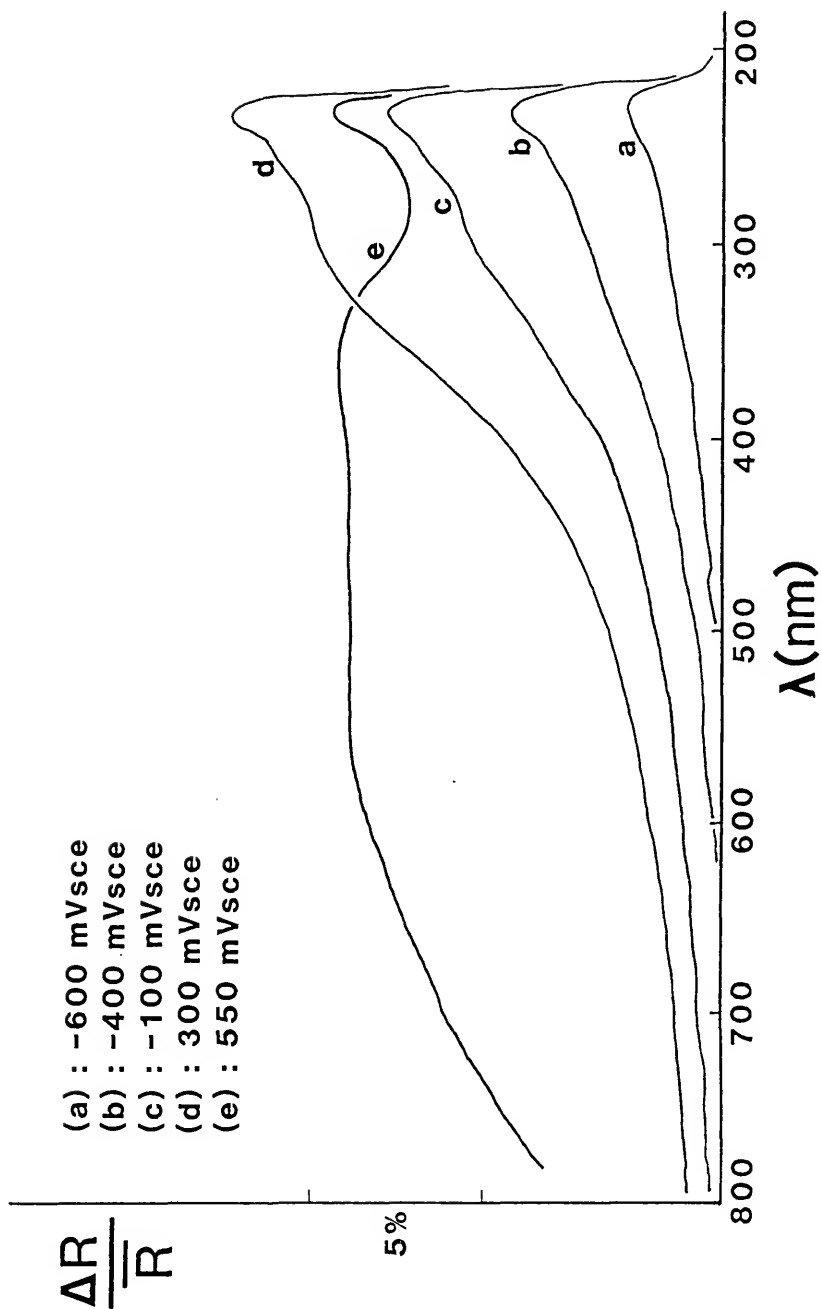


Figure 32. Reflectograms again indicating $\text{Ni}(\text{OH})_2$, NiO and NiOOH in $\text{pH} = 12.0$, deaerated solution.

contrast with the evidence just presented which indicates that Ni(OH)_2 formation is concurrent with the passivation process. There is also notable contrast between the present work and the work published by MacDougall et al. [13,27-30,34-37,44,53]. Employing virtually identical experimental procedure (50 mV potential steps in 0.15 N Na_2SO_4 solution of pH = 2.8 and 8.4) they concluded that NiO was the passivating film, and, furthermore, that NiO was the only film to form on a Ni electrode. A possible explanation for this disagreement lies in the fact that MacDougall et al. electropolished and cathodically pretreated their electrode before running the experiment while the "as polished" electrode is used in the present case. Since it has been shown that the "as polished" film dissolves before the passivation process begins (c.f. Figure 19 and discussion on pages 46-47) it is suggested that the NiO film identified in those experiments by MacDougall et al. may actually be formed in the pretreatment process. This would also explain why the film is always reported to be 9-12 Å thick independent of both potential and solution pH.

Although Ord et al. [33] also report the formation of Ni(OH)_2 on a Ni electrode, they suggest that it forms by hydration of an initial passivating NiO film on multisweep potentiodynamic experiments. In fact, no study can be found in the literature that essentially agrees with the present work as to the composition of the passivating film on Ni in acid solutions.

In contrast to the behavior just discussed for acid solutions, solutions of a high pH (pH = 8.0 open, pH = 12.0 open and deaerated) produce a very thin passivating Ni(OH)_2 film, apparently by a solid state growth mechanism. This film is somewhat more protective as

evidenced by a low current density of $3\text{--}5 \mu\text{A}/\text{cm}^2$ in the passive region. Although not observed in the low pH regime, NiO occurs at intermediate potentials while the transformation of $\text{Ni}(\text{OH})_2$ into NiOOH is apparent near the oxygen evolution potential.

Davies and Barker [39] also reported that a very thin (1 monolayer) film of $\text{Ni}(\text{OH})_2$ was responsible for the passivation of Ni in high pH solution (13.0). They also reported the development of two additional film components at higher potentials but identified these as Ni_2O_3 and NiO_2 , in contrast to the present results. Remarkable agreement is also noted with the work of Schebler-Guzman et al [40] who report the conversion of a passivating $\text{Ni}(\text{OH})_2$ film into NiOOH at a potential near the oxygen evolution potential. The formation of $\text{Ni}(\text{OH})_2$ is also suggested by Lee [41] although no higher oxides are observed in his experiments.

Anodic Behavior of Nickel in .15 N Na_2SO_4 Containing Chlorides

Anodic Behavior at pH = 4.0

When Cl^- ions are added to pH = 4.0 open solution, the prepassive response of the Ni electrode is qualitatively unchanged. As before, a negative peak occurs on the reflectogram (Figure 33) in the initial potential region. The magnitude of the peak in this case is larger, however, indicating that the dissolution of the "as-polished" film is more complete in the Cl^- environment. Active dissolution along with $\text{Ni}(\text{OH})_2$ film growth are observed at potentials slightly cathodic to the initial film dissolution reaction with the film being 25% thicker in this case. The passive potential in the Cl^- environment is slightly

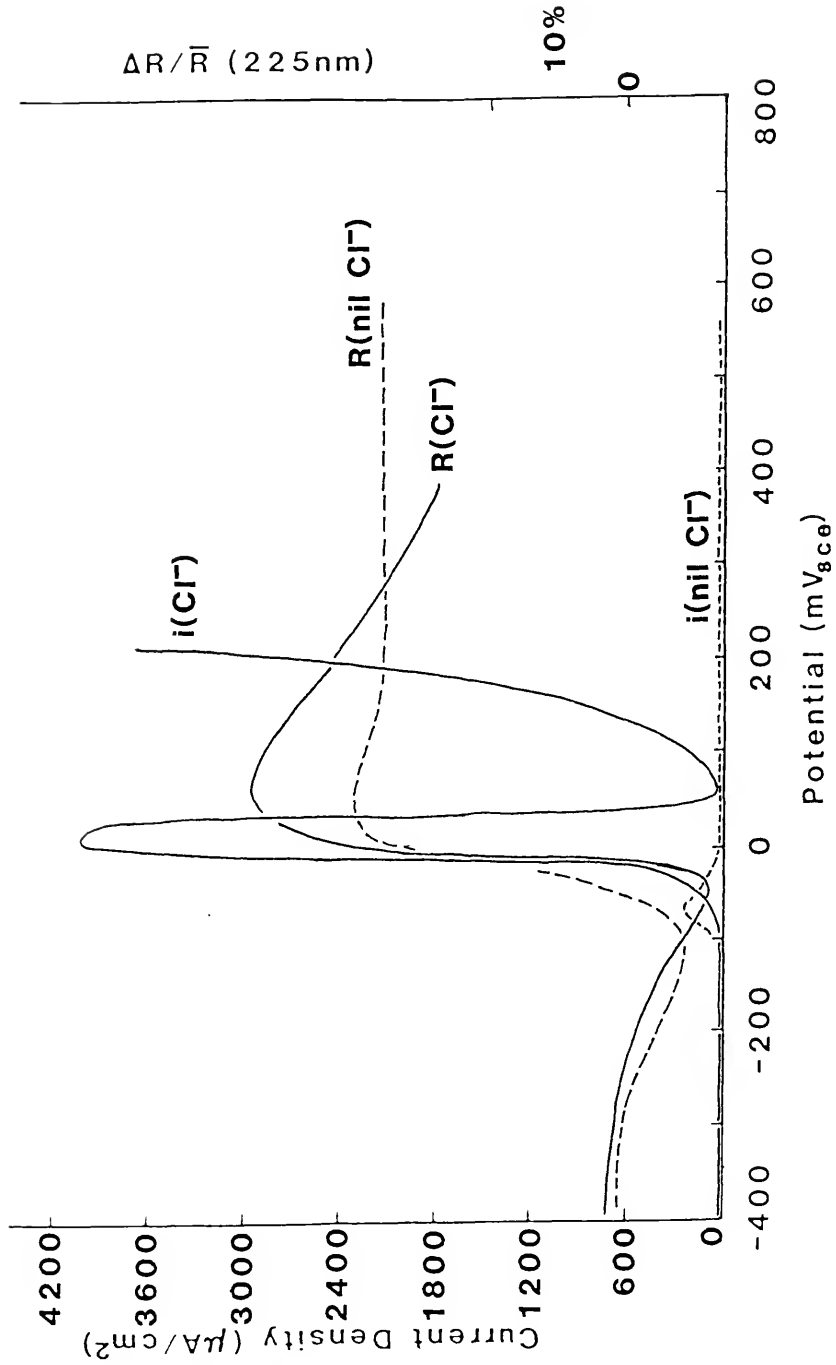


Figure 33. Polarization and reflectivity data for Ni in pH = 4.0, open solution with/without Cl^- .

higher (75 mV) while the current density at this potential is greater by a factor of 16.

Immediately after passivation the current again rises rapidly and is accompanied by a concurrent decrease in reflectivity with the spectra being identical to that obtained in the nil Cl^- solutions. Upon removal from solution, the surface of the electrode appears severely pitted. The decrease in reflectivity during depassivation can be explained either by the initiation and growth of pits, by film thinning, or both.

In the deaerated electrolyte, $\text{pH} = 4.0$, containing Cl^- ions, the passivating current is again higher than in the chloride-free environment (Figure 34). However, passivation in this case is never completed. Rather, breakdown occurs prior to the electrode being truly passive. As was the case in the open solution, Ni(OH)_2 formation is delayed to slightly more anodic voltages but the rate of formation, once initiated, is considerably larger. The Ni(OH)_2 film formed in this deaerated solution is so thick that the DR saturates. Because of this, it cannot be determined whether reflectivity drops off with the loss of passivation as it did before.

Anodic Behavior at $\text{pH} = 8.0$

The response of the nickel electrode in the $\text{pH} = 8.0$ deaerated solution containing chlorides is similar to the behavior just discussed for the $\text{pH} = 4.0$ solutions. Subsequent to active dissolution, passivation occurs but is lost almost immediately (Figure 35). The passivating film is so thick that saturation occurs. A surprising feature of this data, however, is that the passivating current density is approximately 20% less for this solution than for the Cl^- free

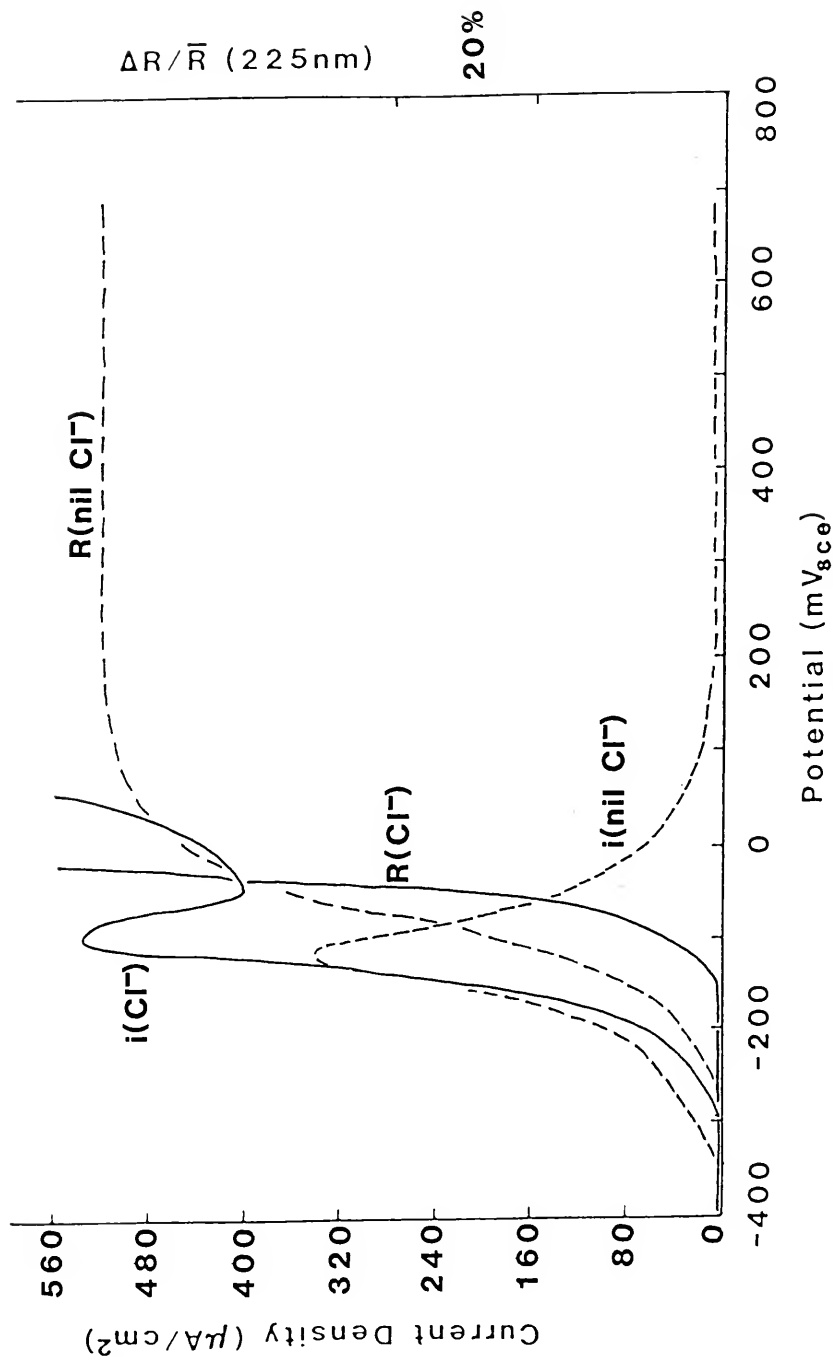


Figure 34. Polarization and reflectivity data for Ni in pH = 4.0, deaerated solution with/without Cl^- .

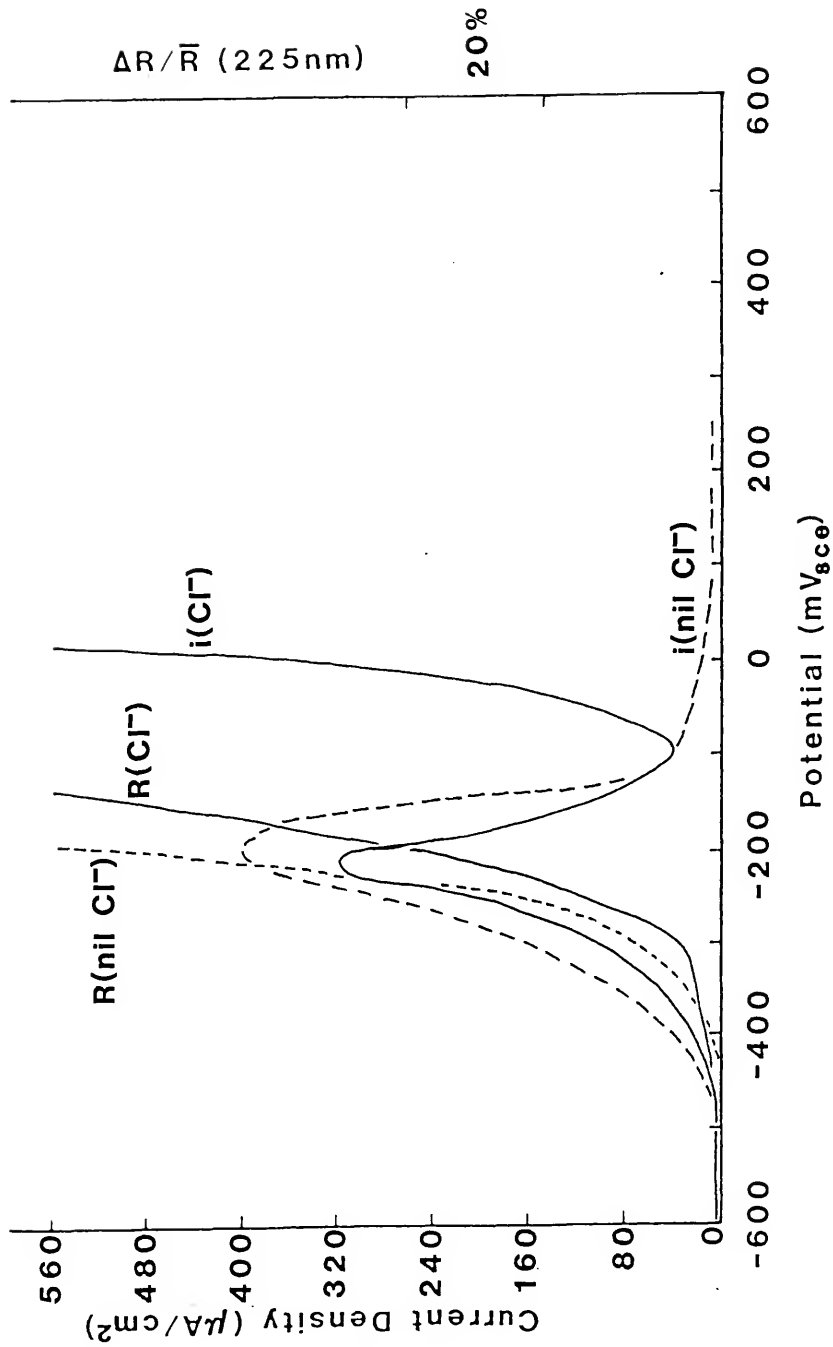


Figure 35. Polarization and reflectivity data for Ni in pH = 8.0, deaerated solution, with/without Cl^- .

electrolyte. The reflectivity data is, nonetheless, consistent with the rest of the data presented to this point in that film growth occurs at slightly more anodic values for the electrode in the Cl^- containing solution. This observation is in agreement with the conclusion reached by T. S. Lee [41].

Since active dissolution occurs at the same or slightly more anodic potentials in all the chloride containing solutions presented so far, it can be concluded that the role of the Cl^- ion is not to facilitate the dissolution mechanism. This conclusion is in contrast with that offered by Kronenberg et al. [48] but is in substantial agreement with the work done by MacDougall [53]. A second contrasting conclusion that can be drawn from the present work is based on the in situ reflectivity data which indicate that the passivating film is identical in composition to the film formed in the Cl^- free solutions. Furthermore, no precursor films are formed. This is in disagreement with the speculation advanced by Vilche and Arvia [49] that NiCl_2 forms on the electrode prior to passivation.

One particularly interesting suggestion made in the literature was offered by Bengali and Nobe [58]. Although they had no specific analytical evidence, they suggested that the Cl^- ions tend to complex the divalent Ni ions immediately subsequent to dissolution. According to their theory the complexing species for acid solutions is NiClH^+ . Such complexing action could explain the behavior discussed in the present study, especially for the electrodes in pH = 4.0 solutions.

If, after dissolution, Ni^{++} ions are complexed into a species such as NiClH^+ , then they are no longer available to participate in the precipitation reaction that results in passivity. Thus, the Cl^- ions, in

effect, lower the Ni^{++} concentration at the surface although the dissolution rate is considerably higher than in the Cl^- -free electrolytes. Once the Cl^- ions near the surface have been complexed, the Ni^{++} ions are free to react with the OH^- species resulting in the precipitation of $\text{Ni}(\text{OH})_2$ onto the surface.

After film formation the Cl^- concentration at the surface of the electrode is replenished by diffusion from the bulk solution. Perhaps these Cl^- ions are able to exchange with the OH^- in the protective film again forming a soluble Ni^{++} complex. Such an exchange would be more likely at defects in the film where the $\text{Ni}(\text{OH})_2$ is chemically less stable. Once initiated, localized attack is likely to continue since depletion of the Cl^- ions near an isolated defect would be unlikely. Once perforation of the film is achieved metal is once again free to dissolve with repassivation being unlikely because of the large sink of Cl^- available for complexing. Thus a pit initiates and grows.

In the $\text{pH} = 8.0$ open solution containing Cl^- ions, the film grows via a solid state mechanism just as it did in the nil Cl^- solution. The film in the present case, however, is appreciably less protective as evidenced by a much thicker film permitting a current density nearly twice that obtained in the Cl^- free environment, Figure 36. Midway through the passive region reflectivity diminishes and the current increases drastically--a clear indication that passivity is lost. The fact that depassivation occurs at + 100 mV in the open solution as compared to -100 mV in the deaerated solution suggests that the OH^- concentration can play a critical role in the response of the electrode in the intermediate pH solutions.

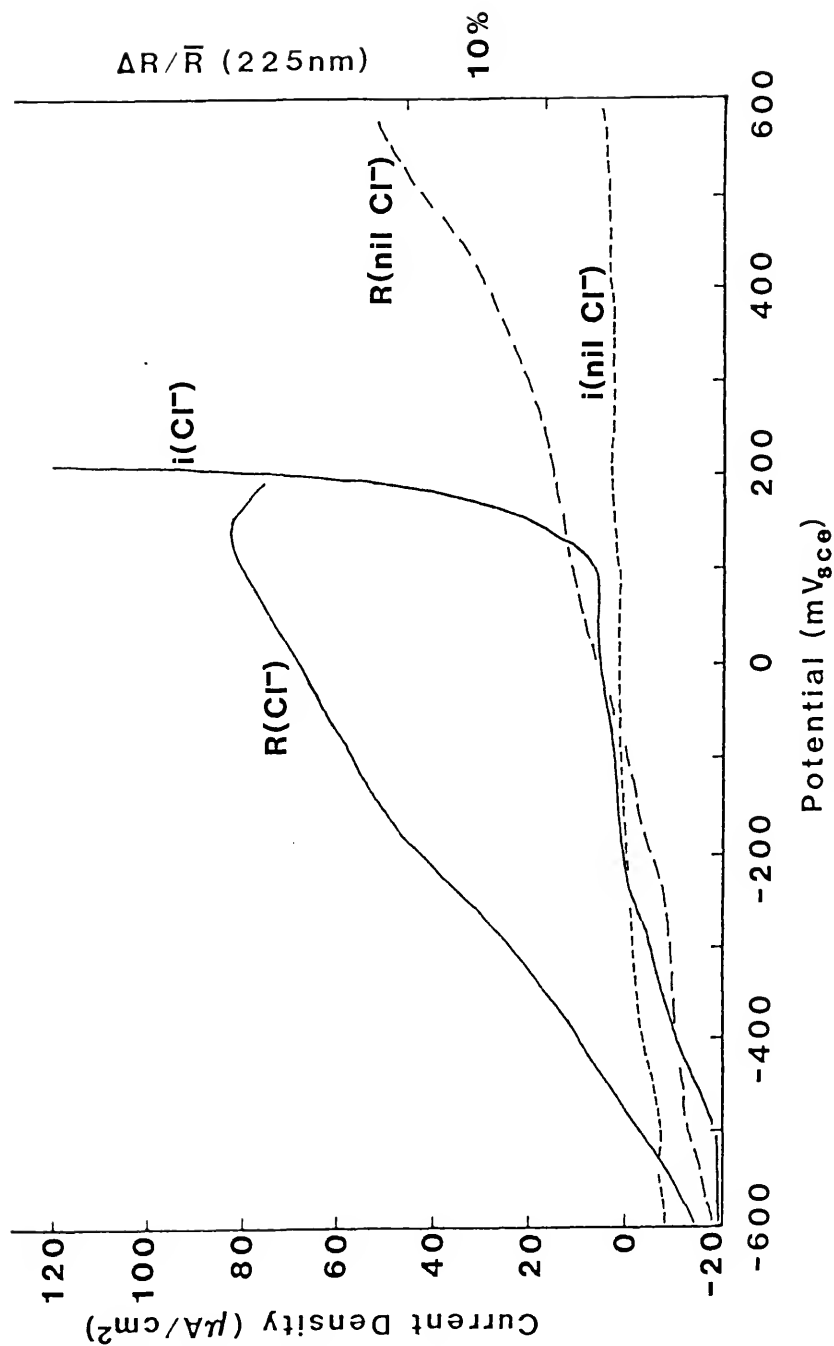


Figure 36. Polarization and reflectivity data for Ni in pH = 8.0, open solution with/without Cl^- .

Anodic Behavior at pH = 12.0

In the pH = 12.0 electrolyte, both open and deaerated, the OH^- concentration is large enough to negate the effects of the Cl^- ions. As seen in Figures 37 and 38 the film growth and current densities for the solutions with and without Cl^- ions are practically identical. This further supports the theory that Cl^- and OH^- compete for the Ni ions.

In summary, although the addition of chlorides to the electrolyte does not influence the composition of the passivating $\text{Ni}(\text{OH})_2$ film, they do severely alter the stability of this film in low pH solutions. This is in substantial agreement with Lee [41] who noted that passivation occurred at mere anodic values when Cl^- were present. Breakdown as well as pitting were reported by Zamin and Ives [50] and also by MacDougall [53]. However, the speculation advanced by Vilche and Arvia [49] that a NiCl_2 layer is formed on the surface is not borne out by the present optical data.

In contrast, the addition of chlorides to the alkali solutions affects neither film composition nor film stability. This suggests that if chlorides cannot be eliminated from a solution, the aggressiveness of the solution towards nickel can be diminished by raising the pH.

Anodic Behavior of Nickel -30 Copper in .15 N Na_2SO_4

Anodic Behavior at pH = 4.0

The Ni-30 Cu alloy exhibits an active-passive transition in the pH = 4.0 open solution (Figure 39) that occurs at a potential approximately 175 mV anodic to the transition for a pure Ni electrode. The passivation current density is greater by a factor of about 20.

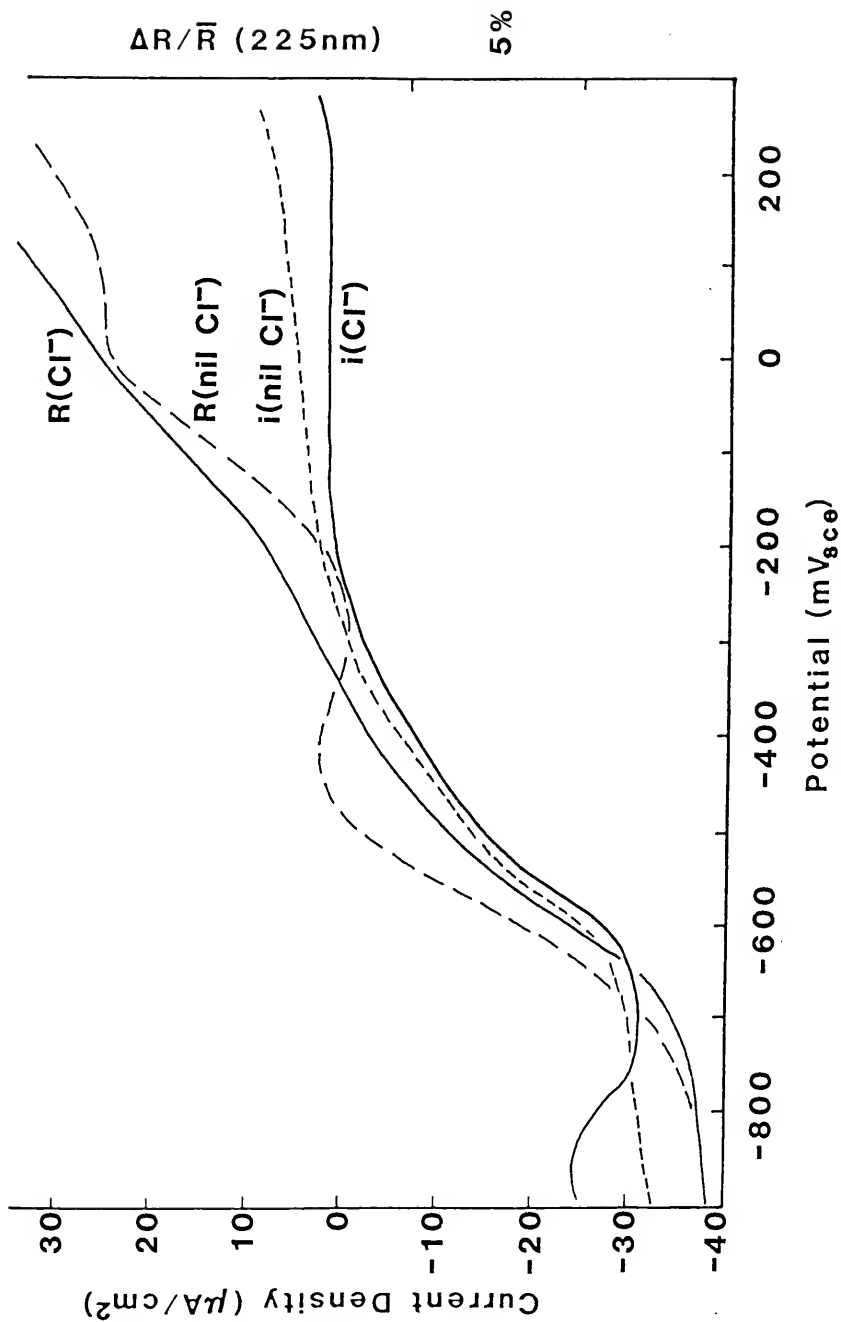


Figure 37. Polarization and reflectivity data for Ni in pH = 12.0, open solution with/without Cl⁻.

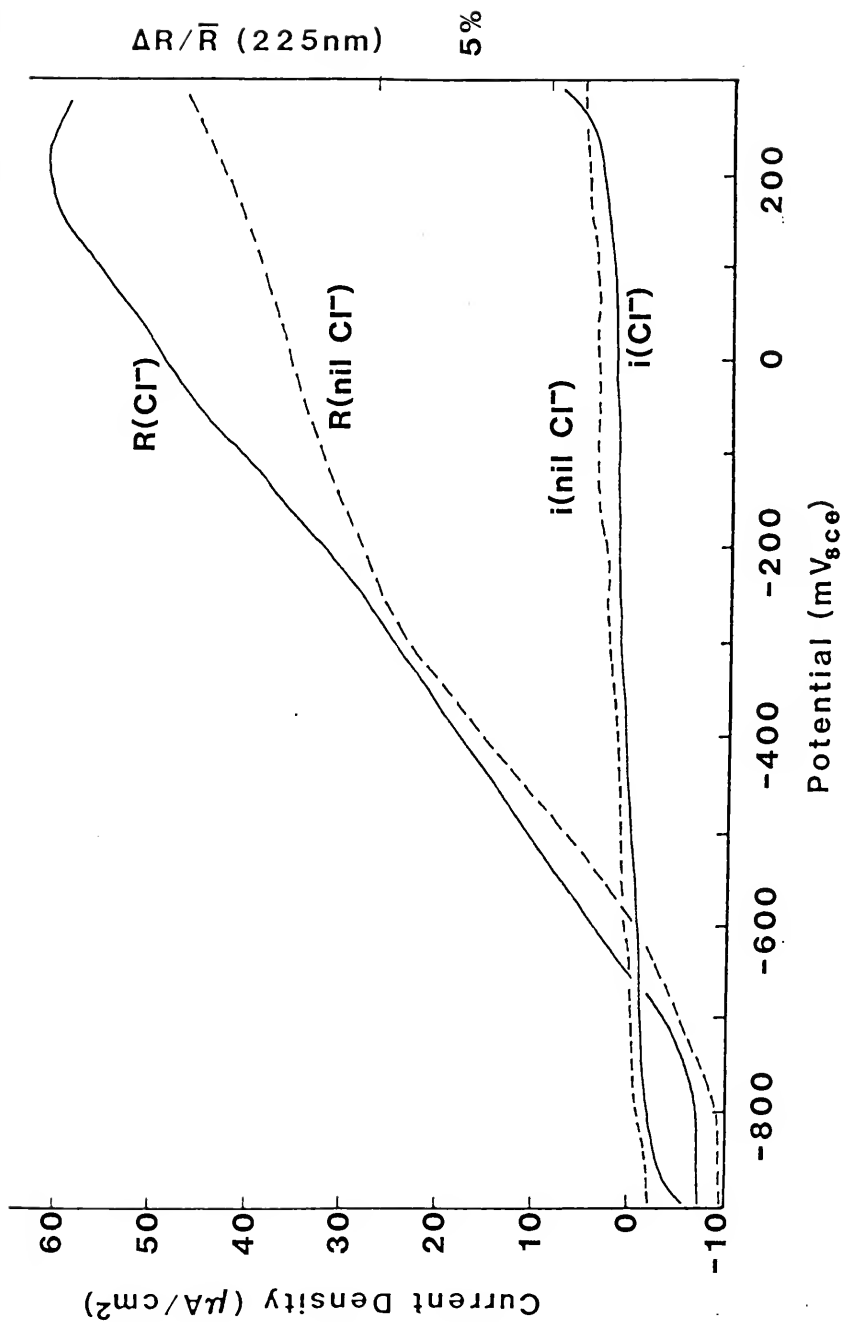


Figure 38. Polarization and reflectivity data for Ni in pH = 12.0, deaerated solution with/without Cl^- .

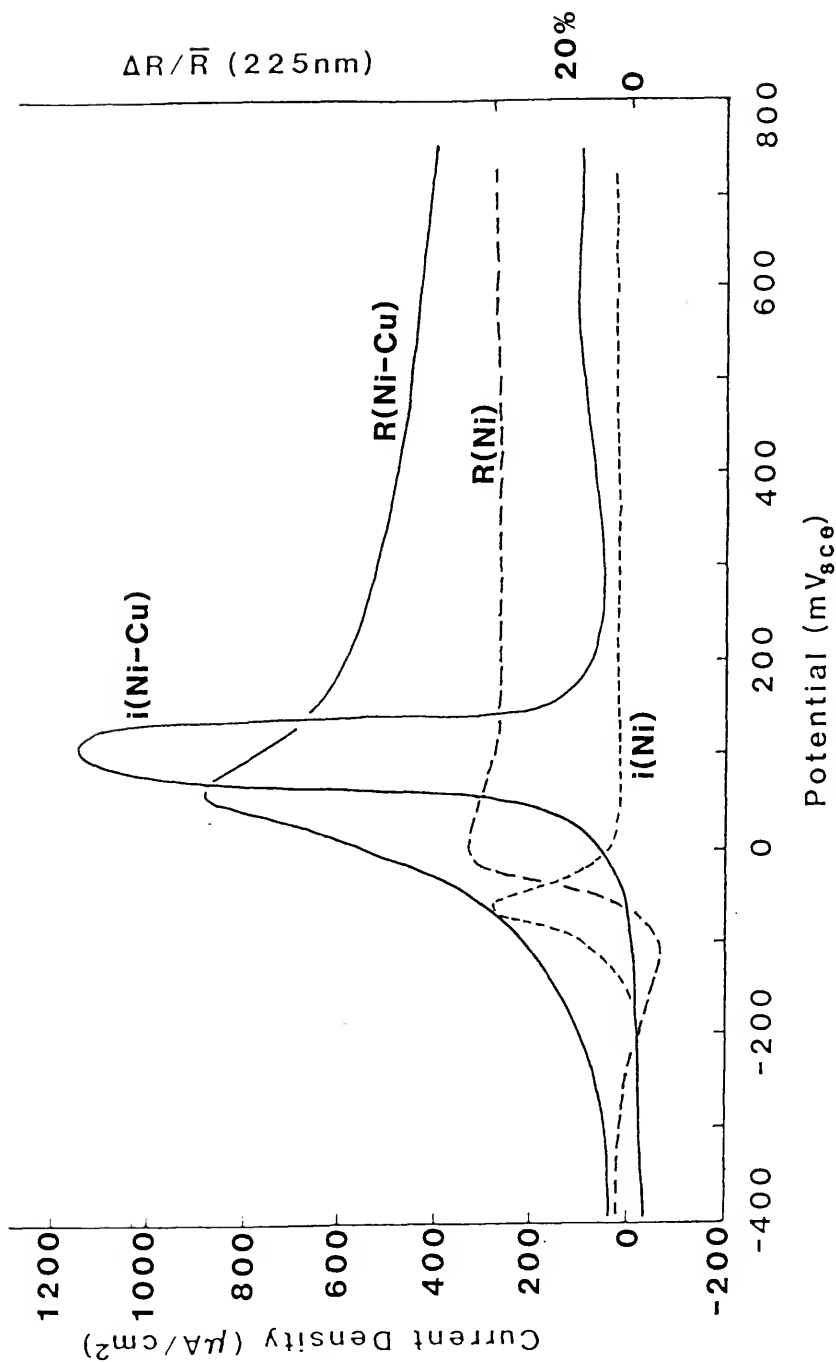


Figure 39. Polarization and reflectivity data for Ni-30 Cu in pH = 4.0, open solution.

Moreover, no initial film reduction is evidenced, but rather a film is actually formed practically from the start of the potential scan (Figure 40). From -150 mV to +100 mV the film appears to be a mixture of Ni(OH)_2 and Cu_2O (Figure 41). However, at somewhat more anodic potentials the reflectivity data indicates that the film is pure Ni(OH)_2 and decreases in thickness as the potential is increased. The thickness of this film is, nevertheless, substantially greater than the film on pure Ni in this solution.

In deaerated pH = 4.0 solution the passivation potential for the alloy is 275 mV more anodic than for pure Ni, while the corresponding current density is four times greater, Figure 42. The passive current density is also greatly affected by the alloying. In addition, unlike the behavior in the open cell just discussed, no surface film develops until -50 mV at which point pure Ni(OH)_2 can be clearly detected (Figure 43).

However, in addition to the Ni(OH)_2 peak at 225 nm, a second structure is present on the reflectogram between 550 nm and 800 nm. As the potential is made increasingly anodic this structure develops further with a more complex curve shape evolving at the lower wavelengths. Analysis of this series of reflectograms indicates that these curves are the result of not only a surface film but also a compositional difference between the optical reference electrode and the working electrode. Note how the reflectogram obtained at +100 mV can be reproduced (Figure 44c) by the addition of a typical Ni(OH)_2 curve to a reflectogram obtained by comparison of a Ni-75 Cu alloy and a Ni-70 Cu alloy (Figure 44b). This suggests that the working electrode is deficient in Cu relative to the optical reference electrode, which is a

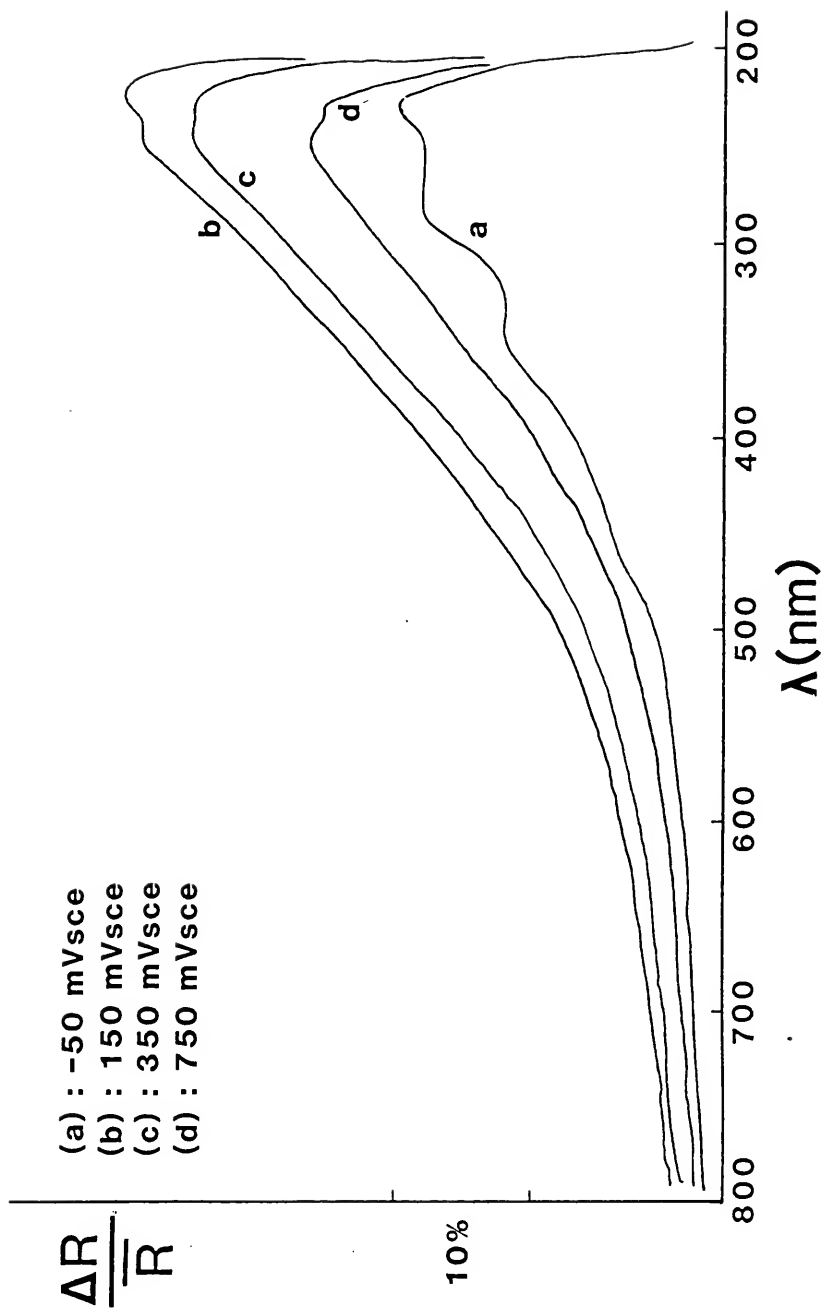


Figure 40. Reflectograms for Ni-30 Cu in pH = 4.0, open solution, which indicate a mixed $\text{Ni}(\text{OH})_2\text{-Cu}_2\text{O}$ oxide and subsequent film thinning.

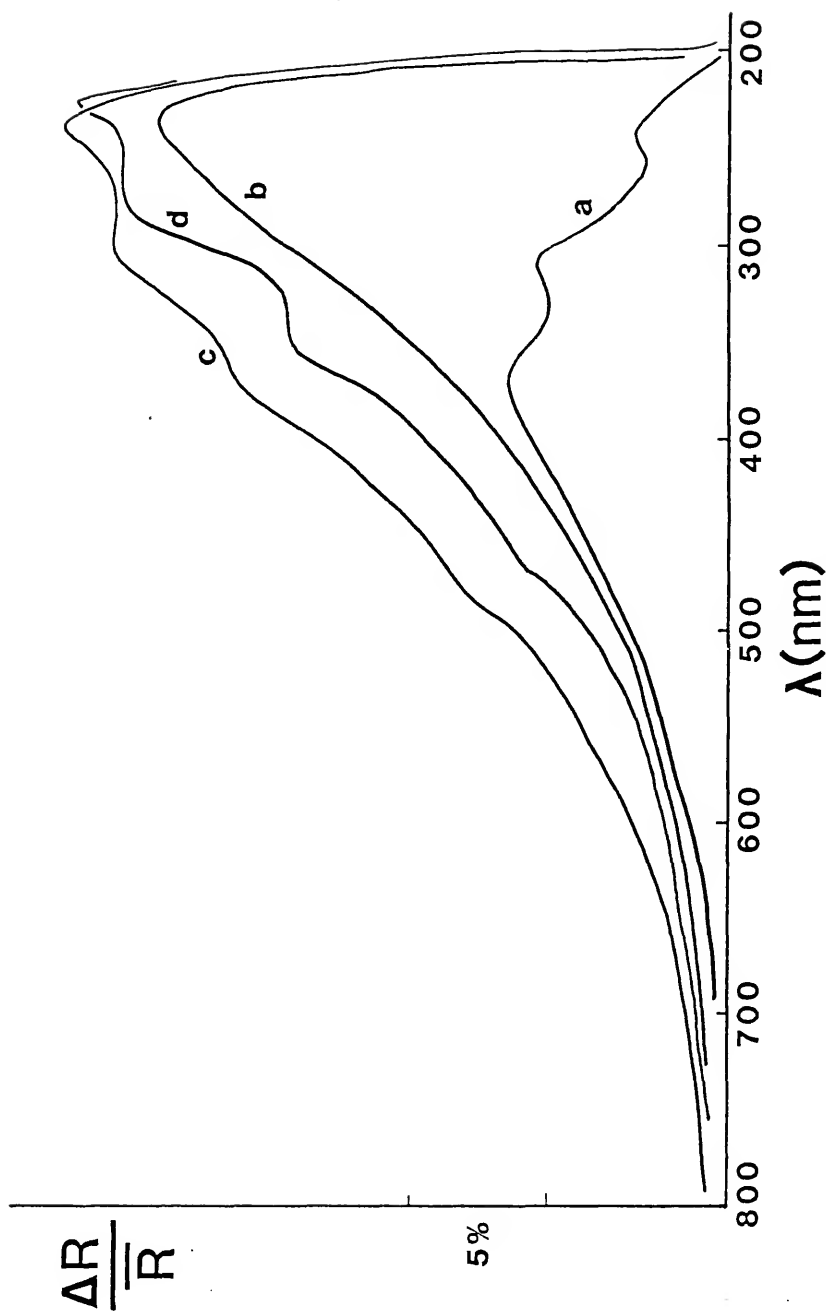


Figure 41. The addition of a Cu_2O curve (a) to a $\text{Ni}(\text{OH})_2$ curve, (b) results in a reflectogram (c) that is very similar to that obtained from the Ni-30 Cu electrode (d) at $-50 \text{ mV}_{\text{SCE}}$ in the $\text{pH} = 4.0$ open solution.

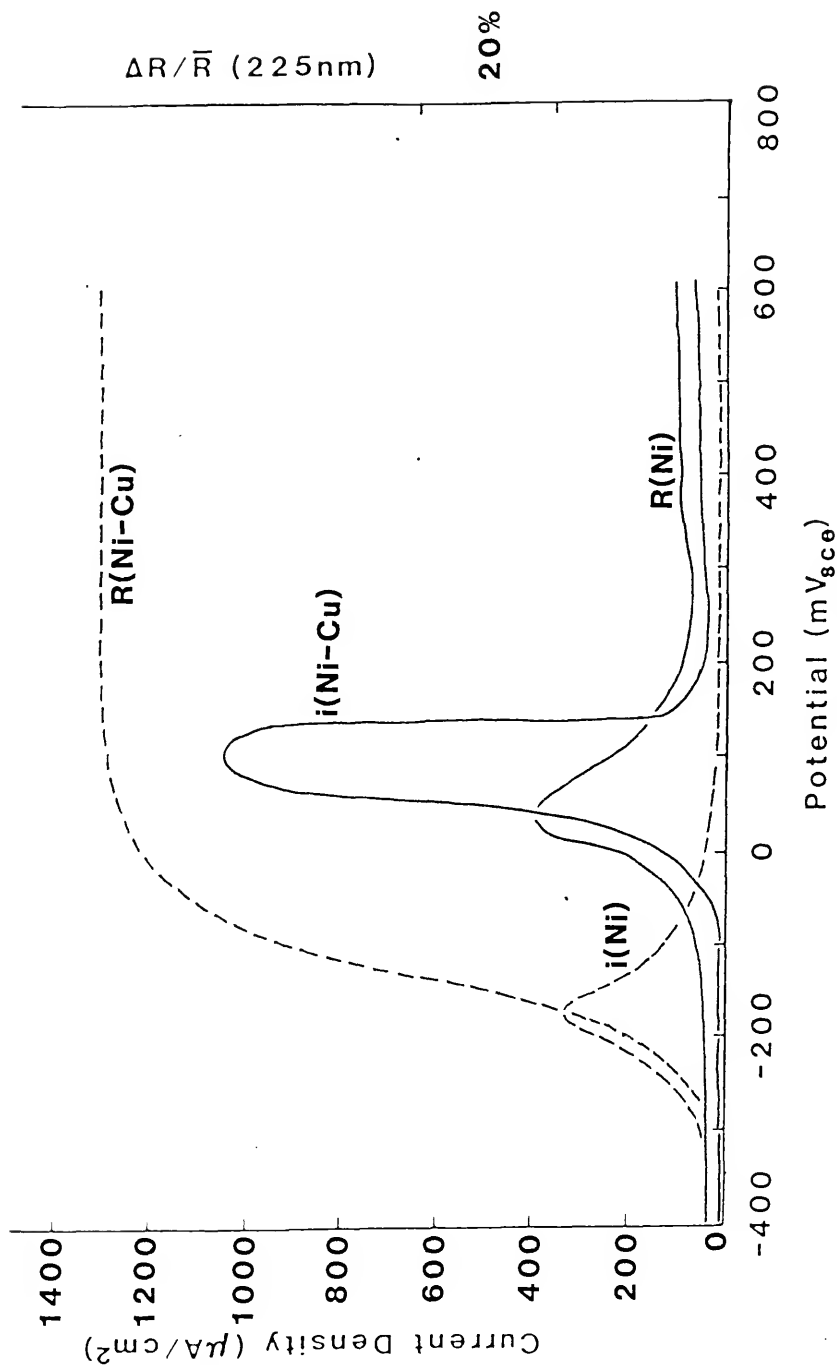


Figure 42 Polarization and reflectivity data for Ni-30 Cu in pH = 4.0, deaerated solution.

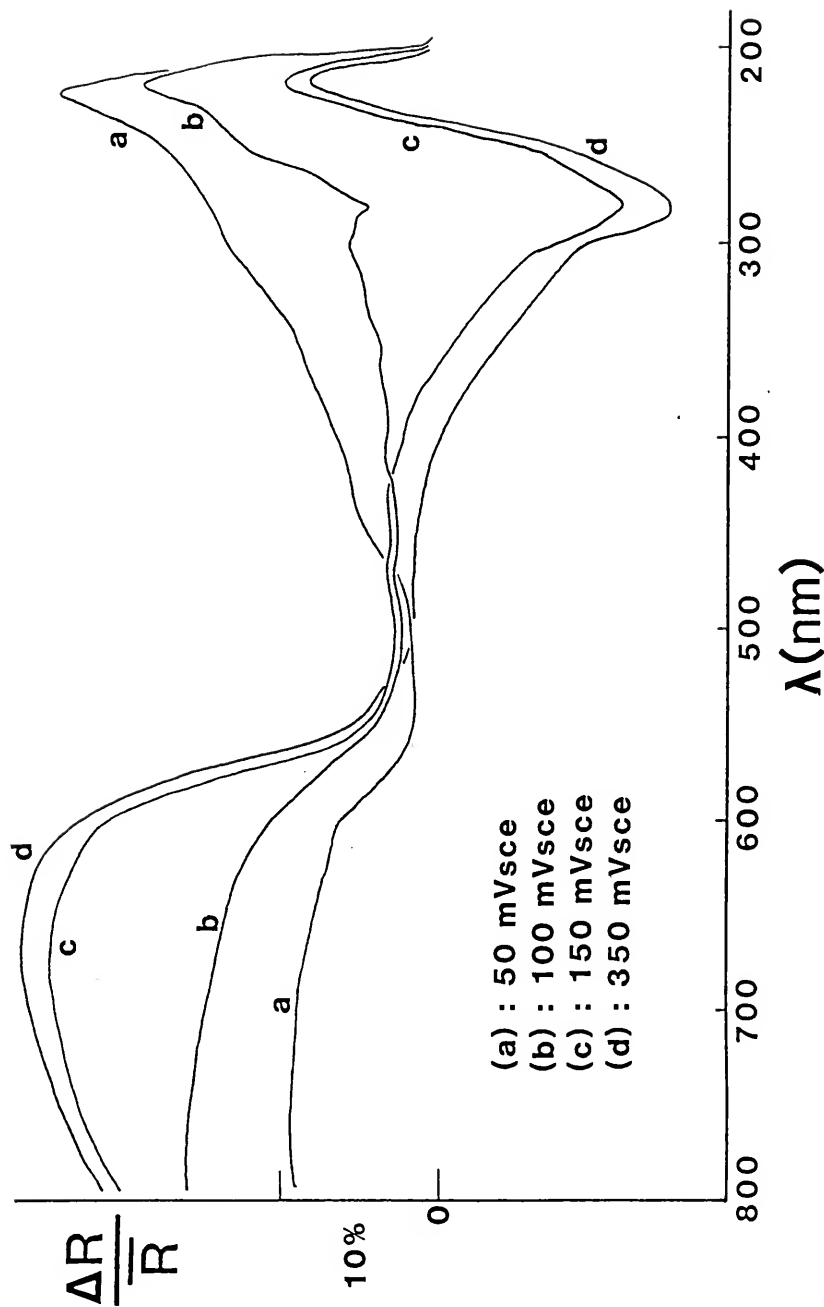


Figure 43. Reflectograms for Ni-30 Cu in pH = 4.0, deaerated solution. A $\text{Ni}(\text{OH})_2$ film is indicated along with the selective dissolution and replating of Cu.

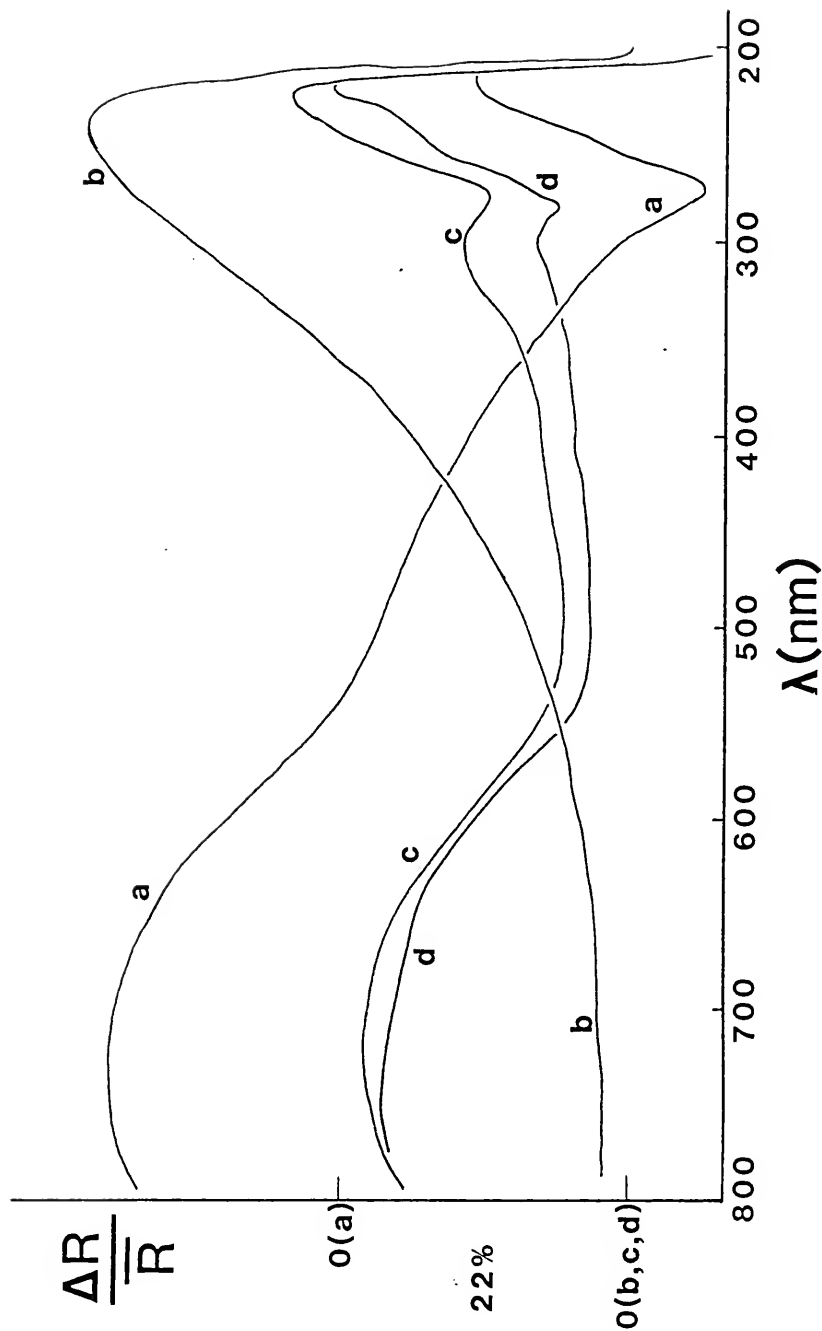


Figure 44. The addition of a 25 Ni-75 Cu/30 Ni-70 Cu compositional modulation curve (a) to a typical Ni(OH)₂ curve (b) results in curve (c) which is quite similar to the reflectogram obtained for the Ni-30 Cu electrode at +100 mV_{SCE} in pH = 4.0, deaerated solution.

clear indication that Cu is preferentially dissolving from the working electrode while the Ni is remaining behind and contributing to passive film formation. In fact, upon removal from solution, a thin metallic copper film is observed to have plated out on the optical reference electrode, which further indicates gross Cu dissolution from the working electrode. Presumably this phenomenon is not observed in the pH = 4.0 open solution because of the higher surface pH created by oxygen reduction. Such a pH increase makes Cu dissolution less likely while increasing the probability of Cu_2O formation (cf with a Pourbaix diagram for pure Cu). Recall that a small component of Cu_2O was detected in the film formed in the open solution.

Anodic Behavior at pH = 8.0

In pH = 8.0 deaerated solution the alloy is passivated at substantially higher potentials (275 mV higher) and by a much larger current density ($\times 2$) as seen in Figure 45. The surface film is once more predominantly $\text{Ni}(\text{OH})_2$ with a minor Cu_2O component (Figure 46) although the thickness is much less than that produced on pure Ni. As was the case for the alloy in the pH = 4.0 open cell, the Cu_2O in the film tends to disappear at higher potentials. In fact, the thickness of the film in general decreases substantially with increasing potential which reflects the behavior noted in the pH = 4.0 solution.

In the pH = 8.0 open solution the response of the alloy (Figure 47) is similar to that of pure Ni since passivation occurs without active dissolution. The current densities and film thicknesses throughout the experiment are also quite similar to that for the pure metal. Figure 48

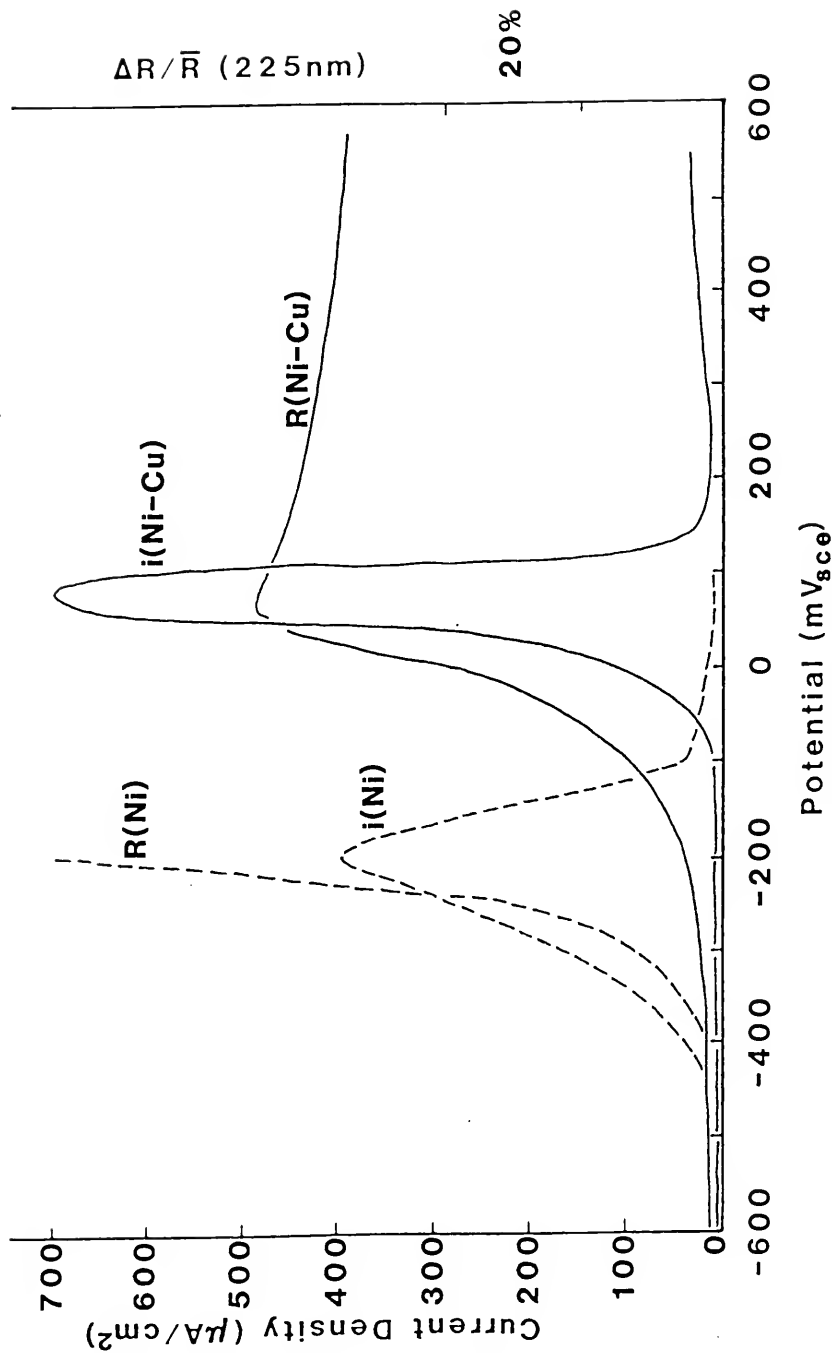


Figure 45. Polarization and reflectivity data for Ni-30 Cu in pH = 8.0, deaerated solution.

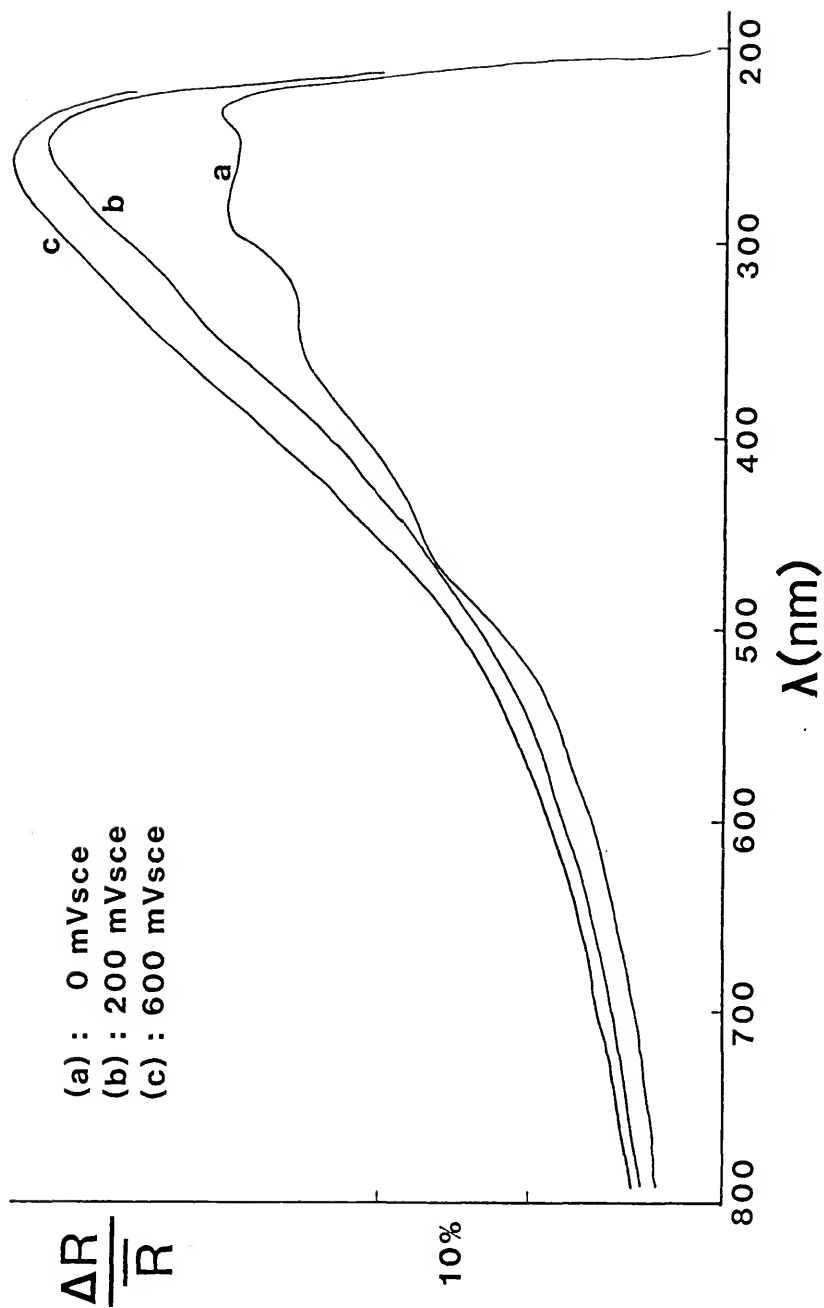


Figure 46. Evolution of a $\text{Ni(OH)}_2\text{-Cu}_2\text{O}$ film on Ni-30 Cu in pH = 8.0, deaerated solution.

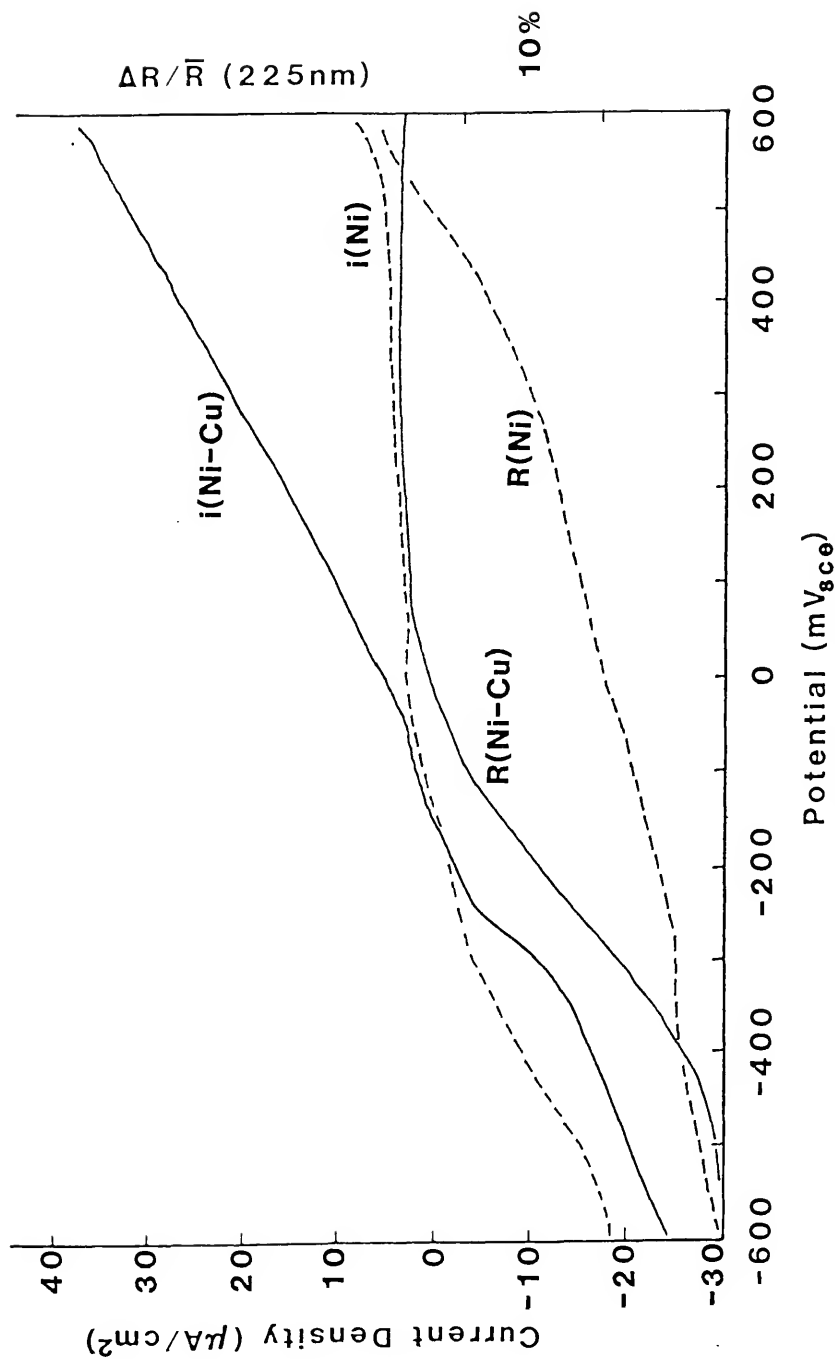


Figure 47. Polarization and reflectivity data for Ni-30 Cu in pH = 8.0, open solution.

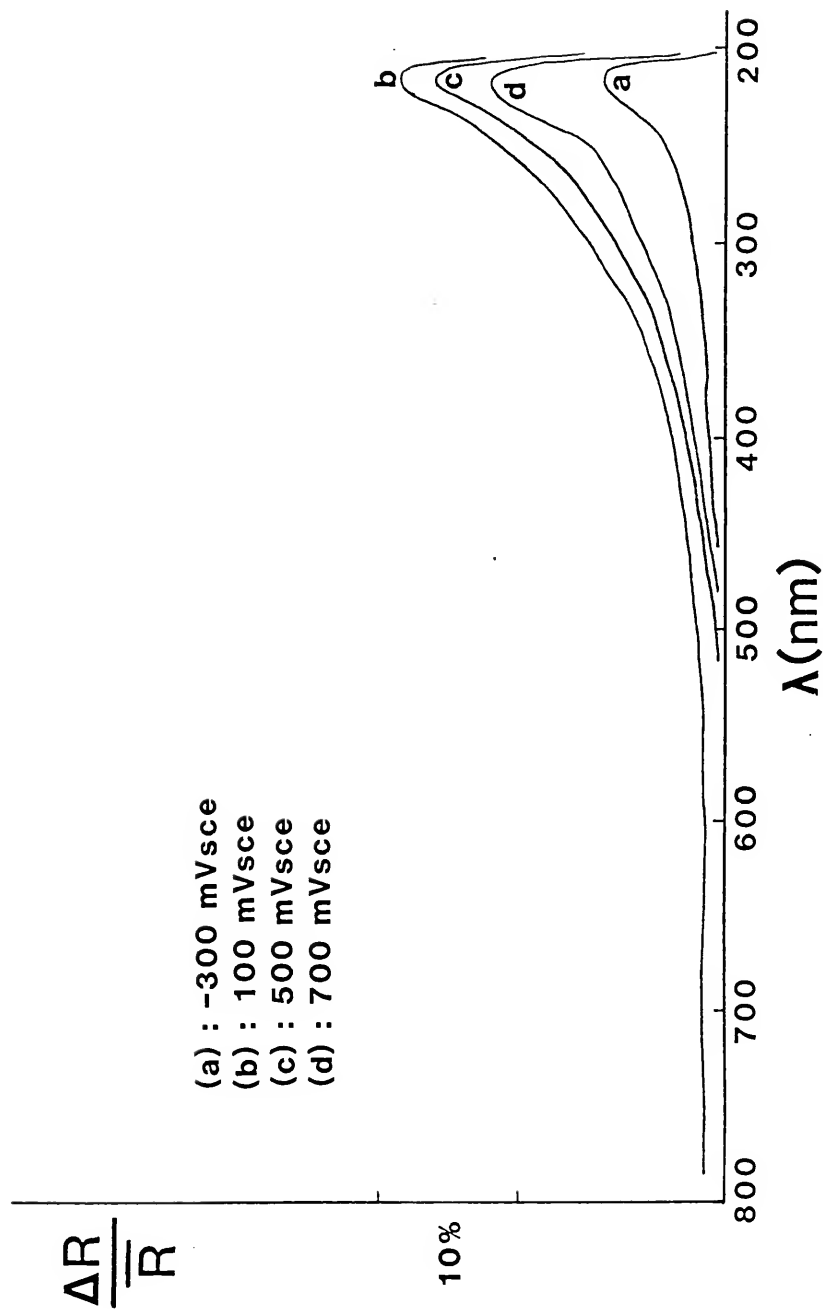


Figure 48. Reflectograms for Ni-30 Cu in pH = 8.0, open solution, indicating pure $\text{Ni}(\text{OH})_2$.

indicates that the surface film responsible for passivation is pure Ni(OH)_2 with no Cu_2O being detected.

Anodic Behavior at pH = 12.0

The electrochemical and reflectivity data obtained for the Ni - 30 Cu alloy in pH = 12.0 open and deaerated solution is virtually identical to that observed for pure Ni (Figures 49 and 50). The passivating film is thin Ni(OH)_2 in both cases (Figures 51 and 52) with no evidence of Cu_2O .

Summary

As was the case for pure Ni, the passivation behavior of the alloy in low pH solutions (pH = 4.0 deaerated and open, pH = 8.0 deaerated) seems to be governed by a precipitation mechanism. Although the presence of Cu has but little influence on the passive film composition, it does effect the passivation potential (at 250 mV more anodic), passivating current density (increased threefold), and passive current density (greater by a factor of five).

Again, imitating the response of pure Ni, the alloy passivates by a solid state mechanism in higher pH solutions. In addition, the passive current density and film thickness in these solutions are practically identical to the values obtained for the pure metal. These observations indicate that the presence of Cu has little effect on the solid state mechanism of film formation and on film coherency while in lower pH solutions the Cu delays metallic dissolution to more anodic values and results in the formation of a less protective film.

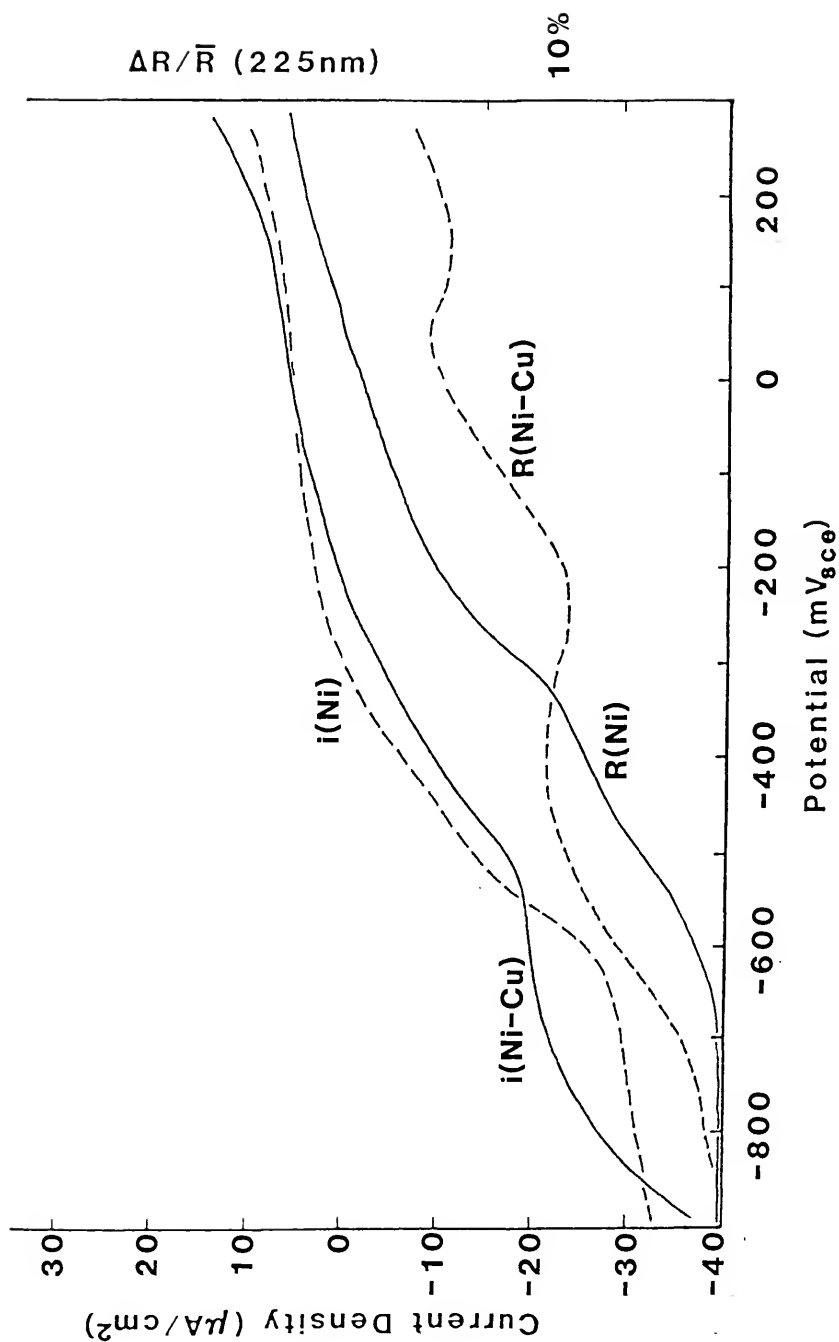


Figure 49. Polarization and reflectivity data for Ni-30 Cu in pH = 12.0, open solution.

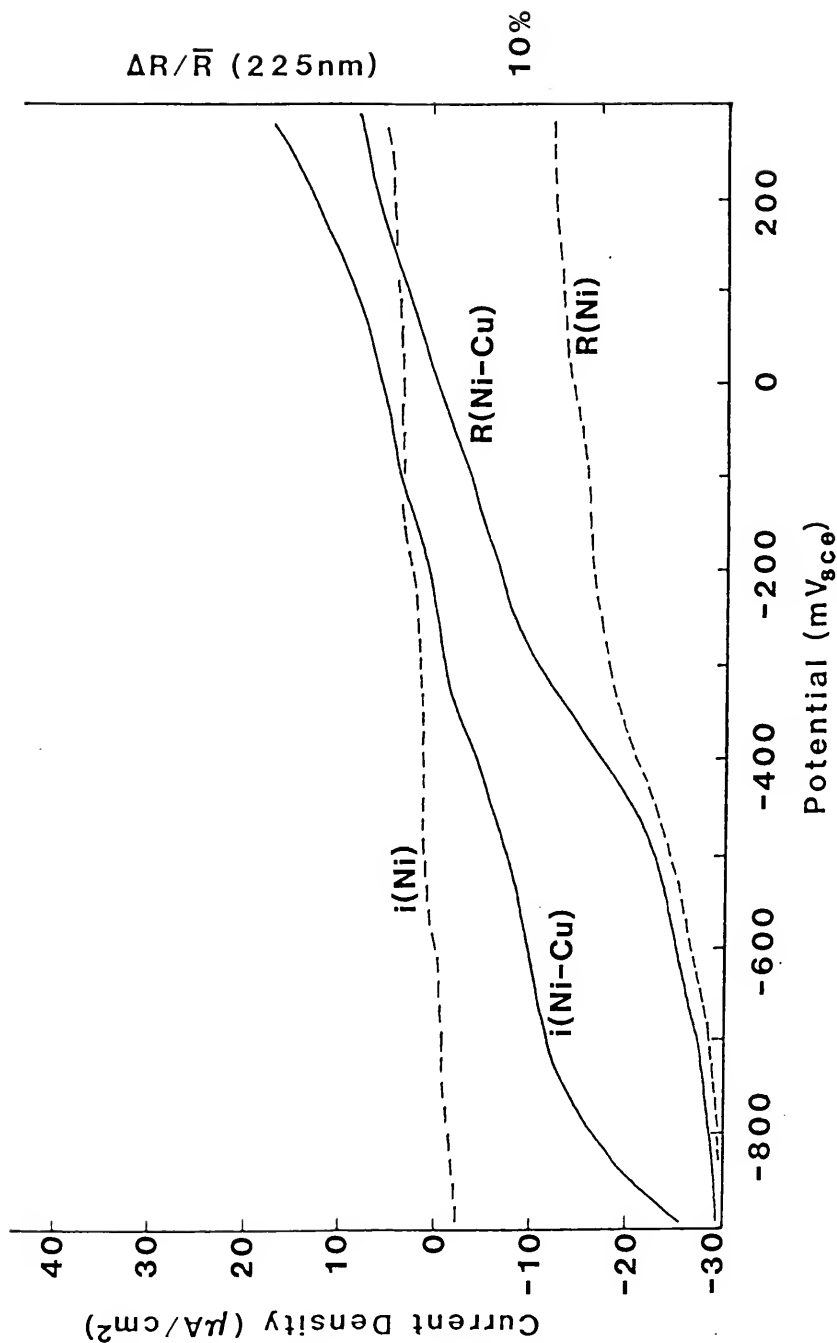


Figure 50. Polarization and reflectivity data for Ni-30 Cu in pH = 12.0, deaerated solution.

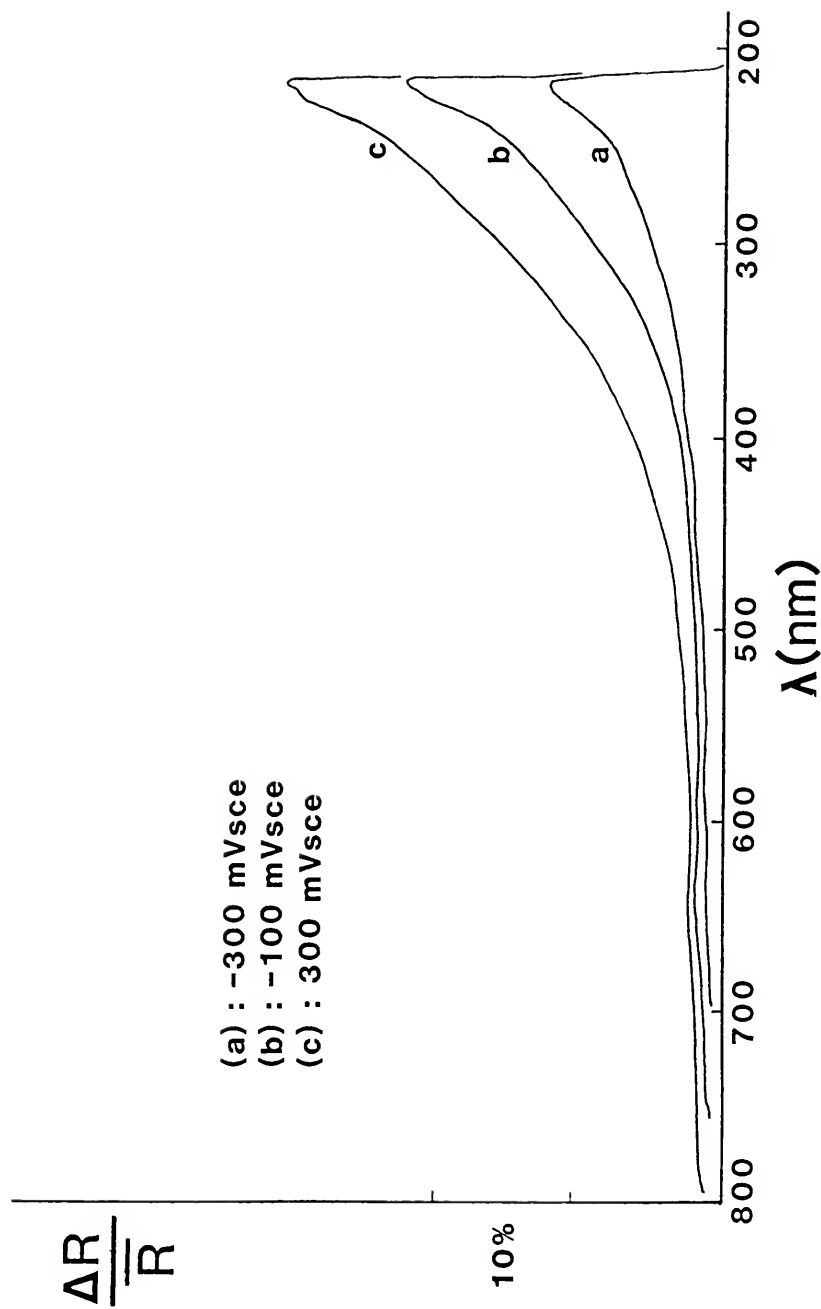


Figure 51. Reflectograms from Ni-30 Cu in pH = 12.0, open solution, indicating pure Ni(OH)_2 .

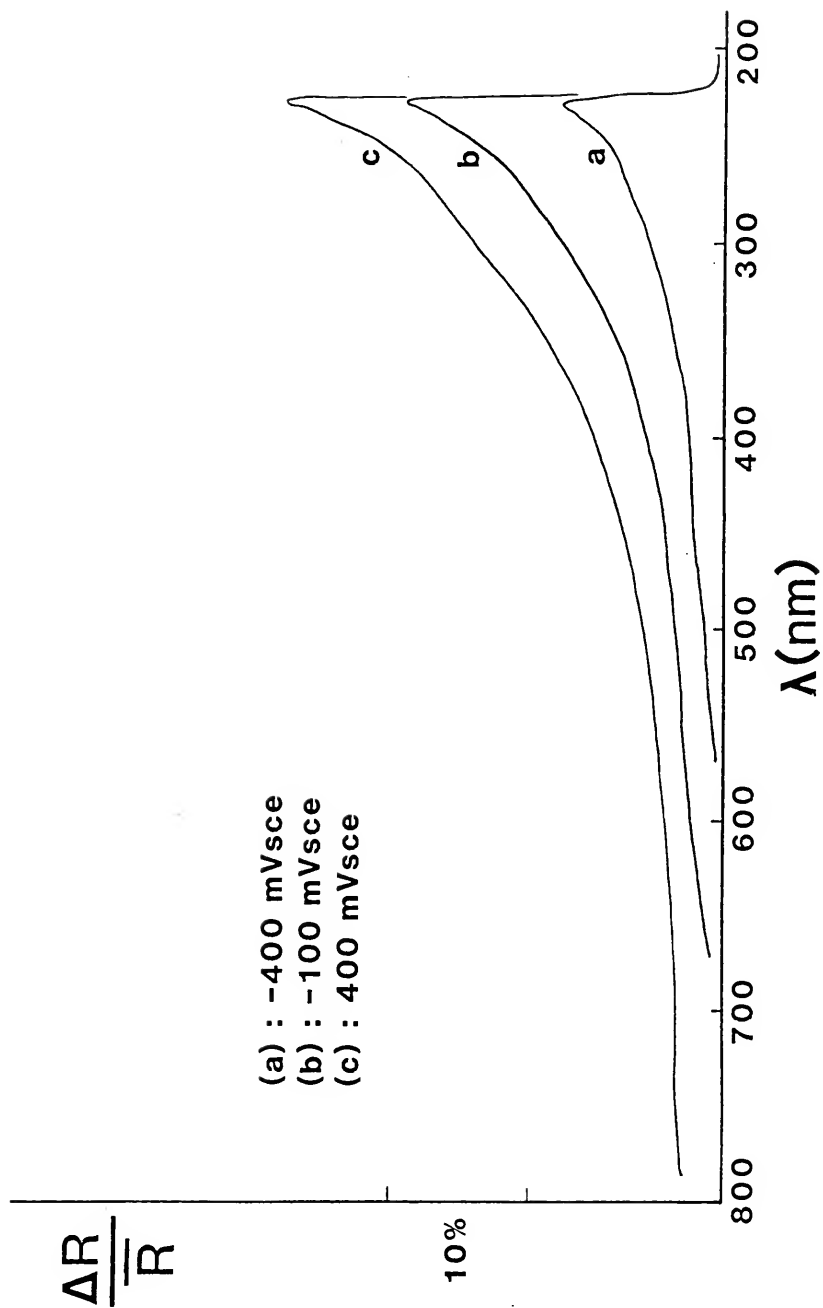


Figure 52. Reflectograms from Ni-30 Cu in pH = 12.0, deaerated solution, indicating pure $\text{Ni}(\text{OH})_2$.

CHAPTER 5 CONCLUSIONS AND SUGGESTIONS FOR FURTHER RESEARCH

It has been shown conclusively that the film primarily responsible for passivating pure Ni in 0.15 N Na_2SO_4 is $\text{Ni}(\text{OH})_2$. In addition, conclusive evidence has also been presented which indicates that NiO can also form on the surface of a Ni electrode but only in solutions of pH greater than 8. The formation of NiO always occurs subsequent to $\text{Ni}(\text{OH})_2$ formation and does not seem to play an active role in the passivation process. The data presented also indicates that in these higher pH solutions the $\text{Ni}(\text{OH})_2$ film partially transforms into a third film type at potentials typically near those required for oxygen evolution. It is suggested that this third film is NiOOH and that transformation proceeds via a deprotonation reaction.

In addition, passive film growth can occur by two different mechanisms depending on solution pH. In low pH solutions (pH = 4.0 deaerated and open, pH = 8.0 deaerated) the $\text{Ni}(\text{OH})_2$ film forms by a precipitation mechanism subsequent to active metal dissolution. This precipitated film, once formed, generally does not change in thickness as the potential is made increasingly anodic. Conversely, the $\text{Ni}(\text{OH})_2$ film formed in higher pH solutions (pH = 8.0 open, pH = 12.0 open and deaerated) grows by virtue of a solid state mechanism. Although the films formed at alkaline pH's are thinner than those formed in the lower pH environments, they are much more protective.

The addition of Cl ions to the electrolyte does not alter the mechanisms by which passive film formation occurs. These ions, however, do seem to complex with the dissolving Ni in the lower pH solutions, which necessitates the passing of a much greater current density to

achieve passivity. The Ni(OH)_2 film that tends proves to be unstable since pitting occurs shortly afterwards. In light of this, it is postulated that the Cl^- in solution exchange with the OH^- in the film creating a soluble Ni complex. Such exchange is localized at defects in the film which leads to perforation of the film and, ultimately, pitting. In the higher pH solutions the Cl ion additions have little, if any, effect on passivation. This confirms that the solid state mechanism of film growth that is operative in this solution produces a coherent film with a relatively low defect density.

The anodic response of a Ni- 30 Cu electrode in the low pH solution is similar in many aspects to that of pure Ni. The film responsible for passivation is Ni(OH)_2 and formation proceeds via the precipitation mechanism which operates during the active dissolution of the electrode. The copper addition results in a considerably higher passivation potential and current density. Although the copper preferentially dissolves in the most acidic environment tested ($\text{pH} = 4.0$, deaerated) it is incorporated into the film as a minor component in the solutions of slightly higher pH. The Cu addition has no detectable effect on the electrode response in the solutions with a pH of 12.

One area of corrosion research currently generating considerable interest deals with the behavior of amorphous alloys in aqueous solutions. The unusually low corrosion rates exhibited by such alloys is attributed to surface films which are suspected to have a very low defect density. It would be interesting to employ an in situ technique such as Differential Reflectometry to analyze the composition of the protective film in an attempt to gain insight into the mechanism(s) of

formation. Work on a Ni-30 Cu alloy could, of course, be compared directly to the present work.

A second, more readily applicable project would be the study of both the short and long term effects of exposure of Monel to sea water. The film composition and thickness could easily be monitored in situ using the SID electrode design.

The usefulness of the present technique could be vastly expanded if a design could be developed which would permit reflectivity measurements to be taken while the SID is being rotated. Such rotation would control corrosion product transport (e.g., copper ions that result from dealloying or hydroxide ions that result from oxygen reduction) and make data interpretation more straightforward.

BIBLIOGRAPHY

1. M. G. Fontana and N. D. Green, Corrosion Engineering, Second Edition, McGraw-Hill, New York (1978).
2. W. Z. Friend, Corrosion of Nickel and Nickel Base Alloys, Wiley, New York (1980).
3. H. H. Uhlig, Corrosion Science, 19, 777 (1979).
4. N. Sato, Passivity of Metals, ed. by R. P. Frankenthal and J. Keuger, The Electrochemical Society, Inc., New York (1978).
5. A. M. Novakouskii and N. Y. Uflyand, Zashchita Metallov, 13, 22 (1977).
6. D. C. Silverman, Corrosion, 37, 546 (1981).
7. T. Smith, P. Smith and F. Mansfield, Journal of the Electrochemical Society, 126, 799 (1979).
8. F. Mansfield, Corrosion, 37, 301 (1981).
9. R. E. Hummel, D. D. Dove and J. A. Holbrook, Physical Review Letters, 25, 290 (1970).
10. J. A. Holbrook, Ph.D. Dissertation, University of Florida (1972).
11. B. MacDougall and M. Cohen, Journal of the Electrochemical Society, 123, 1783 (1976).
12. J. R. Vilche and A. J. Arvia, Corrosion Science, 18, 441 (1978).
13. B. MacDougall and M. Cohen, Journal of the Electrochemical Society, 122, 383 (1975).
14. J. R. Vilche and A. J. Arvia, Journal of the Electrochemical Society, 123, 1061 (1976).
15. G. Okamoto and N. Sato, Trans. Japanese Institute of Metals, 1, 16 (1960).
16. N. Sato and G. Okamoto, Journal of the Electrochemical Society, 110, 605 (1963).
17. N. Sato and G. Okamoto, Trans. Japanese Institute of Metals, 2, 113 (1961).

18. M. Pourbaix, Atlas of Electrochemical Equilibria in Aqueous Solutions, Second English Edition, NACE (1974).
19. R. L. Cowan and R. W. Staehle, Journal of the Electrochemical Society, 118, 557 (1971).
20. V. Mitrovic-Scepanovic and M. B. Ives, Journal of the Electrochemical Society, 127, 1903 (1980).
21. T. S. de Gromoboy and L. L. Shreir, Electrochimica Acta, 11, 895 (1966).
22. J. O'M. Bockris, A. K. N. Reddy and B. Rao, Journal of the Electrochemical Society, 113, 1133 (1966).
23. R. M. Latanision and H. Opperhauser, Corrosion, 27, 509 (1971).
24. J. L. Weininger and M. W. Reiter, Journal of the Electrochemical Society, 110 484 (1963).
25. B. Lovrecek and S. Lipanovic, Corrosion Science, 10, 865 (1970).
26. M. Turner, G. E. Thompson and P. A. Brook, Corrosion Science, 13, 985 (1973).
27. B. MacDougall and M. Cohen, Journal of the Electrochemical Society, 123, 191 (1976).
28. B. MacDougall and M. Cohen, Journal of the Electrochemical Society, 124, 1185 (1977).
29. B. MacDougall, Journal of the Electrochemical Society, 127, 789 (1980).
30. B. MacDougall, D. F. Mitchell and M. J. Graham, Corrosion, 38, 85 (1982).
31. J. Siejka, C. Clerki and J. Yahalom, Journal of the Electrochemical Society, 119, 991 (1972).
32. M. Okuyama and S. Haruyama, Corrosion Science, 14, 1 (1974).
33. J. L. Ord, J. C. Clayton and D. J. DeSmet, Journal of the Electrochemical Society, 124, 1714 (1977).
34. B. MacDougall and M. Cohen, Journal of the Electrochemical Society, 121, 1152 (1974).
35. B. MacDougall, D. F. Mitchell and M. J. Graham, Journal of the Electrochemical Society, 127, 1248 (1980).
36. B. MacDougall and M. J. Graham, Journal of the Electrochemical Society, 128, 2321 (1981).

37. B. MacDougall, Journal of the Electrochemical Society, 130, 114 (1983).
38. S. M. Wilhelm and N. Hackerman, Journal of the Electrochemical Society, 128, 1668 (1981).
39. D. E. Davies and W. Barker, Corrosion, 20, 47T (1964).
40. R. S. Schreiber-Guzman, J. R. Vilche and A. J. Arvia, Corrosion Science, 18, 765 (1978).
41. T. S. Lee, Masters Thesis, University of Florida (1972).
42. M. A. Hopper and J. L. Ord, Journal of the Electrochemical Society, 120, 183 (1973).
43. P. W. T. Lu and S. Srinivasan, Journal of the Electrochemical Society, 125, 1416 (1978).
44. B. MacDougall and M. Cohen, Electrochimica Acta, 23, 145 (1978).
45. M. Datta and D. Landolt, Journal of the Electrochemical Society, 124, 483 (1977).
46. D. Landolt, Passivity of Metals, ed. by R. P. Frankenthal and J. Kruger, The Electrochemical Society, Inc. (1978).
47. N. Sato, Journal of the Electrochemical Society, 129, 255 (1982).
48. M. L. Kronenberg, J. C. Banter, E. Yenger and F. Hovorka, Journal of the Electrochemical Society, 110, 1007 (1963).
49. J. R. Viche and A. J. Arvia, Corrosion Science, 15, 419 (1975).
50. M. Zamin and M. B. Ives, Corrosion, 8, 319 (1973).
51. M. Zamin and M. B. Ives, Journal of the Electrochemical Society, 121, 1141 (1974).
52. A. Bengali and K. Nobe, Journal of the Electrochemical Society, 126, 1118 (1979).
53. B. MacDougall, Journal of the Electrochemical Society, 126, 919 (1979).
54. A. Hickling and D. Taylor, Trans. of the Faraday Society, 44, 262 (1948).
55. H. P. Leckie, Journal of the Electrochemical Society, 117, 1478 (1970).
56. D. W. Shoesmith, T. E. Rummery, D. Owen and W. Lee, Journal of the Electrochemical Society, 123, 790 (1976).

57. D. W. Shoesmith, T. E. Rummery, D. Owen and W. Lee, *Electrochimica Acta*, 22, 1403 (1977).
58. D. W. Shoesmith and W. Lee, *Electrochimica Acta*, 22, 1411 (1977).
59. D. W. Shoesmith, S. Sunder, M. G. Bailey, G. J. Wallace and F. W. Stanchell, *Journal of Electroanalytical Chemistry*, 146, 155 (1982).
60. G. T. Burstein and R. C. Newman, *Journal of the Electrochemical Society*, 128, 2270 (1981).
61. C. W. Shanley, R. E. Hummel and E. D. Verink, Jr., *Corrosion Science*, 20, 467 (1980).
62. C. W. Shanley, R. E. Hummel and E. D. Verink, Jr., *Corrosion Science*, 20, 481 (1980).
63. F. Mansfield and H. H. Uhlig, *Corrosion Science*, 9, 377 (1969).
64. J. Osterwald and H. H. Uhlig, *Journal of the Electrochemical Society*, 108, 515 (1961).
65. M. Kiyoshige and T. Yamane, Z. Melalikde, 70, 392 (1979).
66. S. Hettiarachichi and T. P. Hoar, *Corrosion Science*, 19, 1059 (1979).
67. N. S. McIntyre, T. E. Rummery, M. G. Cook and D. Owen, *Journal of the Electrochemical Society*, 123, 1164 (1976).
68. G. M. Ugiansky and G. A. Ellinger, *Corrosion*, 24, 134 (1968).
69. T. L. Barr, *Journal of Physical Chemistry*, 82, 1801 (1978).
70. N. S. McIntyre, S. Sunder, D. W. Shoesmith and F. W. Stanchell, *Journal of Vacuum Science and Technology*, 18, 714 (1981).
71. N. S. McIntyre and M. G. Cook, *Analytical Chemistry*, 47, 2208 (1975).
72. J. Ali, Ph.D. Dissertation, University of Florida (1983).
73. K. S. Kim, *Journal of Electron Spectroscopy*, 5, 351 (1974).
74. K. S. Kim, *Journal of Electron Spectroscopy*, 1, 254 (1972).
75. K. T. Ng, *Journal of Physical Chemistry*, 80, 2095 (1976).
76. H. Windawi and F. F. L. Ho, *Chemical Analysis*, D. J. Elving and J. D. Winefordner, ed., John Wiley and Sons, New York, p. 89 (1982).
77. D. Briggs and M. P. Seah, *Practical Surface Analysis*, John Wiley and Sons (1983).

78. E. Jones and W. F. K. Wynne-Jones, Transactions Faraday Society, 52, 1260 (1956).
79. P. D. Lukovtsev, Proceedings of the 4th Conference on Electrochemistry of the Academy of Sciences, Moscow (1959).
80. S. F. Uno, Journal of the Electrochemical Society, 107, 661 (1960).
81. R. E. Hummel, Physica Status Solidi, 76, 11 (1983).

BIOGRAPHICAL SKETCH

Randall J. Smith was born April 4, 1959, in Pittsburgh, Pennsylvania. He attended Cedarville College in Cedarville, Ohio, from 1976 to 1978. After leaving Cedarville College, the author then entered Wright State University in Dayton, Ohio, where he graduated with a Bachelor of Science degree in materials science in 1980. The author then entered the University of Florida in 1980 and received a Master of Science degree in materials science in June, 1982, and has pursued the degree of Doctor of Philosophy since that date.

I certify that I have read this study and that in my opinion it conforms to acceptable standards of scholarly presentation and is fully adequate, in scope and quality, as a dissertation for the degree of Doctor of Philosophy.



R. E. Hummel, Chairman
Professor of Materials Science
and Engineering

I certify that I have read this study and that in my opinion it conforms to acceptable standards of scholarly presentation and is fully adequate, in scope and quality, as a dissertation for the degree of Doctor of Philosophy.



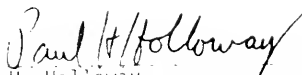
J. R. Ambrose
Associate Professor of Materials
Science and Engineering

I certify that I have read this study and that in my opinion it conforms to acceptable standards of scholarly presentation and is fully adequate, in scope and quality, as a dissertation for the degree of Doctor of Philosophy.



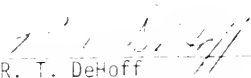
E. D. Verink, Jr.
Professor and Chairman of Materials
Science and Engineering

I certify that I have read this study and that in my opinion it conforms to acceptable standards of scholarly presentation and is fully adequate, in scope and quality, as a dissertation for the degree of Doctor of Philosophy.



P. H. Holloway
Professor of Materials Science
and Engineering

I certify that I have read this study and that in my opinion it conforms to acceptable standards of scholarly presentation and is fully adequate, in scope and quality, as a dissertation for the degree of Doctor of Philosophy.


R. T. DeHoff
Professor of Materials Science
and Engineering

I certify that I have read this study and that in my opinion it conforms to acceptable standards of scholarly presentation and is fully adequate, in scope and quality, as a dissertation for the degree of Doctor of Philosophy.


D. O. Shah
Professor of Chemical Engineering

This dissertation was submitted to the Graduate Faculty of the College of Engineering and to the Graduate School, and was accepted as partial fulfillment of the requirements for the degree of Doctor of Philosophy.

December, 1984


Hubert A. Basis
Dean, College of Engineering

Dean for Graduate Studies
and Research

UNIVERSITY OF FLORIDA



3 1262 08553 5325